

THÈSE

présentée à

L'UNIVERSITÉ BORDEAUX I

ÉCOLE DOCTORALE DES SCIENCES CHIMIQUES

par **Mlle Laura GORACCI**

POUR OBTENIR LE GRADE DE

DOCTEUR

SPÉCIALITÉ : **CHIMIE**

INTERACTION OF SURFACTANTS WITH DNA: A MULTI-TECHNICAL
APPROACH TO THE STUDY OF DNA TRANSFECTION AGENTS

Soutenue le : 9 janvier 2004

Après avis de :

MM. P. Baglioni, Professeur, Università di Firenze
G. Mancini, Docteur, CNR Università di Roma
"La Sapienza"

Rapporteurs

Devant la commission d'examen formée de :

MM. F. Fages, Professeur, Université de la Méditerranée
P. Baglioni, Professeur, Università di Firenze
G. Mancini, Docteur, CNR Università di Roma
J.-L. Pozzo, Professeur, Université Bordeaux I
D. M. Bassani, Chargé de Recherche, Université Bordeaux I
G. Savelli, Professeur, Università di Perugia

Président
Rapporteur
Rapporteur
Rapporteur
Examineur
Examineur

Dottorato in Co-Tutela di Tesi



Università degli Studi di Perugia



Université Bordeaux 1

“La clef de toutes les sciences est sans contredit le point d’interrogation; nous devons la plupart des grandes découvertes au comment? Et la sagesse dans la vie consiste peut-être à se demander, à tout propos, pourquoi?”

Honoré de Balzac (1799–1850)

“La scienza è l’esperienza, e l’esperienza è un manto che si trama a fila di secoli; e più il manto si distende e più la scienza è completa e sicura”.

Carlo Bini (1806-1842)

Alla mia famiglia

Desidero ringraziare in primo luogo il Prof. Gianfranco Savelli per avermi dato l'opportunità di lavorare in un campo tanto affascinante, per tutti i suoi consigli e per la fiducia dimostratami. Grazie anche al Dott. Dario Bassani, per l'entusiasmo che ha dimostrato e per l'appoggio costante, anche a migliaia di chilometri di distanza.

Desidero inoltre ringraziare il Prof. Raimondo Germani, una guida preziosa dentro e fuori il laboratorio, e tutto il gruppo di ricerca di Perugia e di Bordeaux, per l'ambiente sereno e per l'affetto dimostratomi. Infine, un sentito grazie va al Prof. Gabriele Cruciani, per tutto ciò che mi ha insegnato sul Modelling Molecolare, e al Prof. Frederic Fages per avere aperto la strada alla mia esperienza francese.

Grazie alla mia famiglia per il sostegno costante, e per avere sopportato di vivere fra montagne di fogli in questi ultimi mesi...idem per Luisa e la nostra scrivania!Grazie a Guido per la copertina, a Gianluca, Simone e Giuliano per le consulenze tecniche e grafiche.

CONTENTS

CHAPTER 1: INTRODUCTION **1**

1.1	Self-organisation: an overview	1
1.2	The DNA structure	3
1.3	Possible ways of molecule interaction with DNA	7
1.4	A biotechnological application of molecules interacting with DNA: the delivery of DNA in cells for gene therapy	12
1.5	Interaction between DNA and amphiphilic systems	14
1.6	Techniques to investigate DNA-surfactants interactions	17
1.7	Aim of the work	19

REFERENCES **24**

CHAPTER 2: CIRCULAR DICHROISM SPECTROSCOPY **27**

2.1	Introduction	27
2.2	Circular Dichroism of nucleic acids	29
2.3	CD Instrumentation	31
2.4	CD analysis of the DNA-surfactants interaction	32
2.5	Results and discussion	33
2.5.1	Effect of pH on DNA structure	33
2.5.2	Effect of ammonium salts on DNA CD spectra	34
2.5.3	Interactions between DNA and zwitterionic systems	38
2.5.3.a	Effect of the amine-oxide on the DNA structure	38
2.5.3.b	Effect of the carboxybetaine on DNA structure	44
2.5.3.c	Effect of sulfobetaines on DNA	46
2.5.4	Interaction between DNA and zwitterionic non-micellisable systems	48
2.6	Concluding remarks	51

REFERENCES **53**

CHAPTER 3: MOLECULAR MODELLING **55**

3.1	Introduction	55
3.2	Docking procedures	56
3.3	The CHEMODOCK method	60
3.3.1	GRID	60
3.3.2	The GRID Probes	61
3.3.3	The Energy Function	62
3.3.4	The CHEMODOCK procedure	64
3.4	Results and discussion	66
3.4.1	Docking surfactants and DNA	66
3.4.1.a	Docking of cationic surfactants on DNA	70
3.4.1.b	Docking of zwitterionic surfactants on DNA	73
3.5	Concluding remarks	76

REFERENCES **78**

CHAPTER 4 : CIRCULAR DICHROISM EXPERIMENTS SUGGESTED BY MOLECULAR MODELLING **81**

4.1	Introduction	81
4.2	Effect of the Tris-HCl buffer on CD spectrum of DNA	82
4.3	CD spectra of DNA in Tris-HCl upon addition of surfactants	84
4.4	Concluding remarks	88

REFERENCES **90**

CHAPTER 5: FLUORESCENCE SPECTROSCOPY **91**

5.1	Introduction	91
5.1.1	Basic theory of fluorescence	91
5.1.2	Concepts of fluorescence polarisation	96
5.1.3	Quenching of Fluorescence	97
5.2	Ethidium Bromide and Hoechst 33258: fluorescent probes for DNA	100
5.3	DNA-surfactant interaction: the use of fluorescence spectroscopy	104
5.4	Results and discussion	106
5.4.1	Amphiphilic systems	106
5.4.2	Preliminary investigation	108

5.4.3 The use of Hoechst 33258 probe in studying DNA-surfactants interaction	112
5.4.5 Interaction between cationic surfactants and Hoechst 33258	113
5.4.5.a In the absence of DNA	113
5.4.5.b In the presence of DNA	115
5.4.6 Interaction between zwitterionic surfactants and Hoechst 33258	117
5.4.6.a In the absence of DNA	117
5.4.6.b In the presence of DNA	118
5.5 Concluding remarks	128

REFERENCES **130**

CHAPTER 6: CONCLUSIONS AND PERSPECTIVES **133**

REFERENCES **138**

CHAPTER 7: EXPERIMENTAL SECTION **139**

7.1 Materials	139
7.1.1 Commercially available compounds	139
7.1.2 Purification of commercially available compounds	139
7.1.3 Synthesis and purification of cationic surfactants	140
7.1.4 Synthesis and purification of zwitterionic surfactants	153
7.2 Methods	162
7.2.1 Determination of DNA concentration	162
7.2.2 Circular dichroism measurements	162
7.2.3 Fluorescence measurements	164
7.2.4 Absorption measurements	164
7.2.5 Polarization measurements	165
7.2.6 Surface tension measurements	165
7.2.7 Conductivity measurements	166
7.2.8 Molecular modelling studies	166

APPENDIX I: CIRCULAR DICHROISM **169**

APPENDIX II: SURFACE TENSION	177
APPENDIX III: MOLECULAR MODELLING	181
APPENDIX IV: FLUORESCENCE SPECTROSCOPY	183
APPENDIX V: FLUORESCENCE POLARISATION	189

CHAPTER 1

INTRODUCTION

1.1 Self-organisation: an overview

The principle of the self-organisation for the creation of functional units is not an invention of modern natural science. It was already a basic idea of the ancient philosophies in Asia and in Europe: only mutuality of the parts creates the whole and its ability to function. Translated into the language of chemistry this means: the self-organisation of molecules leads to supramolecular systems and is responsible for their functions.

The fascinating phenomena of self-organisation, which can be observed in physical, chemical, and biological systems (either near to or far from thermodynamical equilibrium), are characterised by great variety and complexity. A large number of molecules organise spontaneously, eventually exhibiting well-organised behaviour on the macroscopic scale. The variety of organised states ranges from relatively simple spatial or chronological forms of organisation all the way to the complicated interaction between order and function in biological systems.

Although there are many possibilities for self-organisation, the molecular basis is almost always simple: form-anisotropic or amphiphilic molecules make up the simplest building blocks. These already suffice (as shown in Fig.1) to construct a broad range of substances able to form supramolecular systems, from thermotropic and lyotropic liquid crystals and the manifold micellar systems up to the highly ordered membranes in liposomes and cells.

In material science, the significance of liquid crystals and micellar systems has long been known; it is based on the combination of order and mobility. From the life sciences, we know that no life would be possible without the lipids' self-organisation into the bilayers that form the cell membranes.

Self-organisation and the construction of supramolecular systems is an interdisciplinary area which cannot be understood without the co-operation of different fields of science: chemistry alone does not fulfill that task nor does physics or biology. [1]

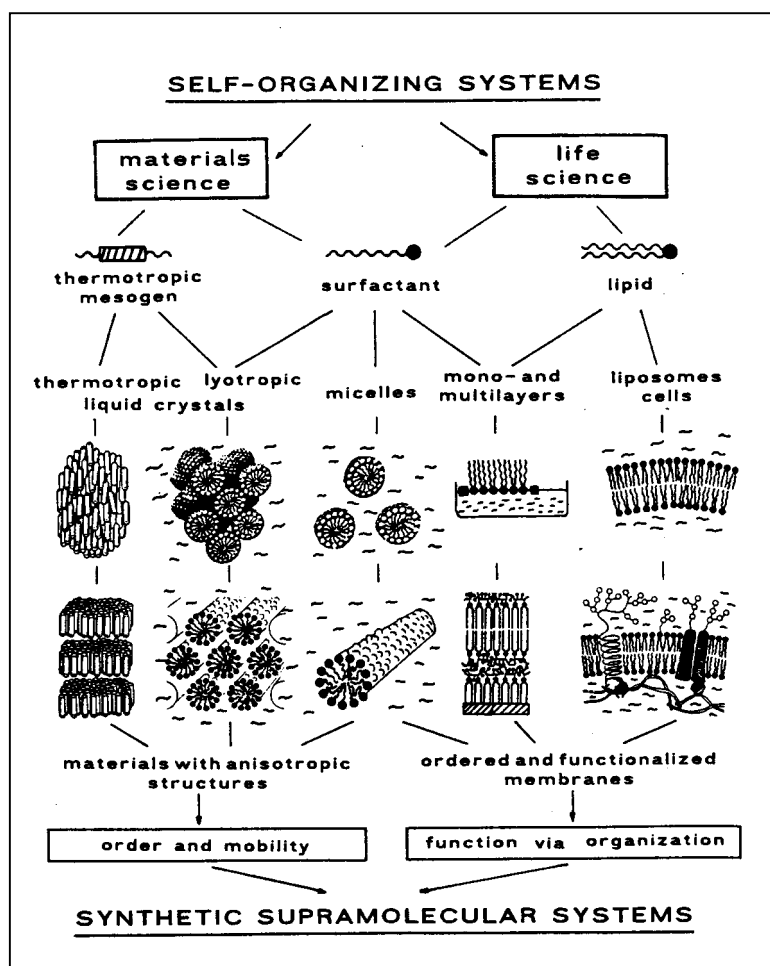


Fig. 1. Self-organisation and supramolecular systems in material science and life science. The supramolecular structures range from simple nematic liquid crystals to complex biomembranes. [1]

1.2 The DNA structure

The discovery that genetic information is coded along the length of a polymeric molecule composed of only 4 types of monomeric units will be regarded as one of the major scientific achievements of last century. This polymeric molecule, known as deoxyribonucleic acid or DNA, is the chemical basis of heredity.

The monomeric units of DNA (deoxyadenilate, deoxyguanylate, deoxycytidylate and thymidilate) are held in polymeric form by 3', 5'-phosphodiester bridges constituting a singled stand. The informational content of DNA resides in the sequence in which these monomers are ordered. One end of the polymer has a 5'-hydroxyl terminus, while the other has a 3'-phosphate moiety. This characteristic is termed as "polarity" of the DNA polymer.

In the early 1950s Watson, Crick and Wilkins proposed a model of a double-stranded DNA molecules. X-ray *diffraction* data obtained by Rosalind Franklin on hydrated fibres of DNA clearly showed that such fibres should have a tridimensional structure that was in some way regular and repetitive. Thus DNA, besides having a primary structure, constituted by the sequence of nucleotidic residues, should have a secondary structure. The diffractograms indicated the presence of a double helix structure, having ten residues for each helical turn. Moreover, the experimental data on the density of such fibres suggested that two filaments of DNA should be in each molecule. A crucial aspect of the hypothesis was the understanding that a helix composed by two filaments could be stabilised by hydrogen bonds between bases of different filaments as long as the bases were coupled in a particular way: the pairing of adenine (A) and thymine (T) by two hydrogen bonds and the pairing of cytosine (C) and guanine (G) by three hydrogen bonds. A consequence of such coupling between a purine and a pyrimidine is that the double helix has a

regular diameter. The model of DNA proposed by Watson and Crick is reported in Fig. 2-A.

The two strands of this right-handed double stranded molecule are antiparallel. This means that one strand runs in 5' to 3' direction and the other in 3' to 5' direction. The two strands are held together by hydrogen bonds between the purine and pyrimidine bases of the respective linear molecules. The restriction imposed by the rotation around phosphodiester bond, the favoured anti configuration of the glycosilic bond, and the predominant tautomers of the four bases allow A to pair only with T, and G only with C (Fig. 2-B).

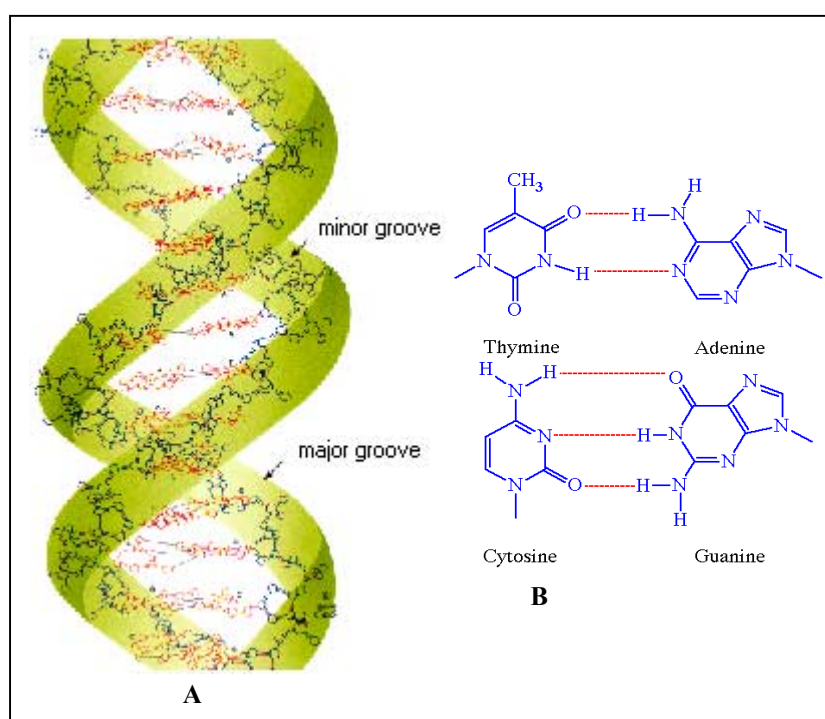


Fig. 2: A) DNA structure in Watson and Crick model; B) interaction between the base pairs.

The hydrophilic skeletons of phosphates and riboses in the helix are on the outside surface in contact to the aqueous medium, whereas the base pairs are stocked on top of each other, with their planes perpendicular to the helical

axis. The superposition of the bases permits strong van der Waals interactions to occur. Each base pair is rotated of 36° with respect to the previous one, and ten base pairs are necessary for each helical turn. The DNA molecule has a pitch of 3.4 nm per turn. Careful examination of the model depicted in Fig.2-A reveals a major groove and a minor groove winding along the molecule parallel to the phosphodiester backbones. These two grooves are very important because, in spite of the fact that the bases (whose sequence codes the genetic information) are in the inner part of the helix, they can be reached from these grooves. In these grooves, proteins can interact specifically with exposed atoms of the nucleotides and thus recognise and bind to specific nucleotide sequences without disrupting the base pairing of the double helical DNA molecule.

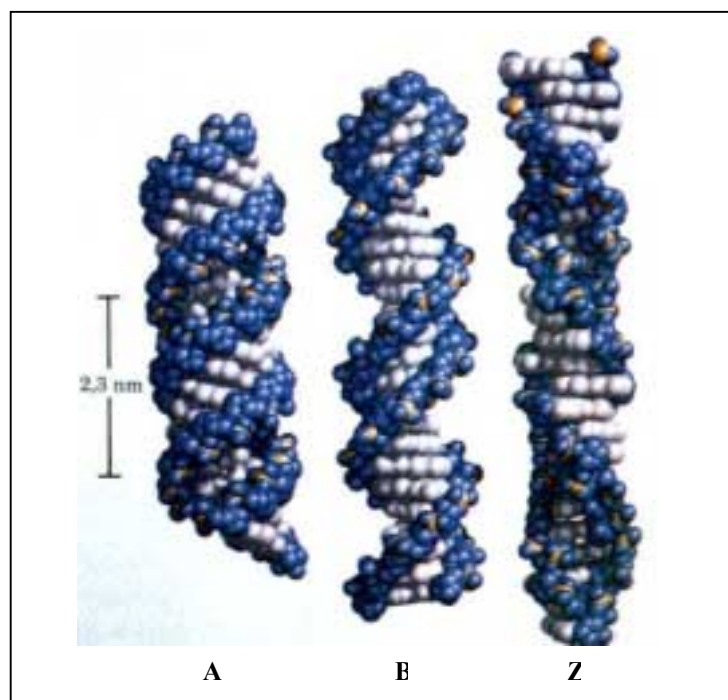


Fig. 3: Structure of A, B and Z DNA. [2]

The model of DNA structure proposed by Watson and Crick is now referred as DNA B. Other two structural variants of DNA, named DNA A and DNA Z, have been characterised (Fig. 3) [2, 3]

The A form is favoured in solutions that are relatively low in water content. Since cells contain a large amount of water, most of the double strand DNA is in the B form or in a form very close to it. In contrast, the Z form of DNA is greatly different from the B form and it appears to be present in prokaryotes and eukaryotes with short DNA sequences, possibly in relation with DNA transcription.

The DNA structure referred to as DNA B will be the one considered throughout this work, since it is the most stable structure under physiological conditions. In living organisms, the DNA molecule is organised in structures called chromosomes. In many viral DNAs, the two ends of the DNA molecule are joined to create a closed circle with no terminus (circular or C-DNA).

In prokaryotic cells, almost all the DNA is contained in a single circular molecule that is often supercoiled and binds to proteins to form a structure called the bacterial nucleoid. In many bacteria, in addition to the greater circular molecule of DNA, there are one or more small circular DNA molecules called plasmids. These often confer to the bacteria resistance to particular antibiotics. Plasmids can vary in length, but they are generally composed only of a few thousand base pairs. Since they can be easily isolated from bacteria, plasmids are useful models for the study of many processes of DNA metabolism. Furthermore, they are a central tool in modern genetic manipulation technologies where they are used to isolate, clone and modify genes. In fact, genes from different species can be inserted into isolated plasmids and then these artificial plasmids can be reintroduced in a normal host cell.

In eukaryotic cells, the genetic material is subdivided amongst than one chromosome, each containing a single molecule of linear DNA. The length of these molecules is generally between 10^7 e 10^9 base pairs. Supercoiling of these molecules around histonic proteins produces nucleosomes. These nucleosomes are further supercoiled to produce fibrils and then chromatin fibres. The peculiar organization of DNA with histonic and non-histonic proteins allow to the long molecules of DNA of many chromosomes to be

contained in the cell nucleus that has the diameter of around five micrometers. A scheme of the organization of DNA is reported in Fig. 4.

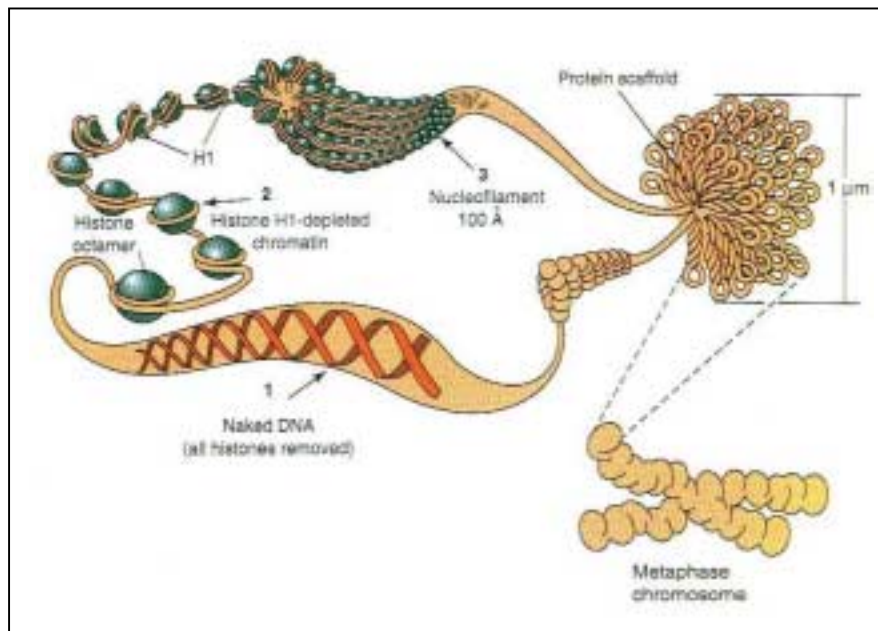


Fig. 4: Organisation of DNA in eukariotic cells. [4]

1.3 Possible ways of molecule interaction with DNA

The study of the interactions of synthetic compounds with DNA is of great interest considering that it is the base of numerous biomedical applications, including drug design, delivery and transfection processes.

Many drugs for cancer chemotherapy are particularly able to specifically interact with DNA and to inhibit DNA replication.[5] This point is obviously very important, although such drugs have the undesirable property of not being able to inhibit the synthesis of DNA in the cancer cell without affecting the DNA synthesis in normal cells. Their value lies in the fact that, in many cancers (e.g. leukaemia), the rate of cancer cells proliferation greatly exceeds normal cell growth. Acridines (e.g. proflavine) and various antibiotics (e.g.

mitomycin C, adriamycin, daunomycin), reported in Fig. 5, are amongst the more well-known non-nucleoside drugs that bind to DNA.

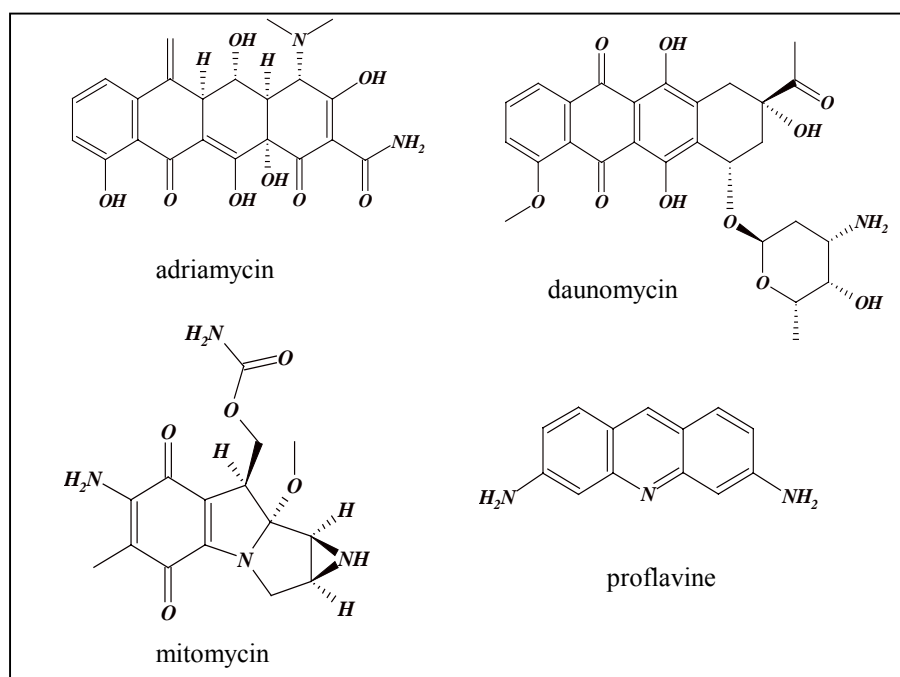


Fig. 5: Structures of some non nucleoside drugs.

In these drugs, binding to DNA is achieved by “intercalation”: The planar ring system of a proflavine, for example, intercalates between the stacked base pair of the double helix and induces a geometrical distortion of the double helical structure. [6, 7] Historically, one of the first studies on the distortion of the double helix by a synthetic compound is the discovery of the interaction between cis-dichlorodiammine-platinum (II) and DNA made by B. Rosenberg in 1969. [8] In the following years a number of mono- and bis-intercalant molecules have been synthesized; among them, some molecules not

only can intercalate into DNA, but are also able to cut DNA structure, as bleomycins can do. 9-13]

An example of the helical distortion due to an intercalating agent is given by the interaction between DNA and the bis-intercalating dye 1,1-(4,4,8,8-Tetramethyl-4,8-Diazaundecamethylene)-Bis-4-(3-Methyl-2,3-Dihydro-(Benzo - 1,3-Thiazole) -2-Methylidene) -Quinolinium Tetraiodide (Toto), as shown in Fig.6.

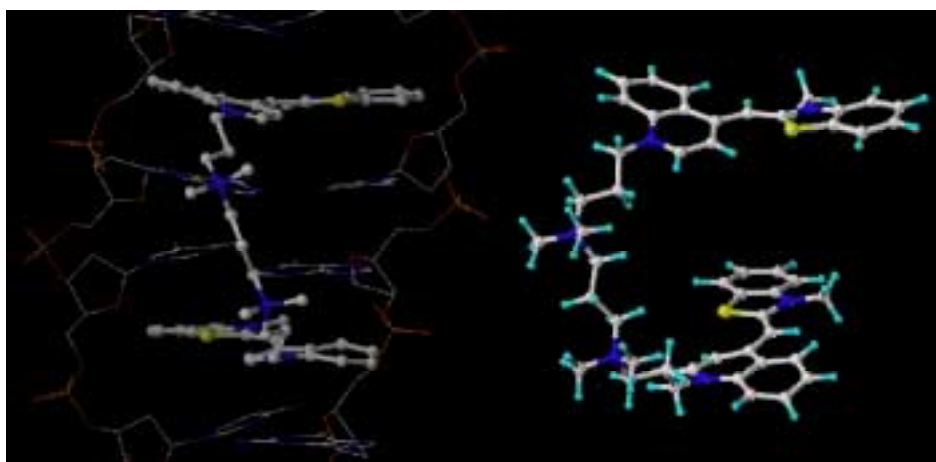


Fig. 6: Bis-intercalation of Toto fluorescent dye into DNA.

The complex formation between Toto and DNA is sequence selective. In fact, it was found that Toto bis-intercalates in a CTAG•CTAG site of DNA, with the benzothiazole ring system sandwiched between the pyrimidines and the quinolinium ring system between the purines, The N-methyl group on the benzothiazole is centered in the major groove. The linker between the two chromophores is positioned in the minor groove crossing from one side of the groove to the other. This probably introduces van der Waals contacts between the linker chain N-methyl groups and the walls of the groove. The length of the linker exactly matches the double strand DNA structural requirements to fulfil nearest neighbor bis-intercalation. [14]

In practice, three different modes of association to DNA are possible:

1. **External binding:** External association of the ligand on the outside surface of the DNA strand.

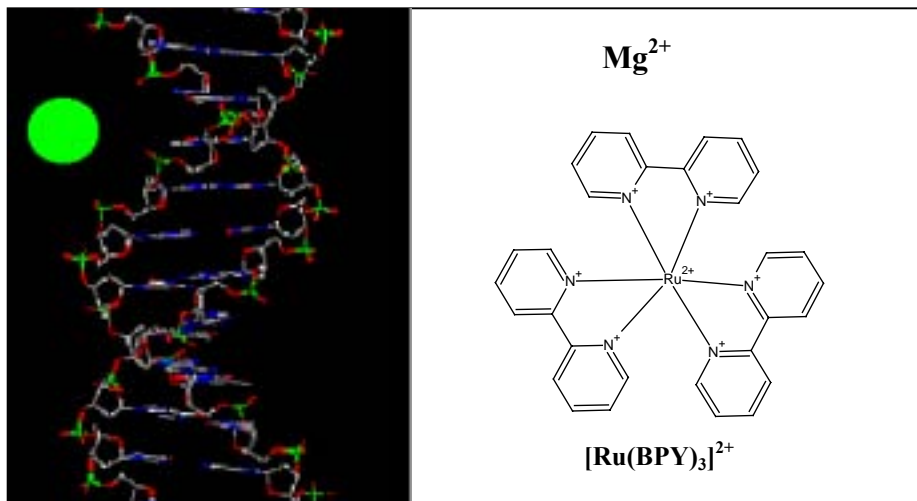


Fig. 7: Example of external binding.

An example of this kind of interaction is given by tris(2,2'-bipyridyl)rutenium(II) ion [Ru(BPY)₃]²⁺. The luminescence enhancement of this complex upon binding to DNA is strongly dependent on the ionic strength, due to the electrostatic nature of the association. Cations such as Mg²⁺ also interact with DNA through electrostatic interactions (Fig. 7). [15]

2. **Groove binding:** Adsorption of a ligand in the DNA groove.

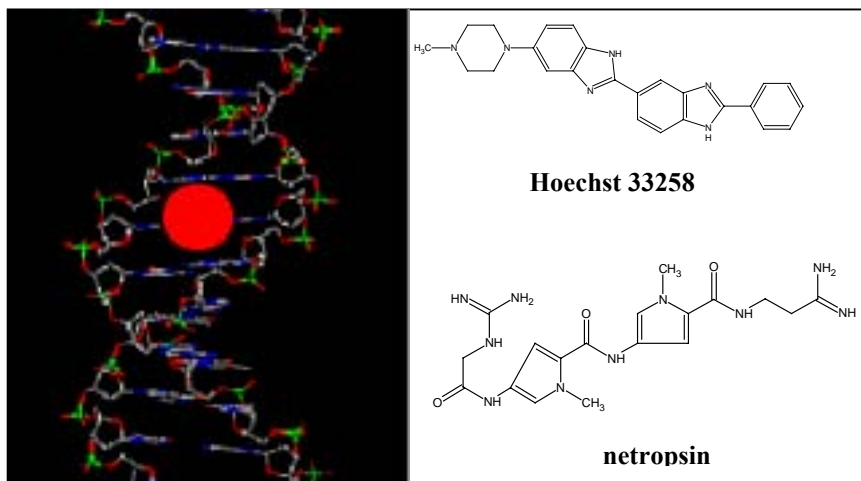


Fig. 8: Example of minor groove binding.

Organic molecules possessing appropriate shape complementarity can bind DNA by insertion within the minor groove of the double helix. Hydrophobic and/or hydrogen bonding are usually important components of this binding process, as well as some electrostatic interaction. The antibiotic netropsin and the fluorescent probe Hoechst 33258 are model groove-binders (Fig. 8). [16, 17].

3. **Intercalation:** Intercalation of a planar ligand between the DNA base pairs.

This mode of association involves the insertion of a planar fused aromatic ring system between the DNA base pairs, leading to significant π -electron overlap. Intercalation is stabilised by stacking interactions, and is therefore less sensitive to ionic strength relative to the two previous binding modes. Favourable π -stacking requires the presence of an extended fused aromatic system as in proflavines, [18] and ethidium bromide (Fig. 9). [19]

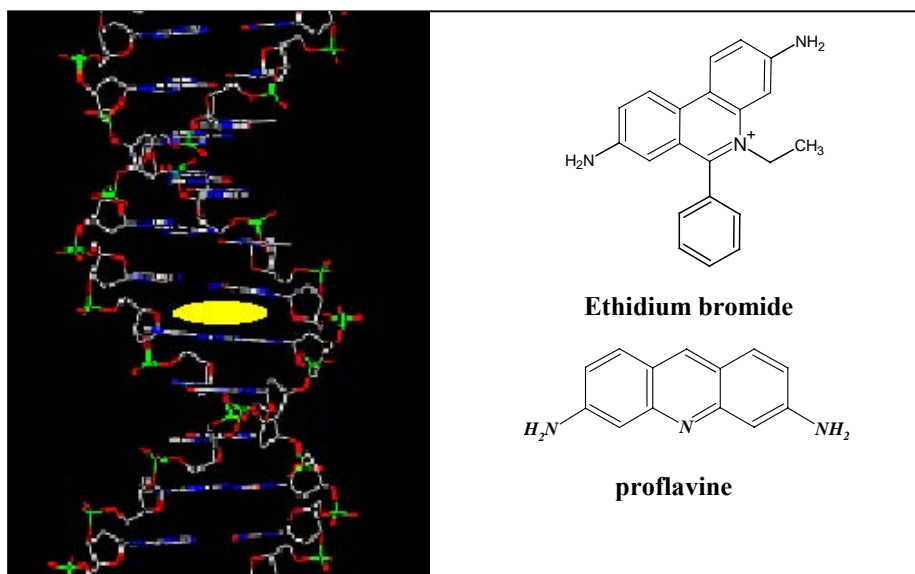


Fig. 9: Example of intercalation process.

1.4 A biotechnological application of molecules interacting with DNA: the delivery of DNA in cells for gene therapy

If in the past few decades the interest for the study of such interactions between synthetic compounds and DNA was mainly focused on the development of intercalating agents of various complexity, the employment of new techniques in the field of gene therapy has recently extended interest to other binding interactions.

Gene therapy, that is a treatment based on correcting, controlling or adding specific sequences of DNA in selected cells, offers tremendous hope for clinical management of chronic and life-threatening diseases. [20]The concept is simple and involves the delivery of a nucleic acid sequence to the target cells in an effort to alter the production of a specific protein, whose expression results in a therapeutic benefit. The entire process is illustrated in Fig. 10.

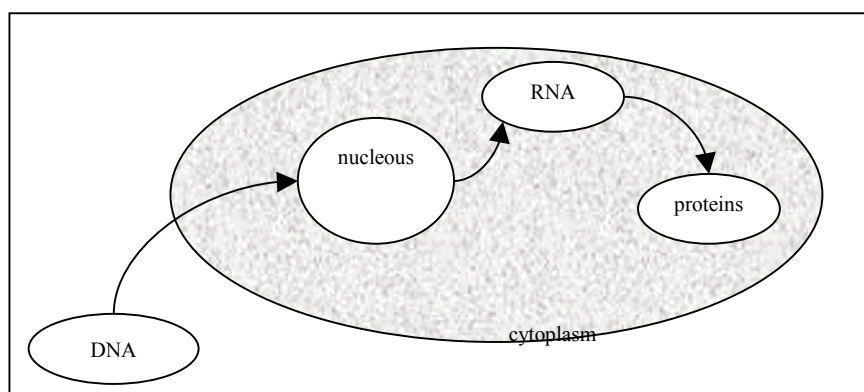


Fig. 10: Scheme of gene therapy processes.

Regardless of whether gene therapy is used to correct a single gene defect, to introduce a gene encoding a protein capable of eliciting a therapeutic response, or in the use of antisense oligonucleotides to disrupt gene function, a prerequisite for effective gene therapy is *efficient delivery of DNA molecules into cells*. To this end, a variety of delivery systems have been developed.

Next to common techniques used for DNA delivery, such as direct microinjection, co-precipitation of DNA with polycations, or through perturbation of the cell membrane by chemical (solvents, detergents, polymers or enzymes) or physical tools, promising results have been obtained by the use of viral vectors. [20] Retroviruses, which replicate themselves by inverting the normal behaviour of the genetic information, have proved to be particularly effective.

A more recent approach to transfer DNA is based on the use of synthetic carriers. [20-23]

Synthetic non-viral vectors for the delivery of plasmid DNA are being developed for gene therapy applications based on the assumption that problems associated with the use of viruses will be difficult to overcome. These problems include antigenicity and a relatively small capacity to carrying genetic information. In addition, it will be difficult to target cells not expressing cell surface receptors required by the virus for binding and entry into the cell. Although the preparation of synthetic vectors has focused on the development of carriers that mimic many viral attributes such as cell binding, membrane fusion triggering and DNA translocating peptides, it would be surprising if these complicated synthetic vectors did not suffer problems similar to those of viral vectors.

One of the attractive features of lipid- and polymer- based systems for DNA delivery is their simplicity. In principle, all that is required is a cationic surface that can bind DNA and reduce repulsion between the biopolymer and the cell membrane, both negatively charged. [24] Obviously, such interactions must not be too strong, otherwise they will hinder the release of DNA in proximity of the cell nucleus. The concept of using lipid-based carriers to deliver DNA to cells resulted from an extensive amount of research on the use of liposomes as drug carriers.

1.5 Interaction between DNA and amphiphilic systems

Amphiphilic systems represent a new class of non-viral vectors for DNA, having the possibility to associate DNA both via electrostatic and hydrophobic interactions. The use of these compounds can eliminate one of the main problems in DNA delivery: the electrostatic repulsion between the cell membrane and DNA, both negatively charged.

The binding of amphiphiles to DNA is co-operative, and become stronger as the concentration of amphiphile increases due to the neutralisation of the most part of the negative charges of the phosphate groups. This phenomenon occurs at various concentration of surfactant,[25] and hydrophobic forces are very important for DNA-surfactant interaction. In fact, with highly hydrophobic cationic surfactant, association occurs at lower concentrations, favourable towards better gene carriers. Kuhn et al. [26] showed that, when the concentration of amphiphilic molecules is low, the counterions preferentially adsorb to the DNA, thus forming a DNA-counterions complex. However, when a critical amount of surfactant is added to the solution, a large number of surfactant molecules simultaneously condense onto DNA strand, and the bound counterions are released back into the solution. This co-operative phenomena is the result of hydrophobic interaction between the hydrocarbon tails of the surfactant monomers.

It is very important to underline that efficient transfection process requires the formation of a small complex, with a very compact structure. The interest towards surfactant molecules as carriers is based on the fact that it seems that they can induce a conformational change in DNA structure, which becomes more compact. Moreover, they can form discrete structures each containing one single DNA molecule of nucleic acid. [27-32]

Amphiphilic systems can be used in different ways to form these complexes. The method of preparation is very important to control the size of the lipid-DNA complex. In Fig. 11, a scheme of the most common methods of preparation is shown. [20]

It has been suggested that lipid-based DNA complexes can be prepared by mixing DNA with preformed cationic liposomes. This initiates an aggregation process resulting in the formation of a heterogeneous group of structures. Careful physical characterisation of cationic liposome-DNA complex structures led Radler et al. to propose a multilamellar structure in which DNA is sandwiched between lipid bilayers.[33] An alternative formulation procedure (Fig. 11, right panel) has been described where a hydrophobic complex is used as an intermediate in the preparation of lipid-DNA particles. This approach relies on the generation of mixed micelles containing detergent, cationic lipids and selected zwitterionic lipids. Under appropriate conditions, cationic lipid-DNA complexes prepared using detergents, spontaneously form intermediate structures that may consist of either monomeric lipids and detergent, or mixed lipid-detergent micelles bound to DNA. Upon dialysis to remove detergent, small particles (<150 nm) are formed. [20]

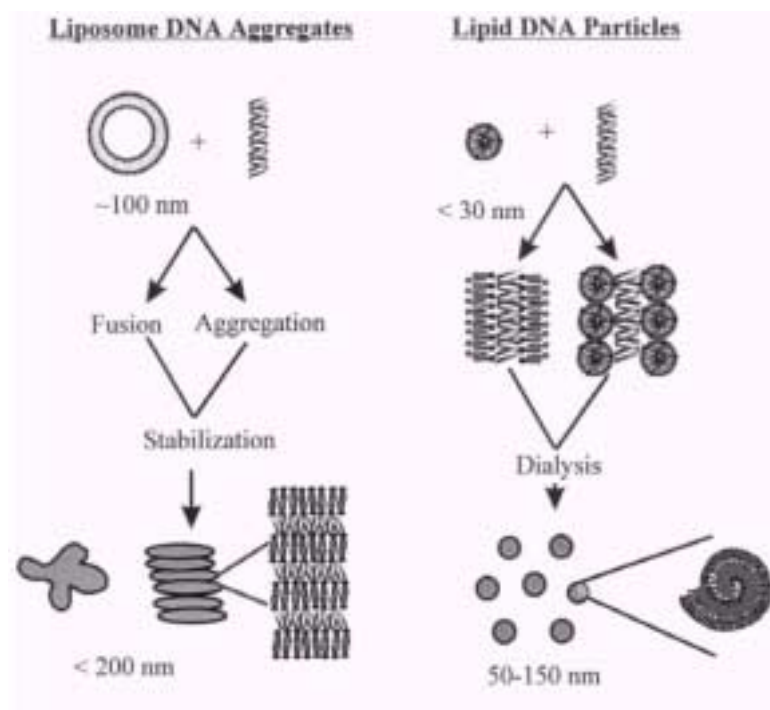


Fig. 11: Possible ways of aggregation in lipid-DNA complexes. [20]

Interaction between DNA and cationic surfactants has been extensively studied in the literature and is most often based on the use of cetyltrimethylammonium bromide (CTABr, Fig. 12) as a model surfactant.

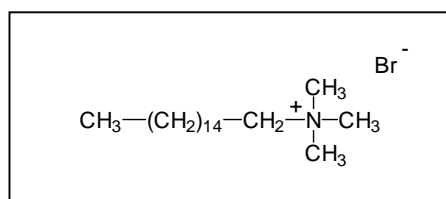


Fig. 12: Structure of CTABr

CTABr is a cationic surfactant able to bind to DNA and induces a modification of the DNA structure, which passes from a linear double helix to the globular form, even at concentration lower than critical micelle concentration (c.m.c.) value. [34]

The nature of the interaction between DNA and CTABr is mostly electrostatic and DNA condensation is a co-operative process. It was observed that binding of cationic surfactants is a reversible process. [23] It was reported that in such interactions the ratio of CTABr to DNA is always less than 1. This is rationalised by comparing the relative sizes of the CTABr polar heads (6.9 Å) to the distance between two phosphate groups in DNA (ca. 5.9 Å). Thus, the polar group of the surfactant is bigger than the distance between charges in DNA and this influences the binding ratio. [27]

Recent studies have also showed condensation of DNA in the presence of zwitterionic amphiphiles such as amine-oxides. Such interactions were studied by spectroscopic methods (fluorescence microscopy and cryo-TEM), and by the use of small angle X-ray scattering (SAXS). It was also observed that the DNA features are very important for the interaction, since large DNA, like T4

fagus DNA (ca.167 Kb) give complexes, whereas smaller DNA (less than 2 Kb) do not. [35, 36]

1.6 Techniques to investigate DNA-surfactants interactions

Many techniques have been used to study DNA-surfactant interactions, mostly relying on the conformational changes in DNA structure induced by such interactions. Amongst these techniques, microscopy, kinetic methods, radiation scattering like dynamic light scattering (DLS), small angle neutron scattering (SANS), small angle X ray scattering (SAXS), [36, 37] fluorescence and UV spectroscopy, circular dichroism (CD), [36, 38] potentiometry, microcalorimetry [30] and gel electrophoresis must be mentioned. [39, 40]

In particular, the use of spectroscopic techniques for the study of biomacromolecules is an area of rapidly growing interest. The use of optical techniques has several attractive features in that measurements can be performed under ambient conditions. As a highly directional probe, optical techniques allow the possibility of *in situ*, non-destructive analysis, which can be used to provide an insight into the structure, dynamics, and interactions of biomolecules. Such information is crucial in order to fully understand the contribution of macromolecules to the biology of the cell. It is also of great importance to investigate changes in the structure and dynamics of biomolecules upon variation of their environment, since they are especially sensitive to changes in the pH, temperature, and solvent polarity. A variety of spectroscopic techniques are currently used to probe biomolecules in solution or at surfaces and give information about different aspects of their structure and stability. A brief overview of some of the most useful spectroscopic techniques is given here.

UV-Visible absorption spectroscopy, being dependent on the electronic structure and the environment of the absorbing chromophore, allows the characterisation or the identification of molecules. Some wavelengths are particularly useful in the study of biomolecules. Amino acids have a strong absorbance around 210 nm, which is frequently used to detect peptides, while nucleic acids absorb strongly at 260 nm. The intrinsic biopolymer chromophores can thus act as reporter molecules of various environmental effects. The most important environmental factors affecting the absorption spectra are the pH, the solvent polarity, and orientational effects. [41] Changes in solvent polarity also often induce changes in the absorption spectrum, in terms of energy, intensity, and shape of the absorption band. These changes are a result of physical intermolecular solute-solvent interactions. [42] The relative geometry of neighbouring chromophore molecules also has an influence on the spectrum. An example is the hypochromicity of nucleic acids. A solution of free nucleotides has a higher absorbance (at 260 nm) than an identical concentration of nucleotides assembled in a single-strand polynucleotide. The single-strand, in turn, has a higher absorbance than a double-stranded DNA helix. [3] Therefore, absorbance can be used to monitor the assembly or melting of DNA strands.

Fluorescence spectroscopy also allows the characterisation or the identification of chromophores. Since most components of biopolymers are non-fluorescent, extrinsic fluorophores are often linked to biomolecules for structural and functional studies. Fluorescence spectra are even more sensitive to environmental effects than absorption spectra. Spectra are strongly affected by the exposure to solvent or the presence of quenchers in the solution. DNA is often detected using fluorescent intercalators, such as acridine orange or ethidium bromide. [42]

Circular Dichroism (CD) spectra, in which the difference in the molar extinction coefficients of left and right circularly polarised light are plotted as a

function of the wavelength, reflect the structure of chiral molecules and is widely used for studying chiral biopolymers, such as proteins and nucleic acids. In nucleic acids, the only chiral component is the pentose sugar. Upon assembly of the nucleotides in polynucleotides and then into double-stranded DNA, the asymmetry of the system increases and hence the strength of the CD spectrum also increases. Differences have been reported in CD spectra due to variation of the nucleotide sequence, G and C nucleotide content, and the stacking conformation of the bases in double-stranded DNA. [43]

1.7 Aim of the work

Although lipid-based DNA delivery systems are being assessed in gene therapy clinical trials, they are still less effective than viral vectors, thus limiting their use. [44] In principle, their synthetic origin, renders modification of their structure to increase the efficiency of such systems possible, but little information exists on the relationship between amphiphile structure transfection efficiency.

The aim of the present work is to contribute to the investigation of the driving forces for the formation of DNA-lipids complexes. To this end, new synthetic surfactants were prepared to have a number of amphiphilic systems widely differing in structure and properties. Considering that anionic surfactants are not able to interact with DNA, only cationic and zwitterionic compounds were considered. With the exception of cetyltrimethylammonium bromide (CTABr), dodecyldimethylamine-oxide (DDAO), dodecyldimethylpropane-sulfonate (SB3-12) and dodecyltrimethylcarboxybetaine (CB1-12) that are commercially available, all other amphiphilic systems used in this work were newly synthesised, purified and characterised. The structures of cationic and zwitterionic surfactants that have been used is reported in Fig.13 and Fig.14 respectively.

Concerning the cationic surfactants, three single-chain systems were considered: cetyltributylammonium bromide (CTBABr) and

paradodecyloxybenzil-trimethylammonium bromide (pDOTABr) are structural analogues of CTABr, in which the size of the head group and the nature of the chain are varied. These changes in the surfactant structure have often shown to be important in the mechanism of aggregation. [45, 46]

Gemini surfactants reported in Fig.13 were synthesised using the same synthetic scheme, but varying the length and the position of the hydrophobic chain. We have already shown by the use of kinetic methods how these variations in structure give aggregates that differ in polarity and amount of water at the microinterface. [47] Recently, it was found that gemini surfactants are, in some cases, good non-viral vectors for DNA transfection. [48]

Finally, a family of the twin-chain amphiphiles was synthesised. In the literature, systems like colin-1616 show transfection ability, probably due to the possibility of such molecules to loose one chain by esterase and thus modulate the release of DNA at the nucleus. [23] Structural changes of this basic structure were performed in terms of length of the chains.

Zwitterionic surfactants, such as amine-oxides, sulfobetaines and carboxybetaines were also considered. In the case of amine-oxides, single chain and gemini surfactants were used, and changes in the nature of the hydrophobic moiety were performed, e.g. in the case of paradodecyloxybenzil-dimethylamine oxide (pDOAO).

structure	name
$\text{CH}_3-(\text{CH}_2)_{14}-\text{CH}_2-\overset{\text{R}}{\underset{\text{R}}{\text{N}^+}} \text{Br}^-$	A) R= -CH ₃ CTABr B) R= -CH ₂ (CH ₂) ₂ CH ₃ CTBABr
$\text{CH}_3-(\text{CH}_2)_{10}-\text{CH}_2-\text{O}-\text{C}_6\text{H}_4-\text{CH}_2-\overset{\text{CH}_3}{\underset{\text{CH}_3}{\text{N}^+}} \text{Br}^-$	pDOTABr
$\text{Br}^- \overset{\text{CH}_3}{\underset{\text{CH}_3}{\text{N}^+}}-\text{CH}_2-\text{C}_6\text{H}_2(\text{R})_2-\text{CH}_2-\overset{\text{CH}_3}{\underset{\text{CH}_3}{\text{N}^+}}-\text{R}' \text{Br}^-$	A) R=-OCH ₃ , R'=-CH ₂ (CH ₂) ₁₀ CH ₃ pXMo(DDA)₂ B) R=-OCH ₃ , R'=-CH ₂ (CH ₂) ₁₂ CH ₃ pXMo(MDA)₂ C) R=-OCH ₃ , R'=-CH ₂ (CH ₂) ₁₄ CH ₃ pXMo(CDA)₂ D) R=-CH ₂ (CH ₂) ₁₀ CH ₃ , R'=OCH ₃ pXDo(TA)₂
$\text{CH}_2-\overset{\text{O}}{\parallel}{\text{C}}-\text{O}-\text{CH}_2-\overset{\text{CH}_3}{\underset{\text{CH}_3}{\text{N}^+}}-\text{CH}_2-\text{CH}_2-\overset{\text{CH}_3}{\underset{\text{CH}_3}{\text{N}^+}} \text{Br}^-$ $\begin{array}{c} \\ (\text{CH}_2)_n \\ \\ \text{CH}_3 \end{array}$ $\begin{array}{c} \\ \text{CH}_2 \\ \\ (\text{CH}_2)_m \\ \\ \text{CH}_3 \end{array}$	A) n=9, m=10 C12-12 B) n=9, m=14 C12-16 C) n=13, m=14 C16-16

Fig. 13: Structures of the cationic surfactants.

structure	name
$\text{CH}_3-(\text{CH}_2)_{10}-\text{CH}_2-\overset{\text{CH}_3}{\underset{\text{CH}_3}{\overset{+}{\text{N}}-\text{O}^-}}$	DDAO
$\text{CH}_3-(\text{CH}_2)_{10}-\text{CH}_2-\text{O}-\text{C}_6\text{H}_4-\text{CH}_2-\overset{\text{CH}_3}{\underset{\text{CH}_3}{\overset{+}{\text{N}}-\text{O}^-}}$	pDOAO
$\begin{array}{c} \text{CH}_3 \\ \\ \text{O}^- - \text{N} - \text{CH}_2 - (\text{CH}_2)_4 - \text{CH}_2 - \text{N} - \text{O}^- \\ \qquad \qquad \qquad \\ \text{CH}_2 \qquad \qquad \qquad \text{CH}_2 \\ \qquad \qquad \qquad \\ (\text{CH}_2)_{10} \qquad \qquad (\text{CH}_2)_{10} \\ \qquad \qquad \qquad \\ \text{CH}_3 \qquad \qquad \qquad \text{CH}_3 \end{array}$	GemAO
$\text{CH}_3-(\text{CH}_2)_{10}-\text{CH}_2-\overset{\text{CH}_3}{\underset{\text{CH}_3}{\overset{+}{\text{N}}}}-(\text{CH}_2)_3-\text{SO}_3^-$	SB3-12
$\text{CH}_3-(\text{CH}_2)_{10}-\text{CH}_2-\overset{\text{CH}_3}{\underset{\text{CH}_3}{\overset{+}{\text{N}}}}-\text{CH}_2-\text{COO}^-$	CB1-12

Fig. 14: Structures of the zwitterionic surfactants.

The studies of the interactions between DNA and the non-micellisable analogue molecules (reported in Fig.15) were performed, as control experiments. The comparison with surfactants gives information about the importance of the amphiphilic nature in the formation of complexes with DNA.

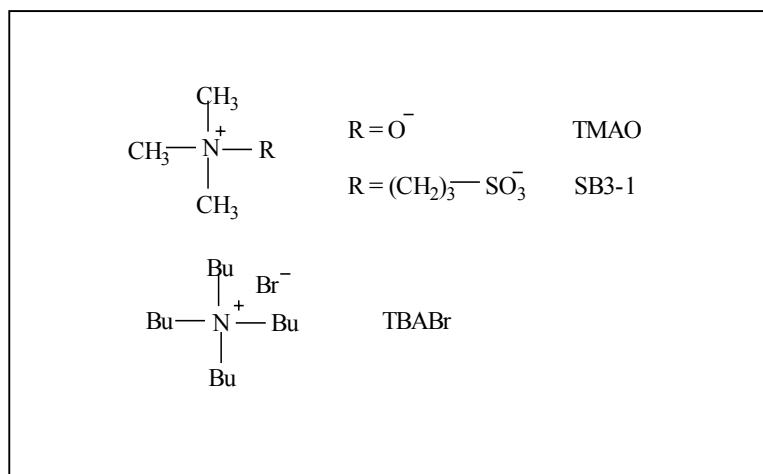


Fig. 15: Non-micellisable systems that have been studied.

Calf Thymus DNA (CT-DNA) was used as the DNA model. It has a molecular weight of ca. 8.6×10^6 Dalton, corresponding to about 13 Kb. CT-DNA is rich in A-T sequences, guanine and cytosine represent 42% of composition. The study of DNA-surfactants interaction was carried out by the use of two very useful spectroscopic techniques, circular dichroism and fluorescence.

In this work, a new approach using molecular modelling to better understand the features of the interaction was undertaken. The results were compared to the experimental data.

Chapters 2, 3, 4 and 5 report the results obtained with the use of Circular Dichroism, Molecular Modelling and Fluorescence Spectroscopy. The theoretical basis of these techniques and their use in these studies will be also briefly described. The overall discussion and the perspectives for future applications represent the content of Chapter 6. Finally, materials and methods, and the synthetic procedures are described in Chapter 7.

REFERENCES

- [1] H. Ringsdorf, B.Schlarb and J. Venzmer, *Angew. Chemie Int. Ed. in English*, **1998**, 27, 113.
- [2] D.L. Nelson and M.M. Cox, "*I Principi di Biochimica di Lenhinger*", 3rd Ed., Zanichelli ed. **2002**.
- [3] L.Streyer, *Biochimica*, Zanichelli ed., **1996**, 919-925.
- [4] T. M. Devlin, *Biochimica con Aspetti Clinici*, 3rd ed, Ed.Idelson-Gnocchi, **1997**, 549.
- [5] H. Dugas, *Bioorganic Chemistry*, Springer ed, **1996**,142.
- [6] K. T. Dugas, *Chem. & Ind.*, **1984**, 738.
- [7] K.T. Duglas, *Chem. & Ind.*, **1984**, 766.
- [8] B. Rosenberg, J. Van Camp, J. Trosko and V.H. Mansour, *Nature* (London), **1969**, 223, 385.
- [9] D. Leòn, C. Garbey-Jaureguiberry, J.B. LePecq, *Tetrahedron Lett.*, **1985**, 26, 4929.
- [10] G.J. Atwell, G.M. Stewart, W. Leupin and W.A. Denny, *J. Am. Chem. Soc.*, **1985**, 107, 4335.
- [11] G.J. Atwell, B.C. Baguley, D. Wilmanska and W.A. Denny, *J. Med. Chem.*, **1986**, 29, 69.
- [12] J.W. Lown, *Acc. Chem. Res.*, **1982**, 15, 381.
- [13] R.P. Herzberg and P.B. Dervan, *J. Am. Chem. Soc.*, **1982**, 104, 313.
- [14] H.P. Spielman, D.E. Wemmer, J.P. Jacobsen, *Biochemistry*, **1995**, 34, 8542.
- [15] J. Kelly, A. Tossi, D. McConnell, Oh Uigin, *Nucl. Acids Res.*, **1985**, 13, 6017.
- [16] J.C. Sutherland, J.F. Duval, K.P. Griffin, *Biochemistry*, **1978**, 17 (24), 5088.
- [17] H. Görner, *Photochem. Photobiol.*, **2001**, 73(4), 339.
- [18] L.S. Lerman, *J. Mol. Biol.*, **1961**, 3, 18.
- [19] J.B. LePecq and C. Paoletti, *J. Mol. Biol.*, **1967**, 27, 87.

- [20] M.B. Bally, Y-P. Zhang, F.M.P. Wong, S. Kong, E. Wasan, D.L. Reimer, *Adv. Drug. Del. Reviews*, **1997**, 24, 275.
- [21] J-P. Beher, *Acc. Chem. Res.*, **1993**, 26, 274.
- [22] D.D. Lasic, N.S. Templeton, *Adv. Drug. Del. Review*, **1996**, 20, 221.
- [23] S. Bhattacharja and S.S. Mandal, *Biochemistry*, **1998**, 37, 7764.
- [24] F.M. Wang, D.L. Reimer and M.B. Bally, *Biochemistry*, **1996**, 35, 5756.
- [25] S. M. Mel'nikov, V.G. Sergeyev and K. Yoshikawa, *J. Am. Chem. Soc.*, **1995**, 117, 9951.
- [26] P.S. Kuhn, M.C. Barbosa, Y. Levin, *Physica A*, **2000**, 283, 113.
- [27] P. Pinnaduwege, L. Schmitt, L. Huang, *Biochim. Biophys. Acta*, **1989**, 985, 33.
- [28] P.S. Kuhn, Y. Levin, M.C. Barbosa, *Physica A*, **1999**, 269, 278.
- [29] S. Maulik, P. Dutta, D.K. Chattoraj, S.P. Moulik, *Colloids and Surfaces B: Biointerfaces*, **1998**, 11, 1.
- [30] S. Maulik, D.K. Chattoraj, S.P. Moulik, *Colloids and Surfaces B: Biointerfaces*, **1998**, 11, 57.
- [31] S.Z. Bathaie, A.A. Moosavi-Movahedi, A.A. Saboury, *Nucleic Acids Research*, **1999**, 27, 4, 1001.
- [32] K. Eskilsson, C. Leal, B. Lindman, M. Miguel, T. Nylander, *Langmuir*, **2001**, 17, 1666.
- [33] J. O. Radler, I. Koltover, T. Salditt, C.R. Safinya, *Science*, **1997**, 275, 810.
- [34] J.P. Clamm, S. Bernacchi, C. Vuilleumier, G. Duportail, Y. Mély, *Biochim. Biophys. Acta*, **2000**, 1467, 347.
- [35] H. Zhang, P.L. Dubin, J.I. Kaplan, *Langmuir*, **1991**, 7, 2103.
- [36] Y.S. Mel'nikova, B. Lindman, *Langmuir*, **2000**, 16, 5871.
- [37] A.V. Gorelov, E.D. Kudryashov, J-C. Jacquier, D. M. Mcloughlin, K.A. Dawson, *Physica A*, **1998**, 249, 216.
- [38] S.M. Mel'nikov, R. Dias, Y.S. Mel'nikova, E.F. Marques, M.G. Miguel, B. Lindman, *FEBS letters*, **1999**, 453, 113.

- [39] Z. Wang, D. Liu, S. Dong, *Biophysical Chem.*, **2000**, 87, 179.
- [40] S.M. Mel'nikov, V.S. Sergeev, K. Yoshikawa, *J. Am. Chem. Soc.*, **1995**, 117, 9951.
- [41] D. Sheehan, *Physical Biochemistry: Principle and Applications*, **2000**, Chichester, Wiley.
- [42] C. Reichardt, *Solvents and Solvent Effect in Organic Chemistry*, **1990**, VCH, New York.
- [43] C. R. Cantor and P.R. Schimmel, *Biophysical Chemistry: Techniques for the Study of Biological Structure and Function*, Vol.II, **1980**, New York, W.H. Freeman and Co., 430.
- [44] M.B. Bally, P. Harvie, F.M.P. Wong, S. Kong, E.K. Wasan, D.L. Reimer, *Advanced Drug Delivery Review*, **1999**, 38, 291.
- [45] R. Germani, P.P. Ponti, T. Romeo, G. Savelli, N. Spreti, G. Cerichelli, L. Lucchetti, G. Mancini, C.A. Bunton, *J. Phys. Org. Chem.*, **1989**, 2, 553.
- [46] L. Brinchi, R. Germani, G. Savelli and L. Marte, *Journal of Colloid and Interface Science*, **2003**, 262, 290,.
- [47] L. Brinchi, R. Germani, L. Goracci, G. Savelli and C.A. Bunton, *Langmuir*, **2002**, 18, 7821.
- [48] P. Camilleri, A. Kremer, A.J. Edwards, O. Jenkins, K.H. Jennings, .I. Marshall, C. McGregor, W. Neville, S.Q. Rice, R.J. Smith, M.J. Wilkinson, A.J. Kirby, *Chem. Commun.*, **2000**, 1253.

CHAPTER 2

CIRCULAR DICHROISM SPECTROSCOPY

2.1 Introduction

Circular Dichroism is a spectroscopic technique based on the use of a linearly polarised beam of light, which is composed of a right-hand and a left-hand beam of circularly polarised light. The difference in the interaction of optically active molecules with the right-hand and the left-hand polarised light in the absence of a magnetic field are used. The optical activity is generated by the rotation of the plane of the linearly polarised light. If it is related to a difference in the refraction index of the two components of the circular polarised light, the phenomenon is called Optical Rotatory Dispersion (ORD). On the other hand, if it is due to the different absorption of the two components the phenomenon is called Circular Dichroism.

Considering the phenomenon of Circular Dichroism from a mathematical point of view, the electric field vector can be expressed as follows (eq. 1):

$$E_{\pm} = E_0 (i + ij)\exp[2\pi i(vt - z/\lambda)] \quad (1)$$

where + and - refer to the two beams of the circular (right and left) polarised light respectively, i and j are the x and y vectors, E_0 is the amplitude of the wavelength and z represents the direction of propagation, while v e λ are the frequency and the wavelength of the light, respectively.

When light goes through an optically active substance, the two components of the circular polarised light not only move with different speed (thus λ_L and λ_R are different), but they are also absorbed to different extent and the electromagnetic radiation results elliptically polarised. When the electric

field vectors of the two circular components are in the same direction, the sum of their amplitudes represents the major semiaxis of the ellipse, while when they are in opposite direction their difference gives the minor semiaxis, (see Fig. 1).

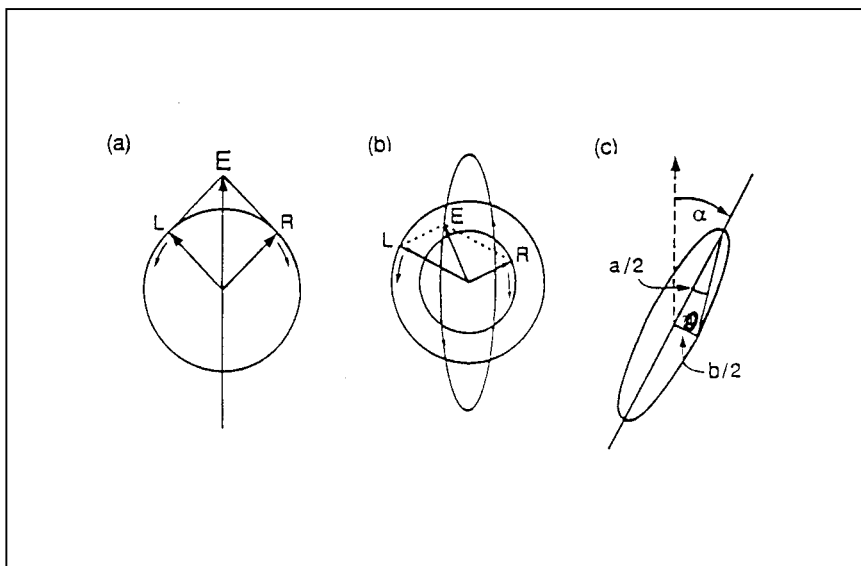


Fig.1: (a) Plane of the linear polarized light where the two circular polarized components are reported. (b) Formation of the elliptical polarized light by the two circular polarized components of different amplitude. (c) The two semiaxes form the θ angle that represents the ellipticity and that is proportional to the circular dichroism, while the α angle represents the optical rotation. It can be shown that when CD exists, optical rotation must exist as well, and they are directly related by a Kronig-Kramers transformation.

If I_0 is the intensity of the incident light and I that of the outgoing radiation, the absorbance calculated by the Lambert-Beer equation is:

$$A = \epsilon cl = \log(I_0/I) \quad (2)$$

where ϵ represents the molar extinction coefficient, c the concentration of the solution and l the optical path length. As mentioned above, considering that in an optically active medium the right-hand and the left-hand components of the circular polarised light are absorbed differently, the equation becomes:

$$\Delta A = A_L - A_R = (\epsilon_L - \epsilon_R)cl = \Delta\epsilon cl \quad (3)$$

where A_L and A_R are the absorbances of the left-hand and of the right-hand circular components, respectively.

In terms of molar ellipticity, the circular dichroism is expressed as:

$$[\vartheta] = \frac{100\vartheta}{cl} \quad (4)$$

By combining equation (4) with the definition of $\Delta\epsilon$, it is possible to approximate the molar ellipticity in a form that is independent of the concentration and of the optical path length (eq. 5):

$$[\theta] = 3298\Delta\epsilon \quad (5)$$

This expression permits to report the circular dichroism spectra as function of the molar ellipticity rather than as a variation of the ϵ values. The circular dichroism spectra are constituted by a series of bands that correspond to specific transitions from the ground-state to an excited state. Each band is characterised by its transition energy, its the shape, and the intensity expressed as $\Delta\epsilon$.

These bands present both positive and negative peaks, depending on the component of the polarised light that is more strongly absorbed. The most part of the bands observed in the CD spectrum of a complex molecule consists of a unresolved sum of vibrational transitions. [1]

2.2 Circular Dichroism of nucleic acids

Nucleic acids are chiral compounds apt to be investigated by the use of Circular Dichroism. With this technique it is possible to observe the formation

and modification of chromophores as well as variations in the secondary structure. [2-6]

Phosphate groups in DNA have electronic transitions only at high energy (wavelengths below 170 nm), whereas deoxyribose units present a weak absorption band located around 190 nm. Thus, the most significant chromophores of DNA are the nitrogen bases that generate moderately intense electronic transitions in the range 180-300 nm. These are allowed π - π^* transitions and are very intense. Also, weakly allowed n - π^* transitions are present, but their amplitude is small and thus more difficult to detect. The nitrogen bases, being planar, do not show intrinsic circular dichroism. Thus, the asymmetry of nucleic acids is due to the presence of the chiral sugar generating a small absorption signal, and the formation of a double helical structure induces a super-asymmetry through the interaction between bases. This gives an intense band that corresponds to the overall electronic transition of the bases.

Taking such features into account and considering that the maximum value of absorption for DNA is at 260 nm, studies concerning structural changes of DNA are performed of wavelength between 210 and 320 nm.

Circular Dichroism has proven to be very useful technique to determine modification in the secondary structure of DNA in solution. Indeed, DNA can assume different conformations, depending on the composition of the bases, the temperature, and the solvent.

The B form of DNA (from Calf Thymus) in aqueous solution at neutral pH and at room temperature, presents a CD spectrum with a maximum around 277 nm, a negative band centred near 240 nm, and an inversion point around 260 nm.

An example of a CD spectrum of CT-DNA is reported in Fig. 2.

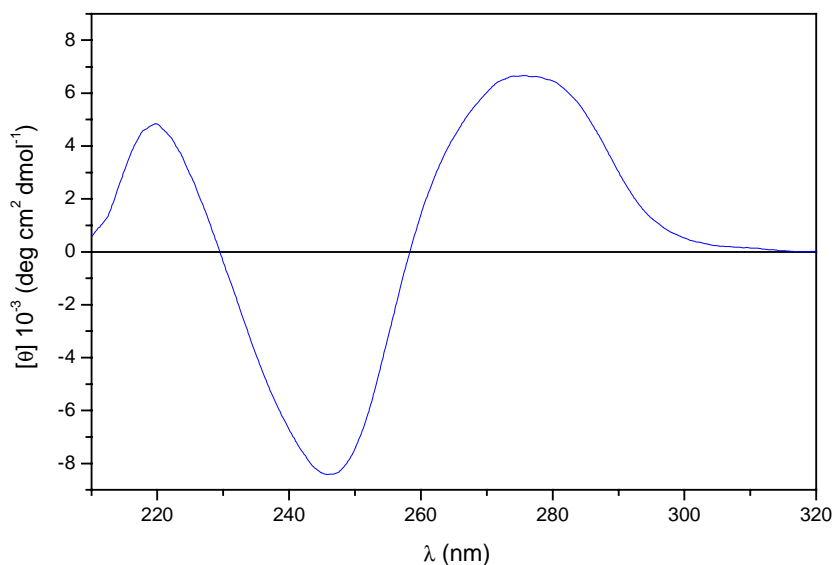


Fig. 2: CD spectrum of calf thymus DNA (pH= 7.0, T= 25.0 °C).

2.3 CD Instrumentation

The instrument for circular dichroism is a spectropolarimeter: a source of light emits a radiation that passes first through a monochromator and then through a polariser. The resulting polarised light passes through the cell containing the optically active substance that can rotate the plane of the polarised light. This rotation is then compensated by the rotation of the analyser and the radiation arrives to the detector that gives the final spectrum. (Fig. 3)

At the beginning the direction of the polarisation of the polariser is perpendicular to that of the analyser and one of the two components is rotated of an α angle to minimise the transmitted light after that it has passed the optically active substance. The measure of α depends on the number of chiral molecules in the sample and thus it is proportional to the optical path. The specific rotation is thus defined as: [7,8]

$$[\alpha] = \frac{\alpha}{l \times c} \quad (6)$$

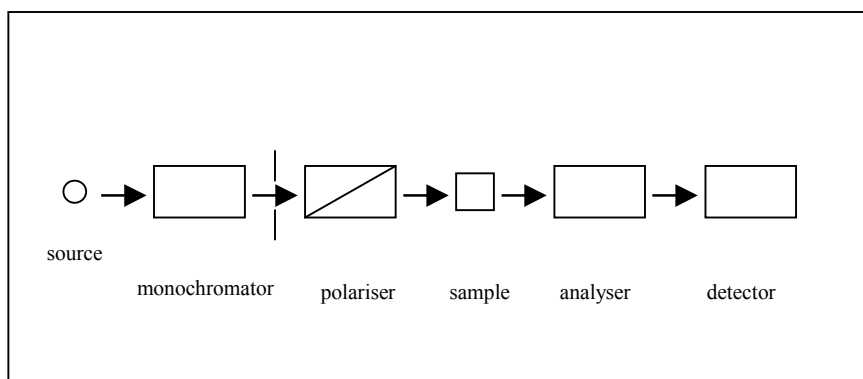


Fig. 3: Scheme of a spectropolarimeter.

2.4 CD analysis of the DNA-surfactants interaction

As previously mentioned, Circular Dichroism is a very useful technique for studying the conformational variations of biopolymers such as proteins, DNA, and RNA. Circular Dichroism has already been applied used to the detection of the conformational changes in DNA structure induced by additives in the solution. For example, it was reported that upon incremental addition of CTABr to calf thymus DNA, the intensity ($\Delta\epsilon$) of both positive and negative bands decreases. However, the overall shape of the spectrum is maintained. This suggests that the binding of DNA with CTABr induces certain conformational changes that are correlated to helix unwinding. [9] Changes in the intensity of the CD peak at 278 nm have been associated to the alteration of hydration of the helix in the vicinity of the phosphate or ionic strength. [10] It was also reported that the addition of sodium dodecylsulfate (SDS) to a solution containing a cationic surfactant-DNA complex leads to a gradual and complete recovery of the CD spectral curve. Thus, the addition of anionic surfactants to cationic amphiphile-DNA complexes permits a recovery of the CD spectrum of native DNA. [11]

2.5 Results and discussion

2.5.1 Effect of pH on DNA structure

A preliminary study was undertaken to verify whether the DNA structure undergoes an important structural variation over a defined range of pH covering the physiological range (pH 5 – 8). At higher or lower pH values, denaturation of DNA may take place. It is known that, in this range of pH, DNA is very stable and any variations in its conformation are a result of interaction with specific molecules like salts or surfactants. [12] To confirm this information, the CD spectra for DNA at three different pH values are reported in Fig. 4.

As shown, only minor variation in the observed the spectra and maximum value of the molar ellipticity $[\theta]$ are observed at 273.8 nm (λ_{\max}). This λ_{\max} value is related to the native form of DNA.

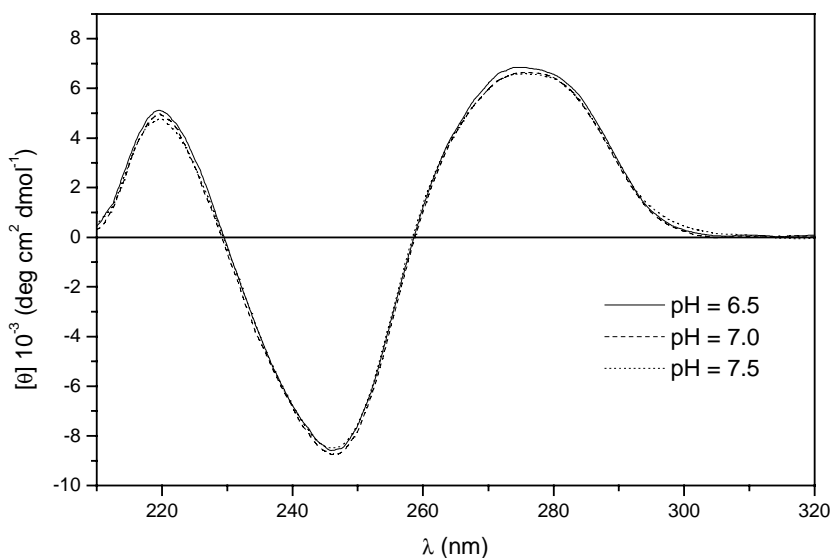


Fig. 4: Effect of pH on aqueous solution of DNA. $[\text{DNA}] = 2.0 \times 10^{-5} \text{ M}$; $T = 25.0 \text{ }^\circ\text{C}$.

2.5.2 Effect of ammonium salts on DNA CD spectra

A study on the effect of the cationic surfactant CTABr on DNA structure was performed by CD. Reference spectra were obtained with identical solutions but omitting DNA. In Fig. 5 the results at pH=7.1 at various surfactant concentration are shown. A concentration dependent shift of the λ_{\max} value and a change of the intensity was observed, indicating the interaction of DNA with the surfactant molecules in aqueous solution. These results are in agreement with the studies mentioned in the previous paragraph, where the variation of the intensity in the CD spectrum in function of the concentration of CTABr is associated to the unwinding of the double helix of DNA. [13]

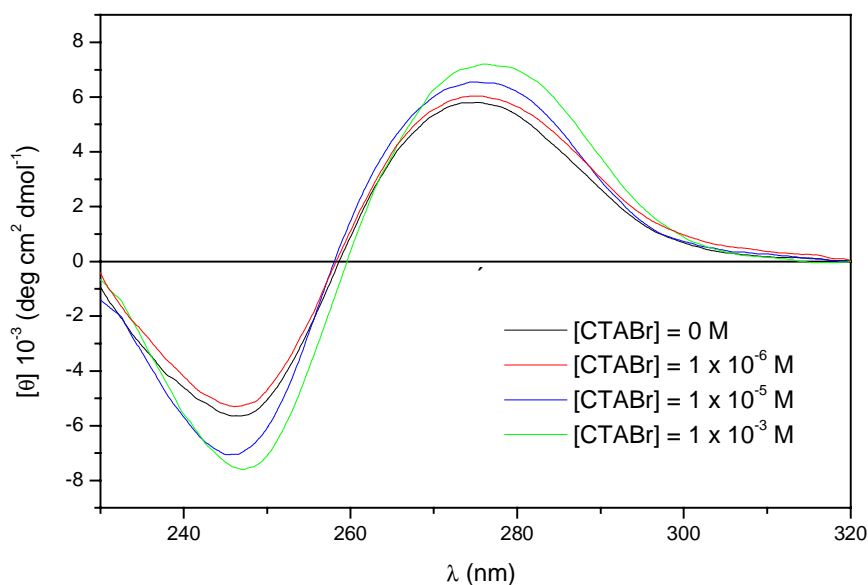


Fig. 5: Effect of CTABr on CD spectra of CT-DNA in aqueous solution. [DNA] = 2.0×10^{-5} M; T = 25.0°C; pH = 7.1

The study was extended to cetyltributyl-ammonium bromide (CTBABr), a cationic surfactant having the same hydrophobic moiety, but with a larger and more hydrophobic head group. It has been shown that the charge density and the hydrophobic feature of the ammonium in CTBABr can change its

interaction with the Br^- counterion and, consequently, could also influence the interaction with DNA. [14] Results obtained with increasing surfactant concentration of CTBABr but at constant DNA concentration are reported in Fig. 6.

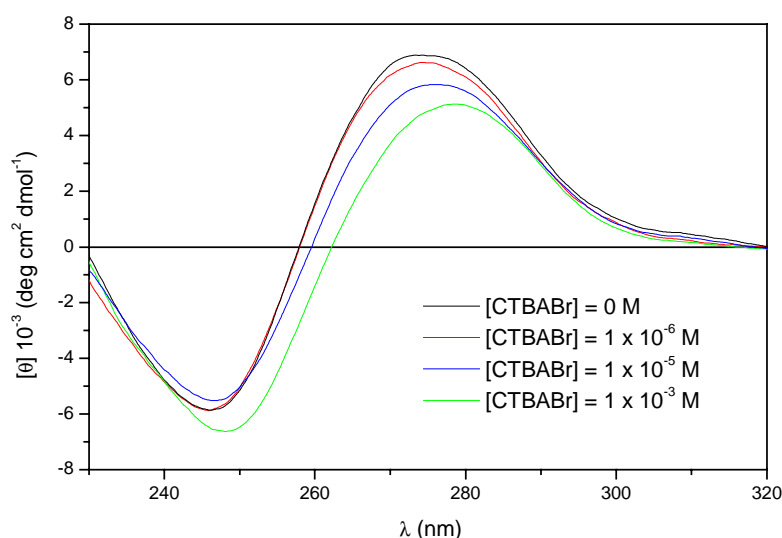


Fig. 6: Effect of CTBABr on CD spectra of CT-DNA in aqueous solution. [DNA] = 2.0×10^{-5} M; T = 25.0 °C; pH = 7.1.

Increasing concentrations of CTBABr caused a bathochromic shift to longer wavelength similarly to what is observed with CTABr, but in this case a decrease in the maximum intensity is also observed. In order to obtain more information on the nature of the interactions between DNA and surfactants, the role of the hydrophobic moiety was also considered. To this end, a simple ammonium salt as tetrabutylammonium-bromide (TBABr), unable to give microaggregates, was used. Circular Dichroism spectra at two different salt concentrations are reported in Fig. 7. It can be observed that in the range 1×10^{-6} M and 1×10^{-3} M salt concentration, the overall contour and the intensity of the spectra does not change, and are coincident with the spectra of native DNA in aqueous solution. These results concur in implying that interactions of amphiphiles with DNA are a synergetic effect due to the presence both of polar ammonium groups and hydrophobic tails.

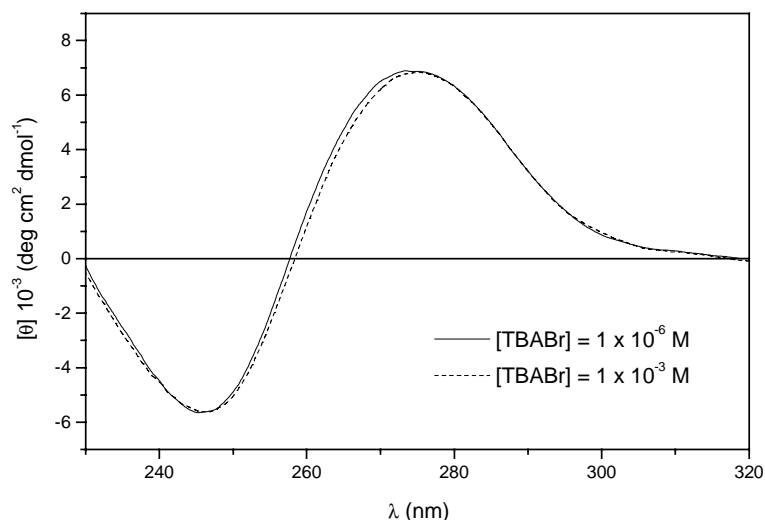


Fig. 7: Effect of TBABr on the CD spectra of CT-DNA in aqueous solution. $[DNA] = 2.0 \times 10^{-5} M$; $T = 25.0 \text{ }^\circ\text{C}$; $\text{pH} = 7.1$.

In Fig. 8, variations of λ_{max} (Tables 1–3, Appendix I) vs. logarithmic value of the additive concentration are reported for the three systems investigated.

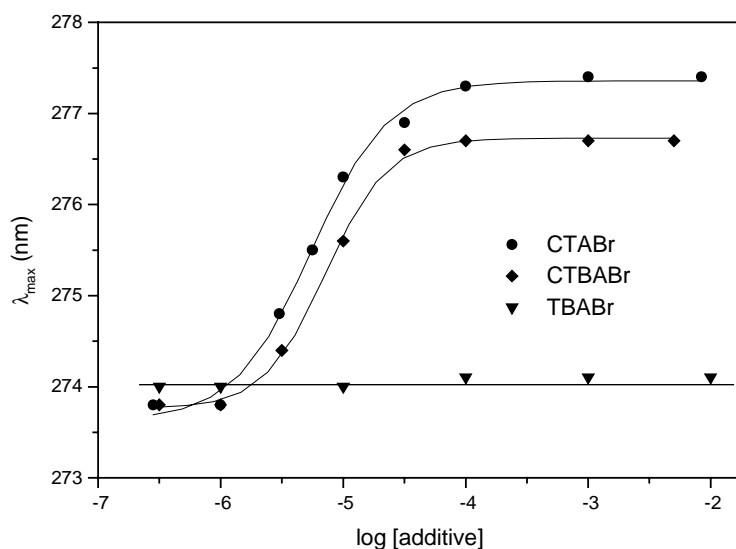


Fig. 8: Variation of λ_{max} as a function of concentration of additive. $[DNA] = 2.0 \times 10^{-5} M$; $T = 25.0 \text{ }^\circ\text{C}$; $\text{pH} = 7.1$.

The logarithmic scale is useful to better represent the behaviour of the transition. These three systems were investigated also at different pH values (Tables 4 – 6, Appendix I), in the presence of DNA and over the physiological

pH range. Similar results were obtained, confirming that the interaction of such systems with DNA is independent of pH.

For CTABr and CTBABr, shifts in λ_{\max} from the values related to the native form of DNA to longer wavelength upon increasing in the surfactant concentration were observed. Conversely, no variation occurred in the case of TBABr. Particularly, the behaviour of CTABr and CTBABr confirm the presence of a co-operative transition that takes place at a concentration of surfactant ca. $\cong 3 \times 10^{-6}$ M, called the critical concentration of aggregation. This sigmoidal behaviour reaches a plateau at concentrations of surfactant of ca. 1×10^{-4} M.

Measurements of surface tension (Tables 1 and 2, Appendix II) of aqueous solution of CTABr, both in absence and in the presence of DNA, give almost the same values of c.m.c. (8×10^{-4} M and 9×10^{-4} M, respectively), showing that the presence of DNA does not have any effect on the c.m.c. of this surfactant. This additional evidence, and the fact that the critical concentration of aggregation for CTABr (i.e. the concentration at which interaction with DNA occurs) is about two fold lower than the c.m.c., confirm that CTABr induces a modification in the structure of DNA before the formation of micelles occurs. Similar conclusions were reached in the case of CTBABr, which has a c.m.c. in water of 2.8×10^{-4} M.

The modification in DNA structure induced by CTABr and CTBABr can be rationalised by assuming that the globular form is responsible for the shift toward higher values of λ_{\max} , and that the native DNA structure exists at lower concentration of surfactant. In agreement with this hypothesis, a non-micellisable system such as TBABr showed no effect upon the DNA structure over the same concentration range used for CTABr and CTBABr. The presence of the hydrophobic chain is thus essential to allow interactions to take place, and this indicates that the nature of the interaction is both electrostatic and hydrophobic.

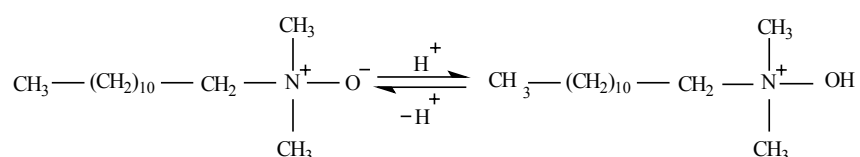
2.5.3 Interactions between DNA and zwitterionic systems

Considering the importance of charged polar head groups in the DNA-surfactant interaction, this study was extended to surfactants having different head groups. Anionic systems were not considered, taking in account that they are not able to interact with the negative charged phosphate groups of DNA. [14, 15] The interest was thus focused on the zwitterionic surfactants, having both a positive and a negative charge in the head group and overall neutral. The charge density of such systems can be modulated, in principle, by the pH, and by the addition of salts that are able of specifically interact with the head group charges.

The zwitterionic systems used in this study belong to two classes. Dodecyldimethylamine oxide (DDAO) and dodecyldimethylcarboxibetaine (CB1-12) are pH-sensitive amphiphiles that can be protonated at physiological pH. On the other hand, dodecyldimethylammonium-propane sulfonate (SB3-12), possesses a higher pK_a, and is in the zwitterionic form over the pH range investigated.

2.5.3.a Effect of the amine-oxide on the DNA structure

Dodecyldimethylamine oxide (DDAO) is a zwitterionic surfactant having a pK_a = 4.95. [16] The charge of this amphiphile depends on the pH of the solution: at basic and neutral pH values it is mainly in the non-ionic form, whereas at acidic pH values it becomes a cationic surfactant. [17] The equilibrium between these two forms in aqueous solution is as follows:



A number of published results have shown that the ionisation of DDAO in water begins at pH values below 7 and reaches complete protonation at pH = 2. [18] The role of pH for this surfactant is thus very important and it is an interesting parameter, in addition to variations of the surfactant concentration, in relation to the DNA- DDAO interaction.

Moreover, it must be taken into account that the presence of DNA in DDAO solution seems to drastically change the degree of ionisation of DDAO to higher values, as compared to the free surfactant in aqueous solution, due to the co-operative electrostatic interactions. [14]

Studies with this surfactant were focused mainly on the effect of varying the pH between 5.5 and 7.5 (Table 7, Appendix I) while monitoring the DNA-DDAO interaction; the CD spectra are reported in Fig. 9, by increasing pH values. Under the reported DNA and DDAO concentrations, the λ_{\max} at pH=7.4 is identical to that of native DNA. It is shifted to higher values when pH was decreased, indicating a variation in the DNA superstructure. These experiments allowed to show not only the presence of an interactions between DNA and DDAO over a wide range of pH, but have also provided evidence of the reversibility of the aggregation process. In fact, increasing the pH from acid to basic values reverses the process and restores the λ_{\max} of native DNA.

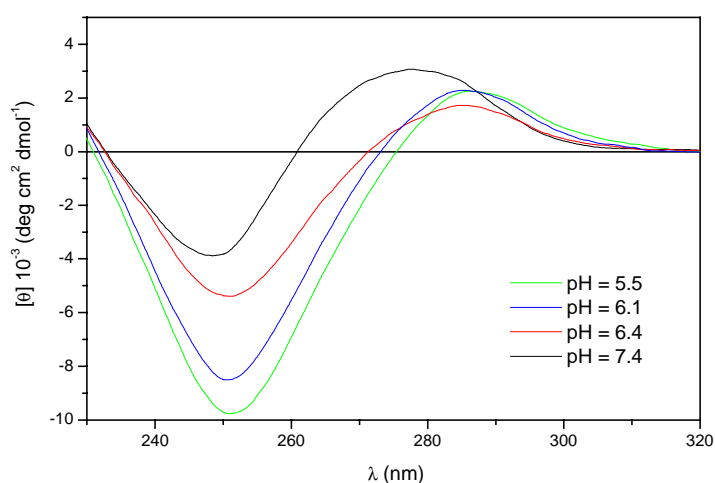


Fig. 9: Effect of pH on CD spectra of CT-DNA at constant DDAO concentration. [DNA] = 2.0×10^{-5} M; [DDAO] = 1×10^{-2} M; T= 25.0 °C.

Further experiments were performed to study the effect of the concentration of DDAO on DNA-surfactant interactions. Figures 10, 11 and 12 show CD spectra of these experiments at three different pH values.

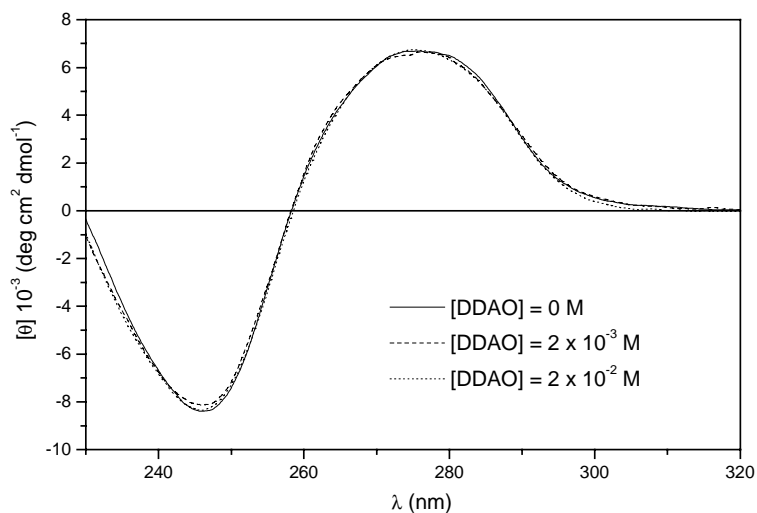


Fig. 10: Effect of the concentration of DDAO on CD spectra of DNA at pH= 7.5. $[\text{DNA}] = 2.0 \times 10^{-5} \text{ M}$; $T = 25.0 \text{ }^\circ\text{C}$.

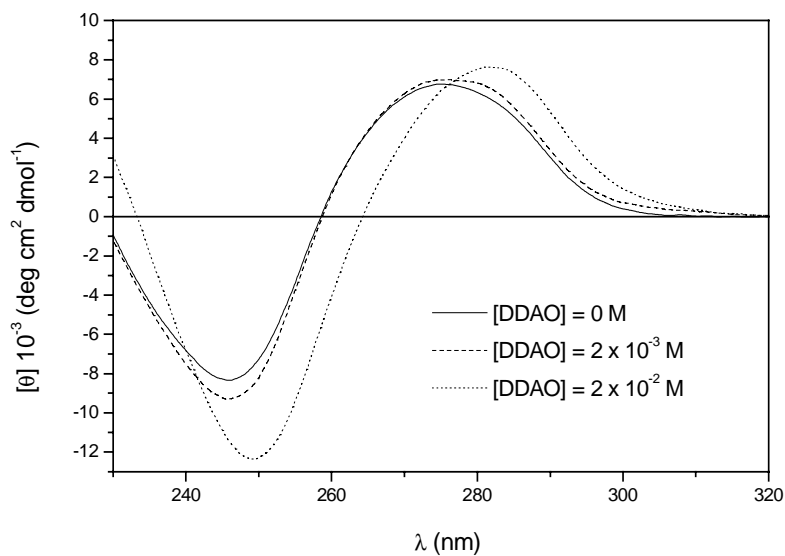


Fig. 11: Effect of the concentration of DDAO on CD spectra of DNA at pH= 7.1. $[\text{DNA}] = 2.0 \times 10^{-5} \text{ M}$; $T = 25.0 \text{ }^\circ\text{C}$.

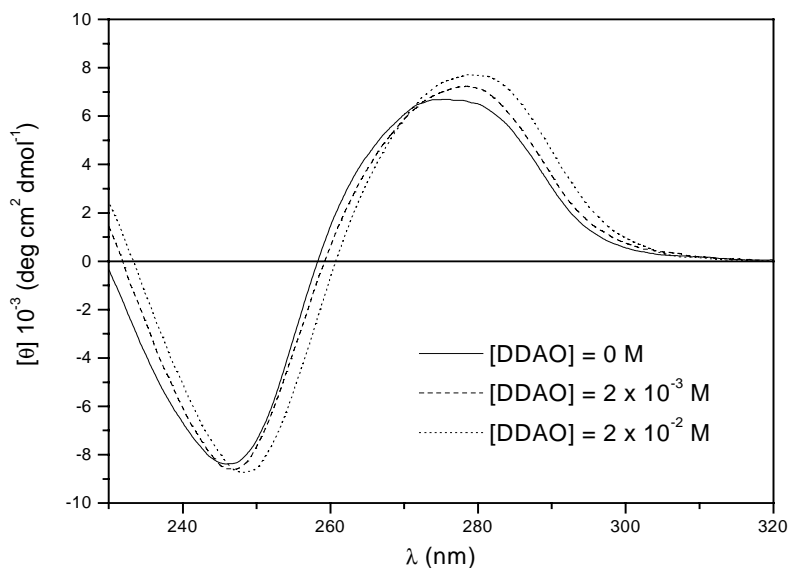


Fig. 12: Effect of the concentration of DDAO on CD spectra of DNA at pH= 6.5. [DNA] = 2.0×10^{-5} M; T = 25.0 °C.

It can be seen that no changes in λ_{\max} are observed upon increasing the DDAO concentration at pH = 7.5. At this pH, the amine-oxide, remains predominantly in the neutral zwitterionic form and, consequently, does not interact with DNA. The plot of the λ_{\max} values as function of the DDAO concentration at the three pH values is reported in Fig. 13 (Tables 8 – 10, Appendix I). When the pH is decreased a rapid increase of λ_{\max} takes place even at relatively low concentration of the surfactant. This shift is significantly greater than that observed in the cationic systems reported above.

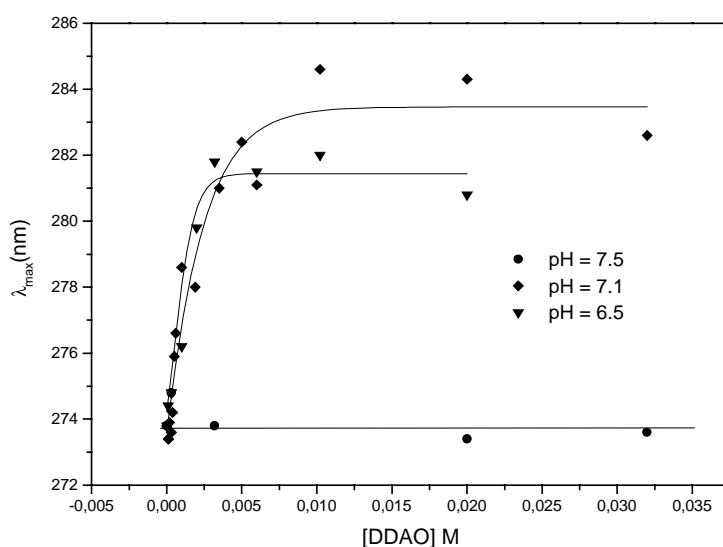


Fig. 13: Variation of λ_{\max} as a function of the concentration of DDAO at three different pH values. [DNA] = 2.0×10^{-5} M; T = 25.0 °C

A critical concentration of aggregation of 3.1×10^{-4} M is determined. This value is very close to the c.m.c. value for DDAO (7×10^{-4} M in aqueous solution).

At pH =7.1, only a small portion of DDAO monomers are present in the cationic form, capable of interacting with DNA. At lower (pH = 6.5), the shift in λ_{\max} is less pronounced than that observed at pH = 7.1. However, the saturation value seems to be reached at lower [DDAO]. This can be related to the larger amount of DDAO in the cationic form at pH=6.5, favouring the interaction of the surfactant with DNA.

So far, these results show that the interaction between DNA and DDAO is controlled by two effects: the concentration of the surfactant, and the pH. Moreover, on the basis of the data concerning the effect of pH on DNA-surfactant interactions, it is possible to establish a range of pH where the transition from the native to the aggregated form occurs. At pH values that are less than 7.1, DNA interacts with DDAO, whereas at pH = 7.5 such interactions are minor. Over this range of pH, changes of λ_{\max} at fixed DDAO concentrations (greater than the c.m.c. in water) are also observed as shown in Fig. 14 (Table 11, Appendix I).

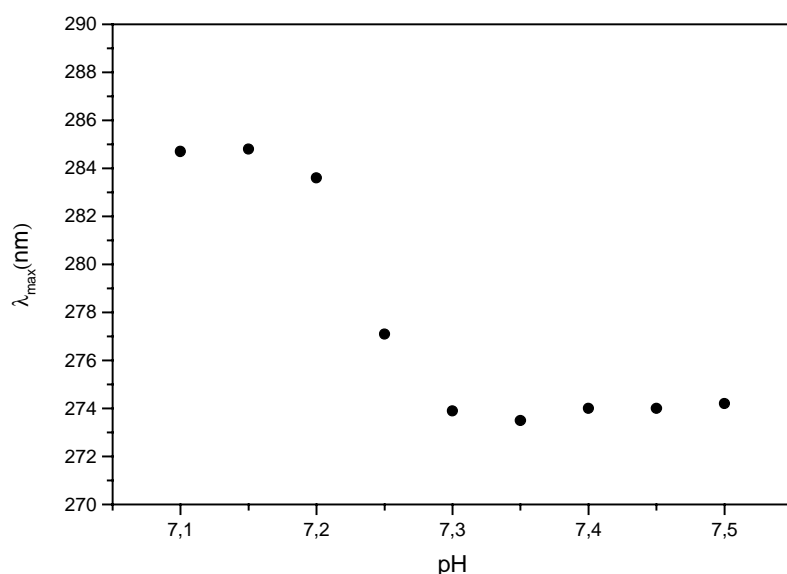


Fig. 14: Variation of λ_{\max} for DDAO-DNA aggregate as a function of the pH. [DNA] = 2.0×10^{-5} M; [DDAO] = 2×10^{-2} M; T = 25.0 °C.

It thus appears that DNA-DDAO interactions end at pH = 7.3 but are still present at pH = 7.2. This means that the range of pH needed to modify the DNA structure from the globular form to the native form is 0.1 units only. This is very interesting because it implies that a small change of pH is sufficient to modulate the interaction DNA-surfactant due to the change in the charge density of the amphiphilic system. The combined role of surfactant concentration and pH in controlling the DNA-DDAO interactions is confirmed by experiments in which the pH is changed while the concentration of the surfactant is maintained below the c.m.c., In this case, interaction is evidenced in the range of pH from 6.5 to 5.0, as reported in Fig. 15 (Table 12, Appendix I).

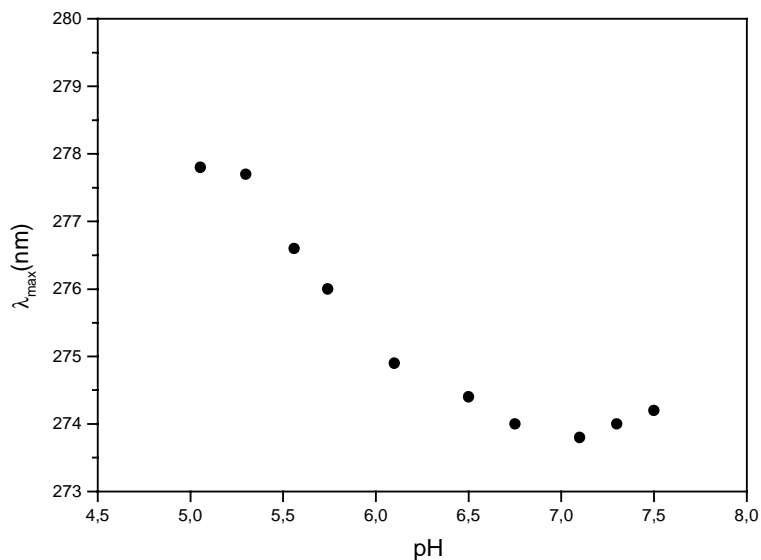


Fig. 15: Variation of the λ_{\max} in function of the pH. [DNA]= 2.0×10^{-5} M; [DDAO]= 8×10^{-5} M; T = 25.0 °C.

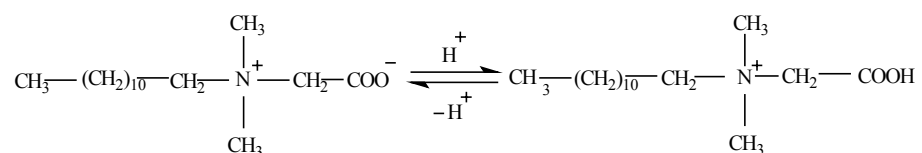
Zwitterionic surfactants such as DDAO prove to be very complex and interesting amphiphilic systems. The effects of pH and concentration in DNA-surfactants interaction seem to be complementary: if the surfactant is sufficiently positively charged (i.e. at low pH values) it can interact with DNA at concentration values above and below the c.m.c.. If the pH is increased, higher amphiphile concentrations are needed for the interaction to occur.

It is important to underline that the c.m.c. values of DDAO are influenced by the pH. It is reported in the literature that a decrease in pH induces an increase of the the critical micelle concentration. [19-21] Measurements of surface tension performed in the presence of DNA at pH = 7.1 and at pH = 5.0 confirm these results. (Table 5, Appendix II).

Moreover, it must be taken into account that the presence of DNA in the DDAO solution seems to affect the way of aggregation of the surfactant monomers. For example, it was observed that the introduction of a highly charged DNA molecule to DDAO solutions induces the formation of rod-like micelles around the polyelectrolyte, [14] whereas, in the absence of DNA rod-like micelles of DDAO can be obtained only by addition of salt at high concentration. [14] On the basis of these observation, it is usually likely to discuss in terms of a generic “critical concentration of aggregation” instead of the c.m.c..

2.5.3.b Effect of the carboxybetaine on DNA structure

Dodecyldimethylammonium-carboxybetaine (CB1-12) is similar to DDAO in that it is a pH-sensitive surfactant, which changes its properties upon variation of the pH. At pH values lower than 5 the surfactant is in the cationic form, whereas at higher pH values it is mostly in the neutral form. [23]



Dodecyldimethylammonium-carboxybetaine has the same hydrocarbon chain as DDAO, but a different head group. The analysis of the interaction between CB1-12 and DNA allows to verify whether or not another pH dependent surfactant having a different hydrophilic moiety also shows a similar behaviour to that of DDAO. Preliminary data were obtained at two concentrations of CB1-12: 2×10^{-3} M and 2×10^{-2} M, as for other systems previously investigated. The CD spectra at $[CB1-12]= 2 \times 10^{-3}$ M are reported in Fig.16.

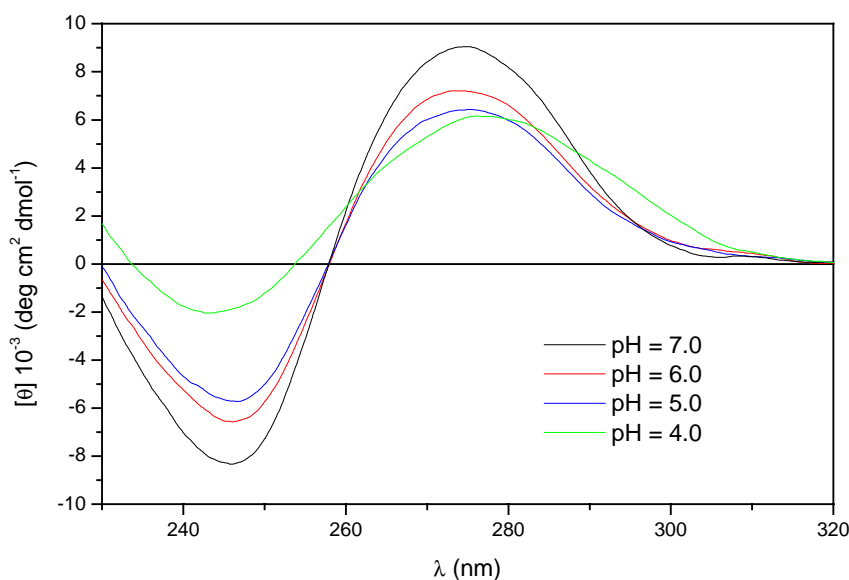


Fig. 16: Effect of pH on CD spectra of CT-DNA at constant CB1-12 concentration. $[DNA]= 2.0 \times 10^{-5}$ M; $[CB1-12]= 2 \times 10^{-3}$ M; $T= 25$

No significant changes of the λ_{max} at pH values above or equal to 5 were obtained, but a decrease of the intensity was observed at acidic pH. At these pH values CB1-12, is in the zwitterionic form and the interaction is not favoured. At pH values lower than 5, the protonation of the carboxylate group of the surfactant favours aggregation with DNA and a broadening of the band shape is observed at pH= 4. To conclude whether any interaction between DNA and CB1-12 are present at pH=4, it is essential to exclude the possibility of denaturation of the biopolymer in such acidic conditions The CD spectra of

DNA obtained at pH=4.0 and 7.1 in the absence of CB1-12 are shown in Fig.17. These spectra indicate a similar change in the DNA structure even if in absence of surfactant at pH= 4 in aqueous solution. Thus, it is difficult to assess whether observed variation in the presence of CB1-12 is due either a small change in the DNA structure at acid pH value or the presence of electrostatic interactions between the positive charges of the carboxybetaine and the negative charges of the phosphate groups.

Because complete protonation of CB1-12 can be obtained only at very low pH, where DNA denaturation occurs, further investigation of this system is complicated.

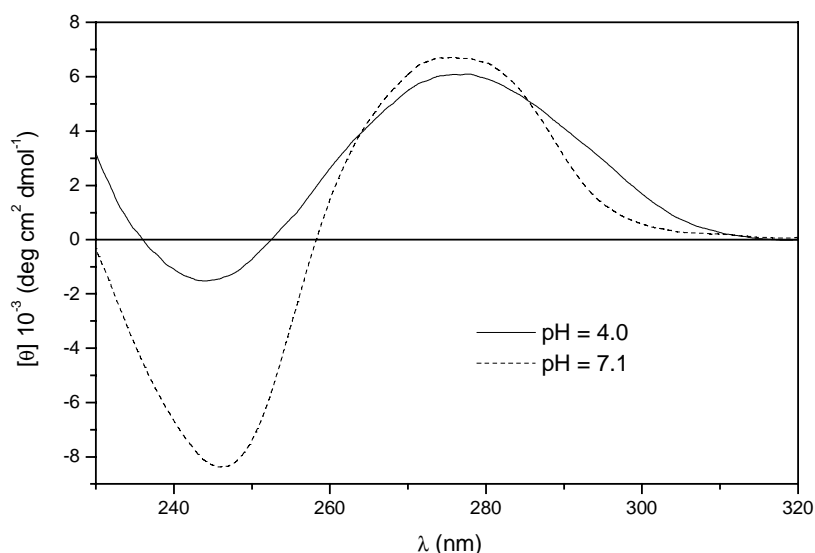


Fig. 17: Effect of pH on the CD spectra of CT-DNA in aqueous solution. [DNA]= 2.0×10^{-5} M; T= 25 °C.

2.5.3.c Effect of sulfobetaines on DNA

It has been shown that pH-sensitive zwitterionic surfactants are able to interact with DNA. The magnitude of the interaction is dependent on the pH and on the concentration. In order to complete the investigation on the effect of the nature of the head-group of the surfactant, dodecyldimethylammonium propane sulfonate was studied (SB3-12). This surfactant has a very high pK_a

value, so it can be considered to be insensitive to pH variation. This is confirmed by results from the pH effect on the interaction between DNA and SB3-12, as reported in Fig.18. It is evident that variations in pH do not influence DNA-SB3-12 interaction, neither in the shape of the spectra, nor in the λ_{\max} value (Table 17, Appendix I).

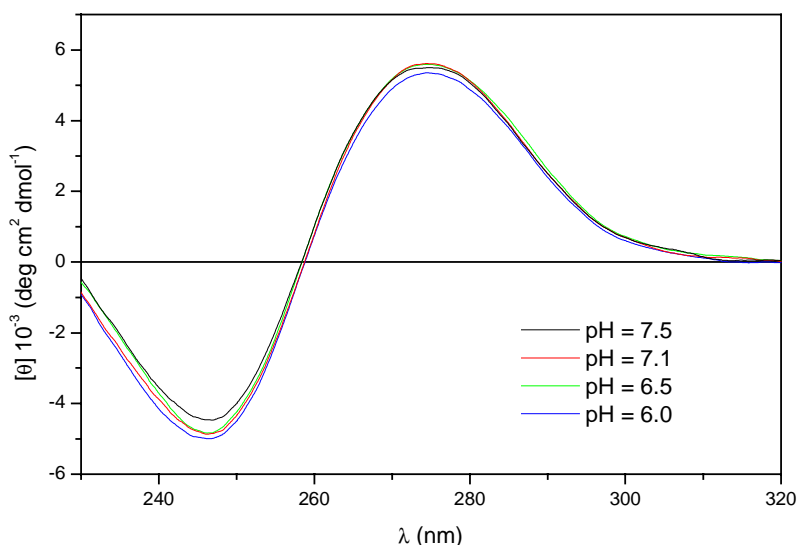


Fig. 18: Effect of pH on the CD spectra of CT-DNA at constant SB3-12 concentration. [DNA]= 2×10^{-5} M; [SB3-12]= 2×10^{-2} M; T= 25°C.

Even at high concentration of the zwitterionic surfactant (above the c.m.c. value) there is no interaction with DNA, which remains in the native form. Moreover, in the range of pH between 7.1 and 7.5, crucial for DDAO interaction, no changes in the CD spectra are found for SB3-12 (Table 14, Appendix I).

The effect of the concentration of the surfactant at a given pH was also investigated. Results obtained at pH=7.1 are shown in Fig. 19. Identical results were obtained at pH= 7.5 (see Table 15, 16, Appendix I). To summarise, even when the concentration of the surfactant is considerably varied above or below the c.m.c., no shifts of the CD band are observed. Thus, it is concluded that no changes in DNA structure take place. Only a slight increase of the maximum intensity is observed upon increasing the concentration of SB3-12.

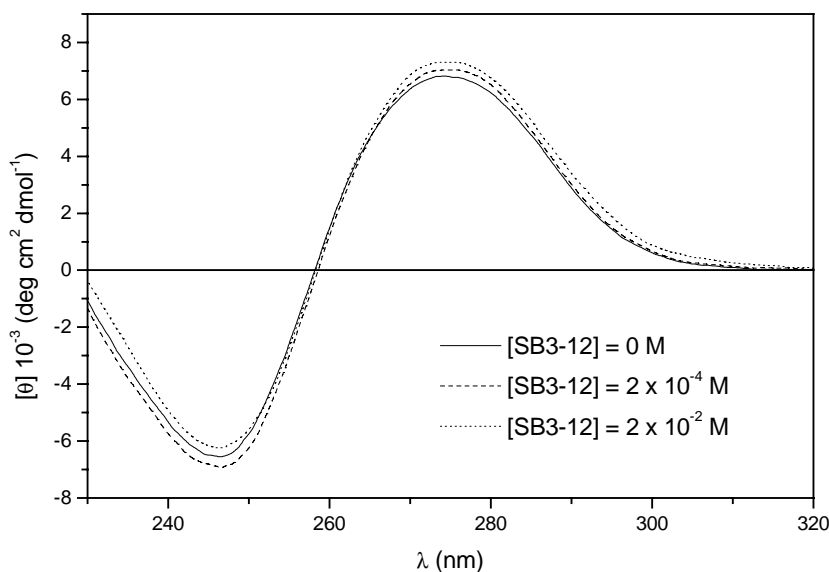


Fig. 19: Effect of the concentration of SB3-12 on CD spectra of DNA at pH= 7.1. [DNA]= 2.0×10^{-5} M; T = 25.0 °C.

It can be concluded from these experiments that in the case of zwitterionic surfactants, the pK_a of the anionic moiety is crucial. In the case of sulfobetaines, which have a very high pK_a , the zwitterionic form is always predominant, and no interactions with DNA are observed. On the other hand, in the case of DDAO and CB1-12, the amount of active protonated form is strongly controlled by the pH. From this aspect, in this case, zwitterionic surfactants act as pH controlled switches for DNA interaction

2.5.4 Interaction between DNA and zwitterionic non- micellisable systems

The experimental data previously reported clearly showed that both for cationic and zwitterionic systems, the presence of an interaction with DNA depends on the charge of the headgroup of such systems. The next question is whether the role of the hydrophobic moiety is important in inducing interaction. To better understand this aspect two other systems were studied,

having a zwitterionic headgroup but lacking the hydrophobic moiety: trimethyl amine oxide (TMAO) and trimethylammonium propane sulfonate (SB3-1). Considering the results previously obtained for TBABr it was expected that for such zwitterionic system, no interactions with DNA would take place. Indeed, under the experimental conditions identical to those used for amphiphilic zwitterionic surfactants, no evidence for DNA interaction was obtained. In the case of TMAO, the effect of pH was also studied, as summarised in Fig. 20 (Table 17, Appendix I).

It is interesting to note that, over the pH range investigated, TMAO has no effect on DNA structure, although it has the same charged moiety as DDAO (which is very effective under identical conditions). Moreover, there is not effect of the concentration of TMAO at pH= 7.1 nor pH = 7.5, whereas for DDAO these represent the upper and lower limit conditions, as shown for pH= 7.1 in Fig. 21 (Tables 18, 19, Appendix I).

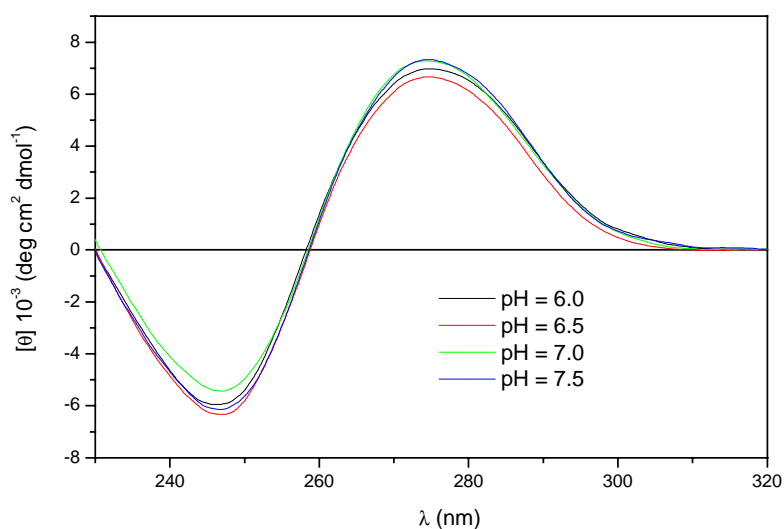


Fig. 20: Effect of pH on CD spectra of CT-DNA at constant TMAO concentration. [DNA] = 2.0×10^{-5} M; [TMAO] = 2×10^{-2} M; T= 25.0 °C.

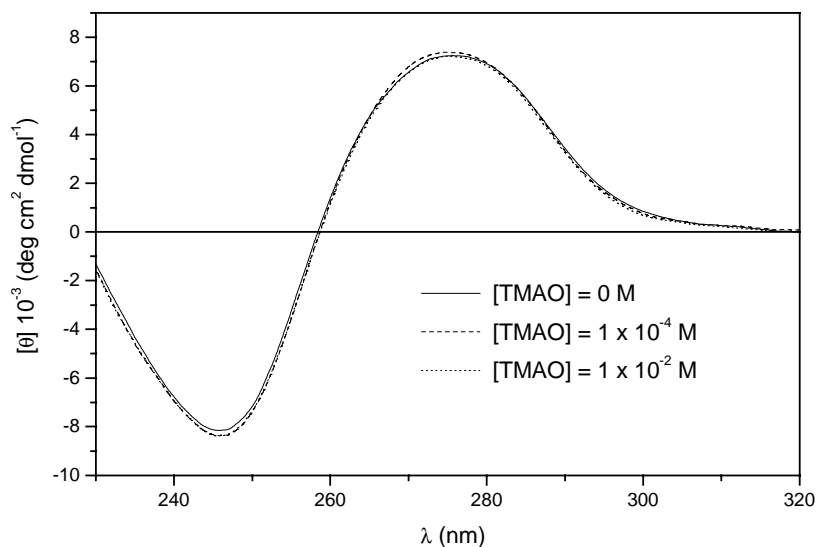


Fig. 21: Effect of the concentration of TMAO on CD spectra of DNA at pH= 7.1. [DNA]= 2.0×10^{-5} M; T = 25.0 °C.

It follows that for the amine-oxides, as for cationic amphiphiles, both the hydrophobic moiety and the head group structure are essential. At pH = 7.5, both systems do not interact with DNA because of their zwitterionic nature, but at lower pH values, DDAO is able to aggregate with DNA whereas TMAO does not.

In the case of SB3-1, in agreement with what has been observed before with SB3-12, we have considered only the effect of concentration, because sulfobetaine systems do not change their charge in function of pH in the considered range of pH. In this case, SB3-1 induces only a minimal decrease in the maximum intensity and no variation in λ_{\max} is observed. (Fig. 22, Table 20, Appendix I).

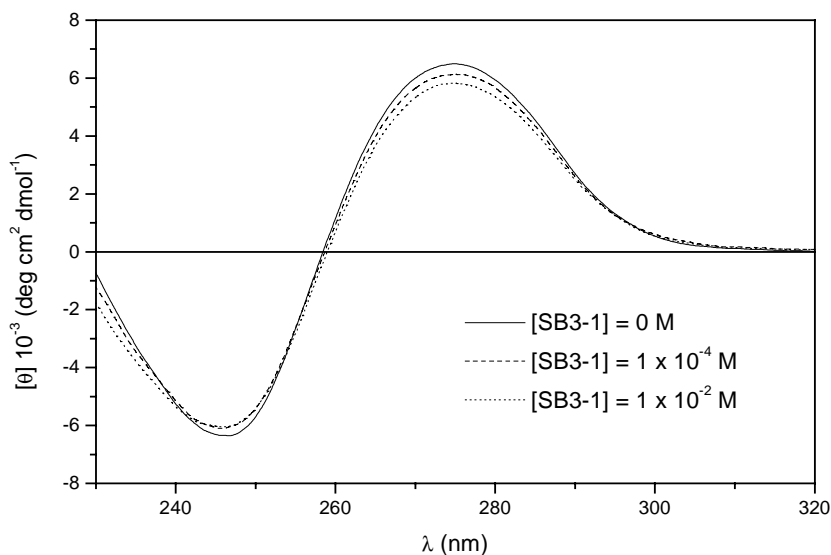


Fig. 22: Effect of the concentration of SB3-1 on CD spectra of DNA at pH= 7.1. [DNA]= 2.0×10^{-5} M; T = 25.0 °C.

2.6 Concluding remarks

Circular Dichroism studies have proven useful obtaining important information concerning the origin of DNA-surfactants interactions. Circular Dichroism spectral shifts toward longer wavelength values are associated with a variation in the DNA conformation from the native form to a more globular compact structure.

As far as cationic surfactants are concerned, it has been shown that both CTABr and CTBABr can interact with DNA even at very low concentrations, well below their c.m.c. in water. The interactions between these two surfactants and DNA appear to be both hydrophobic and electrostatic. In fact, the corresponding ammonium salt, TBABr, (which does not form micelles), does not induce changes in the CD spectra of DNA even at relatively high concentrations.

More interesting results have been obtained using zwitterionic surfactants, in which the pK_a of the anionic moiety resulted to be crucial. The SB3-12 having a very high pK_a , can be considered only in the zwitterionic

form in the pH range studied and no interactions with DNA are observed. On the other hand, in the case of DDAO and CB1-12, the amount of active protonated form is controlled by the pH. Thus, in these cases, zwitterionic surfactants act as molecular controlled switches of DNA conformation..

REFERENCES

- [1] P. Crabbè, in *Optical Rotatory Dispersion and Circular Dichroism in Organic Chemistry*, ed. Holden-Day, **1965**.
- [2] D.D. Lasic, N.S. Templeton, *Adv. Drug Delivery Reviews*, **1996**, 20, 221-266.
- [3] Y. Okamoto, *Prog. Polym. Sci.*, **2000**, 25, 159.
- [4] H. Durchschlag, *J. Molecular Structure*, **2001**, 565, 197.
- [5] A. Parkinson, M. Hawken, M. Hall, K.J. Sanders, A. Rodger, *Phys. Chem. Chem. Phys.*, **2000**, 2, 5469.
- [6] M. Matzeu, G. Onori, A. Santucci, *Colloids and Surfaces B: Biointerfaces*, **1999**, 13, 157.
- [7] W. Curtius Johnson, *Circular Dichroism and the Conformational Analysis of Biomolecules*, ed. G. D. Fasman, New York, **1996**.
- [8] K. Nakanishi, N. Berova, R.W. Woody, *Circular Dichroism: Principles and Applications*, ed. H. G. Schuster, New York, **1991**.
- [9] Z. Wang, D. Liu, S. Doing, *Biophys. Chem.*, **2000**, 87, 179.
- [10] M.J. Carrlin, N. Datta-Grupta, R.J. Fiel, *Biochem. Biophys. Res. Comm.*, **1982**, 108, 66.
- [11] S. Bhattacharya and S.S. Mandal, *Biochemistry*, **1998**, 37, 7764.
- [12] L. Streyer, *Biochimica*, 4th ed., Zanichelli, **1996**.
- [13] S.M. Mel'nikov, V.S. Sergeev, K. Yoshikawa, *J. Am. Chem. Soc.*, **1995**, 117, 991.
- [14] Y. S. Mel'nikova, B. Lindman, *Langmuir*, **2000**, 16, 5871.
- [15] S.M. Mel'nikov, R. Dias, Y.S. Mel'nikova, E.f. Marques, M.G. Miguel, B. Lindman, *FEBS Letters*, **1999**, 453, 113.
- [16] M. Mille, *J. Colloid Interface Sci.*, **1981**, 81 (1), 169.
- [17] D.L. Chang, H.L. Rosano, A.E. Woodward, *Langmuir*, **1985**, 1, 669.
- [18] M. Tuncay, S.D. Christian, *J. Colloid Interface Sci.*, **1994**, 167, 181.
- [19] Y. Imashi, R. Kakehashi, T. Nezu, H. Maeda, *J. Colloid Interface Sci.*, **1998**, 197, 309.

[20] J.F. Rathman, S.D. Christian, *Langmuir*, **1990**, 6, 391.

[21] Xue-Z. Ren, Gan-Zou Li, Hong-Li Wang, Xin-Han Xu, *Colloids and Surfaces A: Physicochem. Eng. Aspects*, **1995**, 100, 165.

CHAPTER 3

MOLECULAR MODELLING

3.1 Introduction

A Main advantage of cationic lipids for DNA transfection is that their physicochemical properties can be varied to facilitate formulation and adaptation to Good Manufacturing Practices. Cationic lipids can, in principle, be designed to combine good transfection efficiency with other desirable features such as lower toxicity and immunogenicity. [1] Although a large number of cationic lipids have been synthesised as potential gene delivery vehicles, few studies on the quantitative structure-activity relationship (QSAR) of the DNA-surfactant interaction have been undertaken and the interest in this approach has increased significantly. [2,3]

Computational approaches to DNA-surfactant interactions are not common in the literature. Some models of these interactions have been reported by Kuhn et al. [4], who formulate a theory for polyelectrolyte-ionic surfactant solutions based on combined electrostatic and hydrophobic interactions. Their predictions were found to be in good agreement with the experimental results of Gorelov et al.. [5]

More recently, molecular dynamics simulation of DNA-surfactant systems were performed [6,7] and, in one case, [6] possible structures of the complex between DNA and surfactant monomers (Fig.1-A) or micelles (Fig.1-B) were proposed. However, molecular dynamic simulations are computationally expensive, and there are practical limits on system size and time scale, so that numerous approximations must be done to reduce complexity.

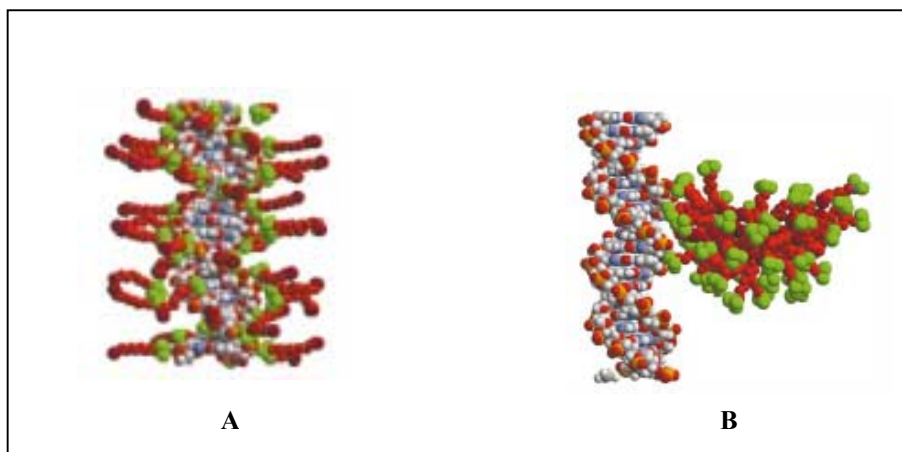


Fig. 1: Models of the DNA interaction with surfactant monomers (A) or micelles (B) proposed by P. Smith. [6]

On the basis of these observations, we undertook modelling of DNA-surfactant systems making use of a different computational approach using docking algorithms. The use of docking can lead to a better understanding of the driving forces of the DNA-surfactant interactions. The experimental data obtained by Circular Dichroism was the starting point to build our computational model. Subsequently, the calculations were extended to other surfactants, to have a more representative sampling diversity. Finally, the predictive ability of our model was tested by designing new experiments in Circular Dichroism and fluorescence spectroscopy.

3.2 Docking procedures

The aim of a docking experiment is to predict the three-dimensional structure (or structures) formed when one or more molecules interact non-covalently to form an intermolecular complex. Generally, this approach is used to investigate protein-ligand interactions, [8-11] but it can be also extended to other biological structures such as nucleic acids, membranes, cytochromes, or single aminoacids. These macromolecular structures represent the Target molecule.

There are essentially two different steps in any docking experiment. First, it is necessary to explore the space of possible receptor-ligand geometries (sometimes called “poses”). Second, it is necessary to score or rank these poses in order to identify the most likely binding mode. Of course, the ranking should prioritise correctly conformers of the same ligand, or different ligands.

In docking, the tridimensional structure of the target molecule must be known as precisely as possible. X-ray crystallography and NMR spectroscopy are useful and common sources of 3D information. Structure by omology models are also used, although the precision of these 3D structures can be a limiting step. Docking procedures can be used both to find the best fit of a known ligand into a receptor or to design a new ligand with specific properties (structure-based ligand design).

The difficulty in dealing with receptor-ligand docking is in part due to the fact that it involves many degrees of freedom. The translation and the rotation of one molecule relative to another involves six degrees of freedom. In addition the conformational degrees of freedom of both the ligand and the biomolecule must be considered. Moreover, the solvent may also play a significant role in determining the receptor - ligand geometry and the free energy of binding even though its role is often ignored.

In some cases, an expert computational chemist may be able to predict the binding mode of a ligand using interactive molecular graphics if he or she has a good idea of the likely binding mode (e.g. if the X-ray structure of a close analogue is available). However, often the manual docking can be very difficult when dealing with novel ligand structures and is clearly impractical for large numbers of molecules.

Docking algorithms are normally classified according to the degrees of freedom that they consider. Early algorithms only considered the receptor as rigid body. The algorithms most widely used at the present enable the ligand to fully explore its conformational degrees of freedom; some programs also permit some limited conformational flexibility to macromolecular Target. [12]

Docking algorithms make use of geometrical or energetic criteria to investigate the complementarity between ligand and receptor and, in some cases, a mixture of both criteria is used. [13] This means that specific Force Fields are used to evaluate the interaction between the two molecules, taking also in account the possible distortions caused by the interaction. Such Force Fields can be represented by the following expression:

$$E_{\text{binding}} = E_q + E_{lj} + E_{\text{HB}} + E_{\text{trasf}} + E_{\text{dist}} \quad (1)$$

in which the total energy of the interaction is expressed by the sum of the electrostatic (E_q), Lennard Jones (E_{lj}), hydrogen bonds (HB), distortion energy (Dist) and electronic transfer (trasf). The main difference in using geometrical or energetic criteria relies in the different contribution of each parameter in equation (1).

The **DOCK** algorithm developed by Kunz and co-workers [14-17] is generally considered pioneering in receptor - ligand docking, and it can be classified as a method based on geometrical criteria. The earliest version of the DOCK algorithm only considered rigid-body docking and was designed to identify molecules with a high degree of shape complementarity to the binding site. Today, shape complementarity is still the driving force of the method, although some corrections for the energetic criteria were added. The first stage of the DOCK method involves building a “negative image” of the binding site. This negative image consists in a series of overlapping spheres of different radii, derived from the molecular surface of the target molecule. Each sphere touches the molecular surface at just two points (see Fig. 2). Ligand atoms are then matched to the sphere centres so that the distances between the atoms equal the distances between the corresponding sphere centres within some tolerance. These pairs of ligand atoms and sphere centres can be used to derive a translation-rotation matrix that enables the ligand conformation to be oriented within the binding site using molecular fitting. [12]

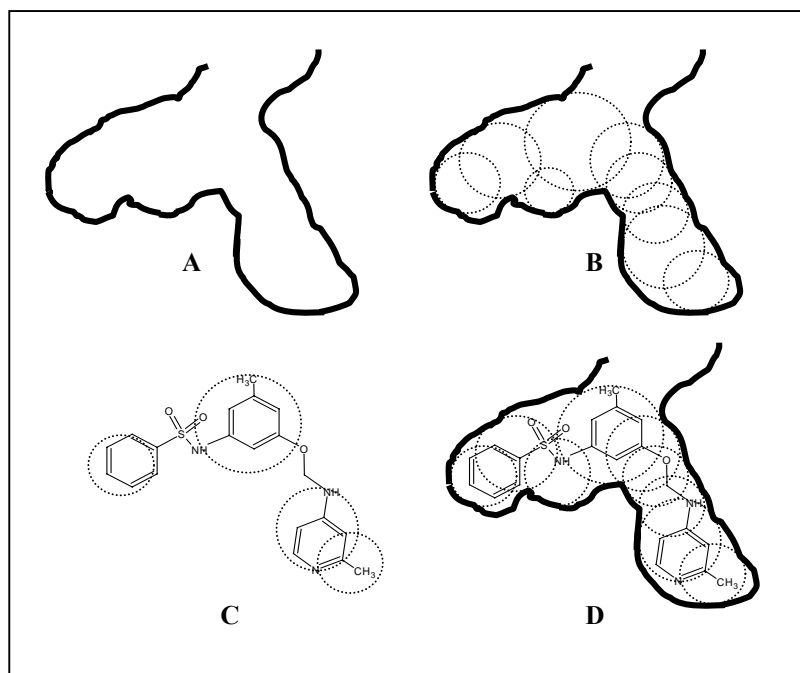


Fig. 2: Scheme of the DOCK procedure. A) Reception site on target molecule; B) Substrate-exclude volume of reception site; C) Identification of ligand conformational space; D) Fitting of ligand to reception site.

Because DOCK lacks a real “Force field” to model the ligand-receptor interactions, a particular scoring function must be used. Ligand conformational space is normally explored using the appropriate conformational search algorithms. Most of these algorithms fall into one of three categories: i) **Monte Carlo** method, ii) **genetic algorithms**, and iii) **incremental construction** approaches. The Monte Carlo method is unique in its ability to overcome small increases in conformational energy: an iterative procedure is used to modify the conformation of the ligand. The new configuration is accepted if its energy (E_{new}) is lower than that of its predecessor (E_{old}) or if the Boltzmann factor $\exp[-(E_{\text{new}}-E_{\text{old}})/kT]$ is greater than a random number between zero and one. Simulated annealing is frequently employed to search for the global minimum.

3.3 The CHEMODOCK method

3.3.1 GRID

The aim of methods based on energetic criteria is to model the energetic interaction of non-covalent bond between the target and ligand molecules. The simulation of the molecular interactions by means of energetic criteria is of more general use, but it is slower and strongly dependent on the chosen Force Field. [13] A well-known docking program that makes use of energetic criteria is **GRID**.

GRID is Force Field designed for studying interactions between molecules in a bioenvironment (such as water), and determining energetically favourable binding sites. The GRID procedure was developed to study the interaction of small chemical groups called “probes” with a protein of known structure, called “Target”. [18, 19] Chemical probes, strictly reflecting individual properties of different chemical groups, are located at each point of the GRID cage established throughout and around the macromolecule, in order to determine the energy values, E_{xyz} , of the interactions with the macromolecule on each point of the GRID cage. Actually, GRID may be used to study individual molecules such as drugs, molecular arrays such as membranes or crystals, and macromolecules such as proteins, nucleic acids, glycoproteins or polysaccharides. [20] The given array of energy values can be combined into an X-matrix in order to apply a statistical approach, especially if GRID is run over a set of targets for Quantitative Structure-Activity Relationships analyses. But it can also be inspected directly: energy iso-contour surfaces (GRID maps) are displayed in three dimensions on a computer graphics system together with the macromolecular structure to identify the regions of attraction and facilitate the interpretation of protein-ligand interactions. GRID is widely used to model biological media. The water solvent molecules can be explicitly treated and organised water molecules can be displaced around and within the macromolecular target. The competition

between water molecules and the ligand, in the active site pocket, can be evaluated, ligand-receptor interactions may be studied in their energy and specific interactions, and flexible target or metal cations can be included in the environment. Finally, there are no limits on the type and size of the macromolecular target.

3.3.2 The GRID Probes

A GRID probe defines one specific atom or small chemical group. The GRID Force Field is designed to calculate the energies of these particular probes when interacting with the target. Many probes are available so that every kind of interaction might be simulated with the appropriate probe. In appendix 2, all the GRID probes are listed and divided in single and multi-atom probes. A whole molecule may be used as probe, and a complete description of the methodology is presented in the GRID manual. [21] An example of the Target-probe interaction is illustrated in Table 1. Glycine is the Target molecule and the chosen probes are WATER (OH₂), DRY and AMIDINE. Each probe interacts differently with glycine, and a diversity of descriptions are generated. Detailed descriptions about each probe is given; all the interactions are plotted as iso-contour energy of -4.0 Kcal/mol, except for the probe DRY, whose interaction is plotted as iso-contour energy of -0.1 Kcal/mol.

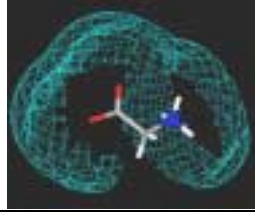
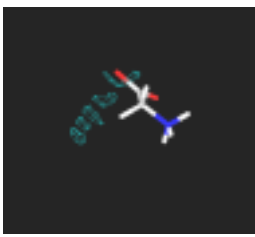
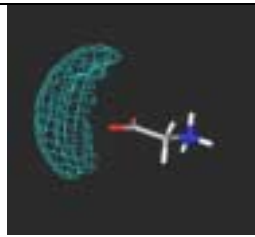
	<p>Probe WATER (OH2): The interaction between glycine and the probe OH2 has the minimum value of -6.6 Kcal/mol. The surfaces in the figure are generated by different interactions of both water lone pairs with NH_3^+ hydrogens and water hydrogens with glycine</p>
	<p>Probe DRY: Glycine is mainly hydrophilic and its hydrophobic regions are strictly limited to the region around the only aliphatic carbon. Its maximum energy value is low (-0.2 Kcal/mol) because the hydrophilic regions, due to the NH_3^+ and COO^- groups, disturb the water hydration shell formed around the molecule, which usually gives the greatest contribution to the hydrophobic energy of the probe DRY. Hydrophobic regions are in fact assumed to induce order in the aqueous environment, producing the resulting Energy. Hydrophilic regions, with their polar interaction with the water shell, break this order and reduce the hydrophobic energy. More details on hydrophobic energy are presented in the next section.</p>
	<p>Probe AMIDINE: The aliphatic AMIDINE probe consists of two sp^2 NH_2 groups, both of which are bonded to an sp^2 carbon which itself is bonded to another (beta) methylene group. It contains four hydrogens and it can donate up to four hydrogen bonds, two internal and two external. It has also a net electrostatic charge of $+1$. These features make the amidine interaction with COO^- very strong, therefore its minimum value, between the two oxygen atoms of glycine, is -13.1 Kcal/mol.</p>

Table 1: GRID fields describing the interaction of glycine molecule with probes OH2 and DRY.

3.3.3 The Energy Function

The non-bonded interaction energy E_{xyz} of the probe at each xyz grid position is calculated as the sum of many different components: [22]

$$E_{xyz} = \sum E_{lj} + \sum E_{el} + \sum E_{hb} + S \quad (2)$$

where E_{lj} is the Lennard-Jones potential, E_{el} is the electrostatic contribution and E_{hb} is the hydrogen bond potential. Each individual term is the sum of all the interactions between the probe and each atom of the Target; finally, S represents the entropic term.

The Lennard-Jones potential approximates the non-bonded attraction (London) and repulsion interaction between proximed atoms:

$$E_{lj} = \frac{A}{d^{12}} - \frac{B}{d^6} \quad (3)$$

where d is the distance between a pair of non-bonded atoms, A and B are calculated parameters. The Lennard-Jones contribution is a short-range interaction, so E_{lj} is set to zero whenever the probe and the Target atom are more than a certain distance apart (generally 8 Å). Cut-off may not be applied to the electrostatic interaction, because E_{el} does not diminish rapidly with distance.

The hydrogen bonding function is dependent on the length and orientation of the hydrogen bond and also on the chemical nature of the hydrogen bonding atoms, [23] and is calculated with this equation:

$$E_{hb} = E_r * E_t * E_p \quad (4)$$

where E_r describes the separation of the hydrogen-bonding atoms, and E_t and E_p describe the dependence on the angle made by the hydrogen bond at the target and probe atom, respectively.

The hydrogen bond potential was formulated to give GRID fields in agreement with experimental data; E_t and E_p functions were chosen by fitting to experimental data on hydrogen bond geometries in crystalline structures of small organic molecules and proteins, observed by X-ray or neutron diffraction.

The entropic effect, S , is calculated starting from the entropic component, called WENT (Water ENTropy), for an ideal flat hydrophobic surface: it represents the contribution to the Free Energy of solvent water molecules,

organised in an ordered manner around an ideal hydrophobic surface. When polar groups are present in the target, variation in global energy are due to the interaction between water molecules and target polar groups, especially when hydrogen bonds are formed, replacing bonds between water molecules. At the same time, when two hydrophobic surfaces come together there will be a favourable induction/dispersion interaction between the two molecules, and Lennard-Jones contribution (ELJ) is used to estimate this component. Therefore the entropic term is the result of two opposite effects: the favourable one originates from the well-organised water shell around the target and to the dispersion and induction forces, while the unfavourable one is due to the interaction of the water shell with a polar group of the target that disrupts the order in water-water interactions. The overall energy of the hydrophobic probe is thus computed at each grid point as:

$$S = (WENT + ELJ) - EHB .$$

3.3.4 The CHEMODOCK procedure

CHEMODOCK is a program to do docking calculations using the GRID Force Field. CHEMODOCK considers the ligand as a combination of probe groups. Fig.3 exemplifies the fragmental approach used by CHEMODOCK when a known ligand is recognised and parametrised. A molecule is first dissected into chemical fragments. Each fragment represents a normal GRID probe. Attractive or repulsive interaction regions are then generated for each probe over the whole protein active site. In addition to the probes representing the ligand, the water (OH2), hydrophobic (DRY) and hydrogen (H) probes are always considered. The attractive interaction regions are used to fit the ligand over them. CHEMODOCK can move the ligand, in its rigid form determined by its conformation, inside the pocket and over these defined regions, until energetically favourable positions are found; repulsive interactions tend to be minimised at each step of the iterative procedure. When the global minimum is reached the molecular coordinates are stored and another docking inside the active site goes on, according to an iterative procedure.

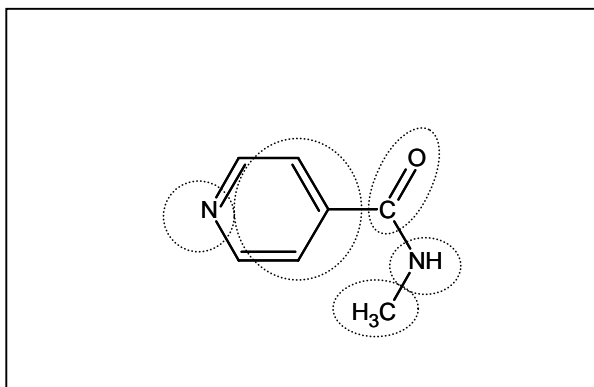


Fig. 3: The ligand as perceived by CHEMODOCK. Four different probes are used to simulate the chemical behaviour of the molecule: the pyridinic nitrogen, the carbonyl oxygen, the amide nitrogen and two hydrophobic regions (benzene ring and methyl group).

When all the regions have been evaluated, the most energetically favourable ones are taken into account and the entire molecule is considered as a multi-probe. This allows the global interaction with the target environment to be evaluated. Small movements are allowed in order to find the best global solution and the final solutions are stored. Each solution is characterised by the new cartesian coordinates and by the interaction energy with the macromolecular Target. Unlike the latest version of CHEMODOCK, the version used in this work does not take into account molecular flexibility, so an external conformational analysis is needed. The number of the docking solutions increases exponentially with the number of the sites of interaction in the target and in with the number of probes in the ligand. For a normal protein or DNA tridecamer, it is not unusual to find millions of possible “poses”. Each pose must be energetically evaluated. CHEMODOCK is the only docking programme that evaluates all the possible poses, without any limitation and the evaluation is extremely fast. At the end of the procedure the solutions retained are optimised, and the energy values are evaluated for each solution. The energetic equation that is used to calculate such energy values is based on the same contributions considered in the GRID energy equation.

3.4 Results and discussion

3.4.1 Docking surfactants and DNA

Since the B-conformation of DNA is the most stable under normal biological conditions, a thirty base-pair DNA fragment was modelled in this conformation. The DNA fragment was made in such a way to contain an AT/GC base pair ratio of 50%. The base sequences were randomly distributed. In the absence of counterions, the DNA molecule would have a large net anionic charge, so one potassium counterion was added to each phosphate (except for the terminal phosphates, to which one magnesium counterion was added). Each cation was placed radially at 7.0 Å from the corresponding phosphate group so that it was not directly bound to DNA. This resulted in an uncharged system for computational studies, well-suited to avoid overestimation of the electrostatic component.

Surfactants have been modeled as ligands, without considering the counterion. The version of CHEMODOCK utilised in this work did not consider the flexibility of the ligand. Of course, especially in the case of surfactant molecules, flexibility can be of great importance. To take flexibility into account, 100 conformers have been randomly modeled for each surfactant molecule, starting from the original structure, making use of a specific external program. Thus, the docking procedure has been repeated on all 101 conformations.

In order to exemplify the whole procedure utilised, the case of cetyltrimethylammonium bromide (CTABr, Fig.4) is reported in a schematic flow-chart:

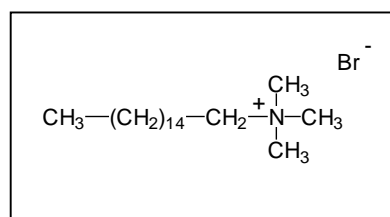


Fig. 4 CTABr structure.

STEP 1. The DNA structure is modelled as previously reported, and it is used in the same conformation for each surfactant. The structure of CTABr is modelled, without considering the counterion.

STEP 2. 100 conformers of the original CTABr structure are randomly generated by using OMEGA program. [24] All these conformers are recorded in a single file and are singularly considered, as independent ligands.

STEP 3. CTABr is analysed by the program to select the best chemical probes able to simulate the interaction of the ligand with DNA. In the case of CTABr, the most representative selected probes were:

H = the hydrogen atom probe;

DRY = the hydrophobic probe;

OH2 = the water probe;

N1+ = the probe representing a positive charged nitrogen with H-bond donor capability.

STEP 4. The probes are used to calculate the corresponding molecular interaction fields (MIF) with the DNA Target. In Fig.5, the MIF obtained with the OH2 probe interacting with DNA is reported.

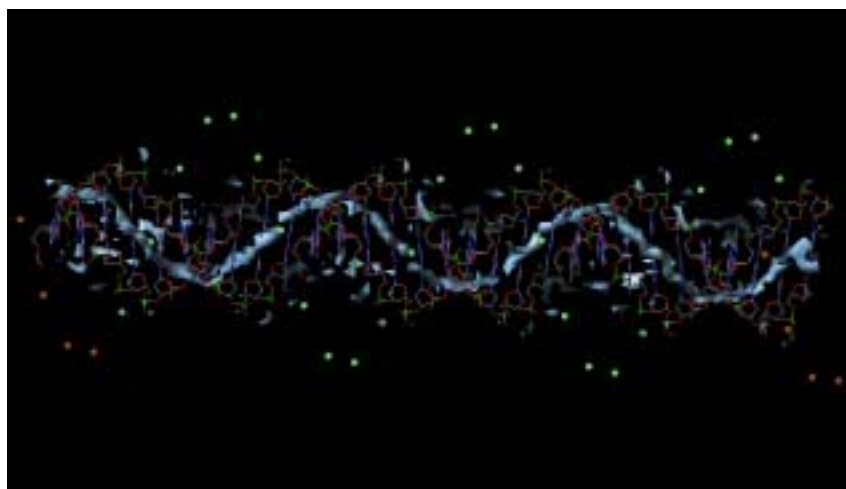


Fig. 5: The blue region represents the MIF obtained with the OH2 probe on DNA. The green and the orange spheres represent the potassium and the magnesium counterions respectively.

To individuate the possible “site points” that are present on the target, the local minima in each interaction region are temporarily condensed in specific points. Because the number of local minima (site points) can be very large, in Fig. 6 only three points needed for one docking solution are reported.

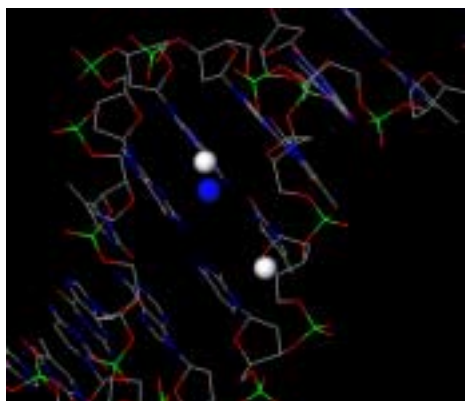


Fig. 6: Condensation of the information in points of minimum energy.

In each of these points, CHEMODOCK tries to locate the corresponding probes found in the ligand structure. (Fig. 7)

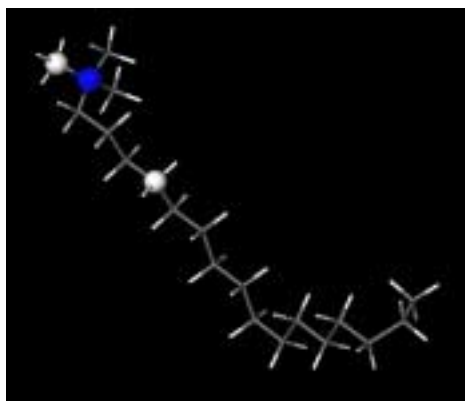


Fig. 7 : Probes on the ligand.

Starting from a vertex of the grid, CHEMODOCK will set an atom P1, which chosen among the polar ones, in a minimum position in the correspondent energetic map. This position will be considered as a favourable position for the atom P1. After positioning atom P1, attention will be focused

on a second atom P2, to find the corresponding point of favourable interaction on the target. Obviously, in the case that a target that is very large, there will be many favourable positions for each heavy atom of the ligand. The distance that must be observed between the atoms P1 and P2 is critical to drastically decrease the number of the possible solutions. For each atom subsequently considered, the position of the previously positioned atoms will be taken in account. In fact, after fixing the position of the first two atoms, the molecule may only rotate around the axis passing through P1 and P2, to search the position in which a third atom could be positioned. At this point, after having fixed also the third atom, the ligand is blocked and its orientation leads to the best correspondence between the triad of points of energetic minimum on the target surface and the complementary triad of points on the ligand (Fig. 8).

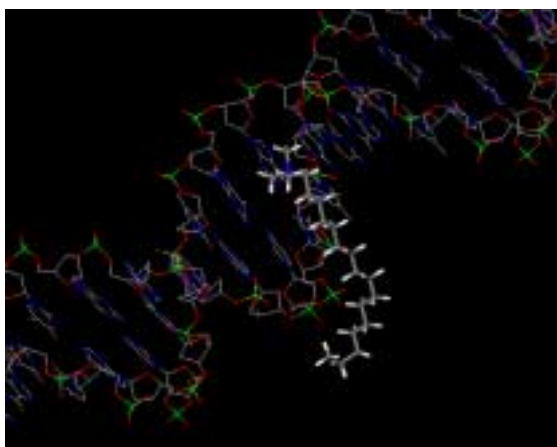


Fig. 8: Positioning of the ligand on the Target by CHEMODOCK procedure.

The same procedure has been performed for each one of the 101 conformers and, at the end of the calculation, the solutions have been reported in one output file. A visualisation of the output file for CTABr is shown in Fig.9. Obviously, the obtained image is not a picture of the “real” DNA-surfactant interaction, because each monomer does not “feel” the surrounding monomers. The number of the docked solutions is related to the occurring probability of each interaction. The greater the number of the solutions, the greater the possibility of interaction. Moreover, the analysis of the position of

each solution allows understanding of the location of the most favourable sites of interaction in the double helix, and the interaction pattern which are the chemical features involved in the interaction.

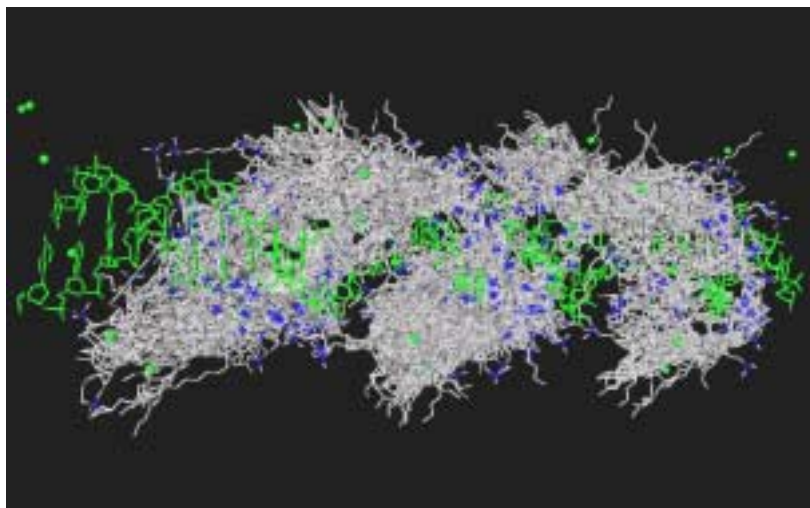


Fig. 9: Visualisation of the docking solutions obtained for CTABr

3.4.1.a Docking of cationic surfactants on DNA

The cationic systems considered in docking calculations are reported in Fig. 10.

Three different classes of amphiphilic systems, single-chain (CTABr, pDOTABr), twin chain (C16-16), and gemini (pXMo(DDA)_2), were selected. The comparison of the results obtained for CTABr and pDOTABr gave information on the role of the hydrophobic moiety of the surfactant in its interaction with DNA. Moreover, we calculated the docking interactions also with the 2-amino-2-hydroxymethyl-1,3-propane diol (TRIS) ammonium salt. The choice of this salt was related to the fact that TRIS is often used as a buffer solution in experimental studies of DNA-surfactants interactions. Thus, the docking performed with this salt allows one to see if a competition between cationic surfactants and the buffer occurs.

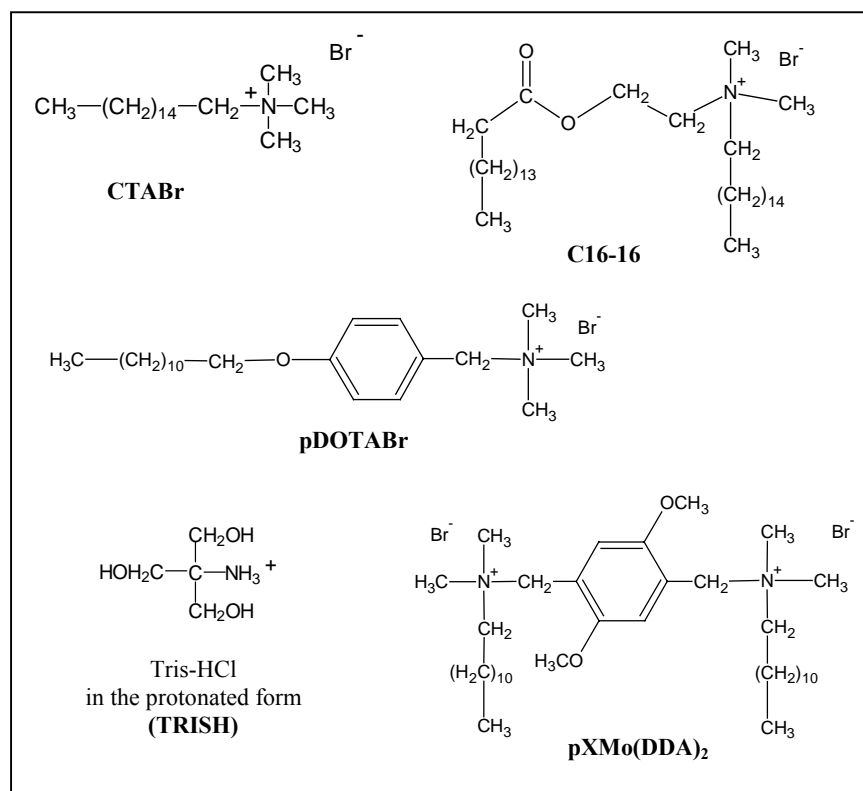


Fig. 10: Structures of cationic systems that have been modeled.

Table 2 reports the number of the solutions found for each system, together with the energy values. By constructing a histogram of the energy of the solutions, it is possible to make a comparison of the range of energies for the different systems. Obviously, no histograms were needed for TrisH, since only few docking solutions were found. It is important to point out that energy values obtained by docking are not useful as absolute values. In fact, since they may take into account different energetic contribution, the comparison must be better considered as an index of the ability of the ligand to interact with the target. In Fig.11 the histogram obtained for CTABr is reported as an example.

Cationic System	Number of Docking solutions	- ΔE (Kcal/mol)
CTABr	770	1 - 15
pDOTABr	779	1 - 15
C16-16	604	1 - 18
pXMo(DDA)₂	542	2 - 28
TrisH	9	1,4 - 3,5

Table 2: Docking results for cationic systems.

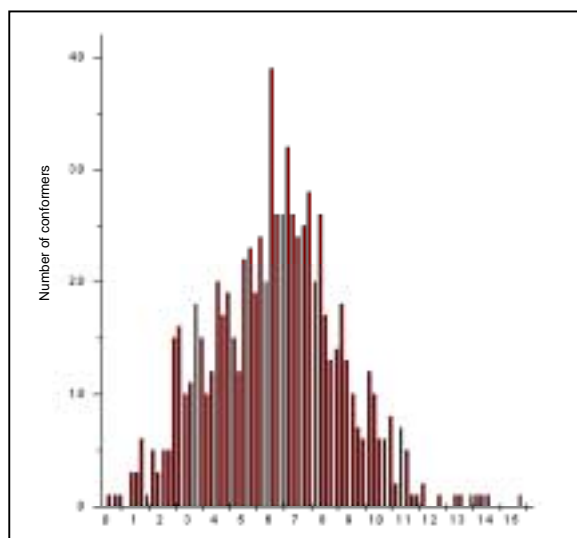


Fig. 11: Energy distribution for the docking solution of CTABr.

Considering both the docking solutions and the energy values, it seems that the four surfactants have similar ability to interact with DNA. It was already shown by the CD experiments, that CTABr could interact with DNA even at low concentrations. On the basis of this result, we can argue that the three other cationic surfactants could interact with DNA as well. Moreover, the presence of the two positive charges in pXMo(DDA)₂ structure seems to have a positive effect in increasing the interaction with the DNA target.

On the contrary, for TRISH salt, only nine docking solutions (and with low energy) were found. This result allow suggests that the study of interactions between cationic surfactants and DNA should not be invalidated by the presence of TRIS buffer in solution.

Additional information can be obtained from the whole conformational set docked into the DNA (e.g. Fig.9 for CTABr). In all the cases studied, the most favourable sites for cationic surfactants position the polar head-group oriented toward a phosphate group, while the hydrophobic tail is located on the DNA surface in proximity of the major groove. It is interesting to note that, since some drug molecules interact primarily on the major groove, such surfactants may also modulate the DNA-drug recognition.

3.4.1.b Docking of zwitterionic surfactants on DNA

A limiting factor in using cationic surfactants as vectors for transfection processes is the DNA release into the nucleus: if DNA-surfactant interactions are too strong, the release of DNA is hindered. On this basis, great interest has been devoted to zwitterionic surfactants, especially to amine-oxides amphiphiles. Amine-oxides as dodecyldimethylamine oxide DDAO possess a $pK_a \cong 5$ so that, around physiological pH, monomers are partially in the protonated form. Due to this property, the interaction between DDAO and DNA can be regulated by the pH and surfactant concentration, as shown in Chapter 2. In order to have a better comprehension of these experimental results, docking studies on zwitterionic systems were performed by modelling both the zwitterionic and the protonated form. In addition to DDAO, a number of diverse amine-oxides systems in terms of head group size and hydrophobic tail were considered.

The structures considered for modelling are reported in Fig.12.

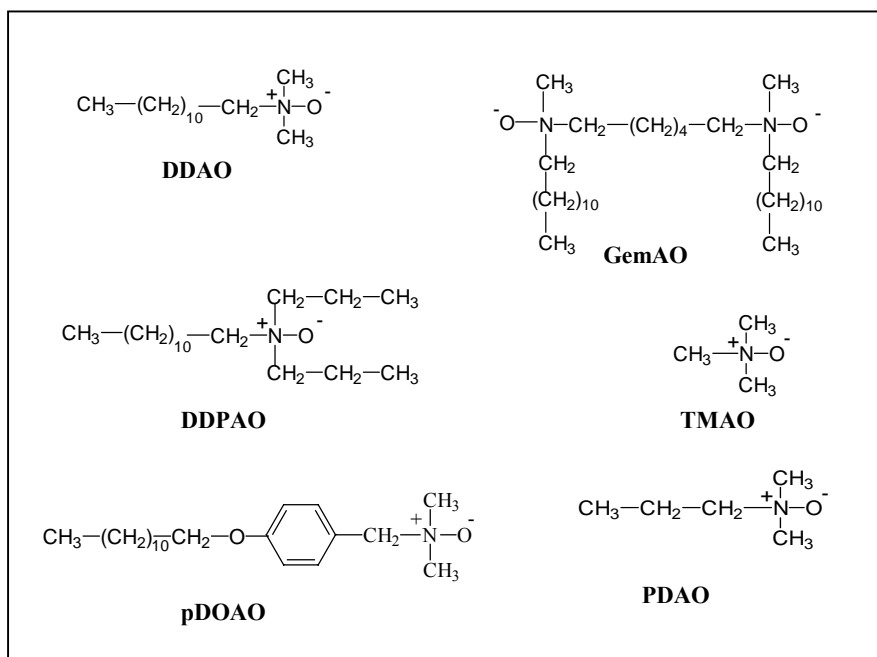


Fig. 12: Structures of zwitterionic systems that have been modelled.

First, we considered the DDAO system to better apprehend the results obtained with Circular Dichroism.

The docking solutions for the zwitterionic and the protonated forms of the amine-oxides DDAO, TMAO and PDAO are reported in Table 3. Focusing on the first two rows of Table 3, one can see that the number of docking solution found by CHEMODOCK is almost the same in both cases. However, when the energy values is associated to these solutions and the energy distribution plot is used, it is possible to appreciate that the energy values related to the zwitterionic form are lower than the cationic (Fig.13).

Zwitterionic systems	Number of Docking solutions
DDAO	999
DDAOH	870
TMAO	0
TMAOH	0
PDAO	0
PDAOH	0

Table 3: Docking solutions for DDAO, TMAO and PDAO both in zwitterionic and in protonated form.

It seems that zwitterionic DDAO can weakly interact with DNA due to the lack of the electrostatic interactions. Probably, conformational changes on DNA structure can not be induced.

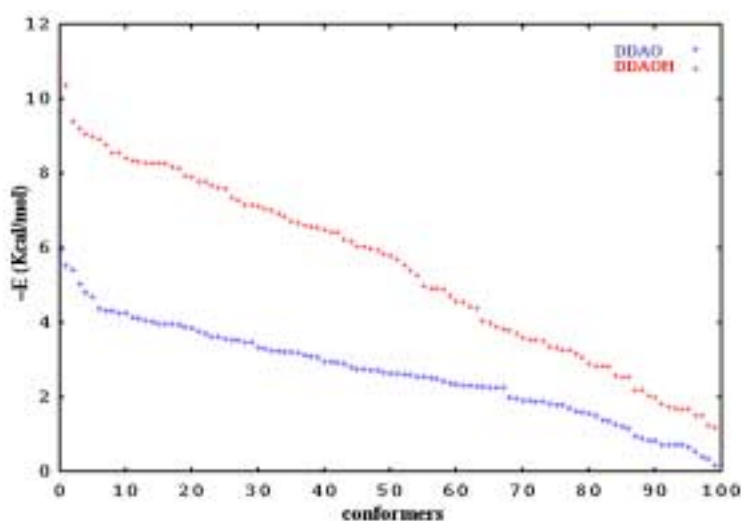


Fig. 13: Comparison of the energy values of the docking solution of DDAO and DDAOH.

From a comparison between the energetic distributions of the docking solutions for CTABr and DDAO in its protonated form (DDAOH, see Fig.14), it seems that DDAOH has a weaker interaction energy compared to CTABr, having a maximal value around 2 Kcal/mol.

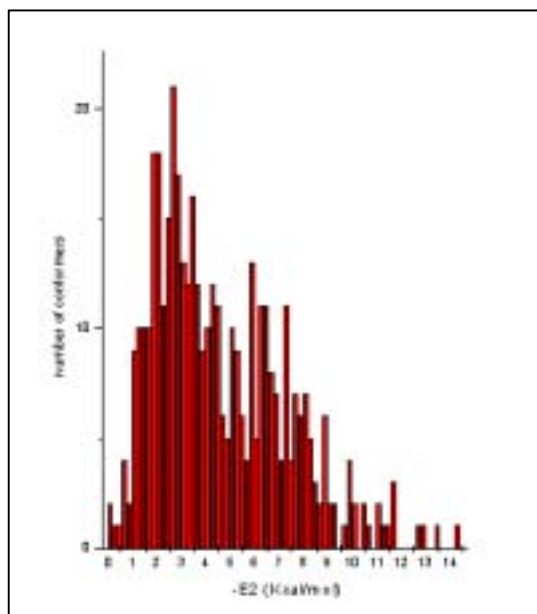


Fig. 14: Energy distribution for the docking solution of DDAO.

On the basis of this observation it would appear that, using DDAO, a competition with Tris buffer is possible. It is therefore important to consider this point before designing experiments on DNA-DDAO interaction in this buffer.

The experimental data obtained by Circular Dichroism for trimethylamine oxide (TMAO), a non-micellisable system, led to the conclusion that the presence of the hydrophobic moiety is essential to for interaction with DNA. In fact, no changes in the DNA CD spectra were observed in the presence of TMAO in solution.

Docking with TMAO was performed in order to verify the goodness of the procedure and, as expected, no docking solutions were found for this system (Table 3). This indicates that there is a good correspondence between

the experimental data and the docking results. Moreover, we have tried to perform Docking with an intermedieate system like propyldimethylamine oxide, another non-micellisable system. Again, no docking solutions were obtained (see Table 3) Finally, pDOAO and GemAO were considered, and the number of solutions found is reported in Table 4.

Zwitterionic systems	Number of docking solutions
pDOAO	926
pDOAOH	537
GemAO	625
GemAOH	582

Table 4: Docking solutions for pDOAO and GemAO in both the zwitterionic and protonated form.

Comparing the distribution energy of the docking solutions for the zwitterionic and the protonated form gives an analogous behaviour to Fig. 14 was obtained (Appendix 3, Figures 1 and 2).

3.5 Concluding remarks

On the basis of the obtained data using CD, new studies of molecular modelling were undertaken. The aim was to obtain a computational model for the DNA-surfactants interactions, able to provide a better understanding of the forces involved and to predict the interaction ability for surfactants non yet tested. The results of this new study are very promising. Particularly, docking studies have demonstrated the important role played by the hydrophobic moiety of the surfactant when interacting with DNA, in addition to the normal electrostatic forces.

With the zwitterionic dodecyldimethylamine oxide surfactant, CD experiments showed that a small change of pH, from 7.1 to 7.3, was able to modulate the DNA-surfactant interactions. This observation led us to the

hypothesis that DDAO protonation could be of importance in determining interaction. Docking studies on this system showed that the protonation of DDAO leads to a significant increase in the energy of the DNA-surfactant interaction, although the energetic values are lower than those obtained from cationic surfactants such as CTABr.

Furthermore, the interaction between the Tris-HCl buffer and DNA was studied, to investigate if this buffer could compete with surfactants in the interaction with DNA. Docking studies suggest that the energies and probabilities of interaction of Tris-HCl with DNA are very low, so we could hypothesise that the presence of this buffer in solution should not affect our studies. However, the energy of the interaction of amine oxide systems with DNA is also low. Thus, we performed further CD studies on the interaction between DNA and zwitterionic systems (DDAO and pDOAO) in TRIS-HCl buffer, to verify whether or not the presence of the buffering compound might introduce artefacts in the experimental data. Results concerning these experiments are reported in Chapter 4.

Finally, in order to check the external predictivity of the model, new amphiphilic systems have been modelled without having previous information by Circular Dichroism experiments. Then, these surfactants have been experimentally studied using fluorescence spectroscopy, to evaluate the prediction obtained by the pure model, and the experimental results are reported in Chapter 5.

We found a good ability of prediction for the model, as it will be better discussed the next chapters.

REFERENCES

- [1] Ledley F.D., *Current Opin. Biotechnol*, **1994**, 5, 626.
- [2] C. McGregor, C. Perrin, M. Monk, P. Camilleri, A.J. Kirby, *J. Am. Chem. Soc.*, **2001**, 123(6), 6215.
- [3] G. Byk, B. Wetzler, M. Frederic, C. Dubertret, B. Pitard, G. Jasline, D. Scherman, *J. Med. Chem.*, **2000**, 43, 4377.
- [4] P.S. Kuhn, Y. Levin and M.C. Barbosa, *Chem. Phys. Lett*, **1998**, 51, 298.
- [5] A.V. Gorelov, E.D. Kudryashov, J.C. Jaquier, D. McLoughlin and K.A. Dawson, *Physica A.*, **1998**, 249, 216.
- [6] P. Smith, R.M. Kynden-Bell and W. Smith, *Phys. Chem. Chem. Phys.*, **2000**, 2, 1305.
- [7] M. Karttunen, A.L. Pakkanen, P.K.J. Kinnunen and K. Kaski, *Cell Mol. Biol. Lett.*, **2002**, 7 (2), 238.
- [8] J.M. Blaney and J.S. Dixon, *Perspective in drug discovery and design*, **1993**, 1, 301.
- [9] R. Abagyan and M. Totrov, *Current opinion in chemical Biology*, **2001**, 5, 375.
- [10] R.D. Taylor, P.J. Jewsbury and J.W. Essex, *J. Computer-Aided Molecular Design*, **2002**, 16, 151.
- [11] I. Halperin, B. Ma, H. Wolfson and R. Nussinov, *Protein: Structure, function and genetics*, **2002**, 47, 409.
- [12] A.R. Leach and V.J. Gillet, *An Introduction to Chemoinformatics*, Kluwer Academic Publishers, **2003**, 171.
- [13] G. Cruciani, "Tecniche Computazionali per il Disegno di Farmaci", in *Biologia Molecolare dei Recettori e Drug Design*, Società Chimica Italiana, **1996**, 217.
- [14] I.D. Kunz, J.M. Blaney, S.J. Oatley R. Langridge and T.E. Ferrin, *Journal of Molecular Biology*, **1982**, 161, 269.

- [15] R.L. Desjarlais, R.P. Sheridan, G.L. Seibel, J.S. Dixon, I.D. Kuntz and R. Venkataraghavan, *Journal of Medicinal Chemistry*, **1988**, 31, 722.
- [16] I.D. Kuntz, *Science*, **1992**, 257, 1078.
- [17] I.D. Kuntz, E.C. Meng and B.K. Shoichet, *Account of Chemical Research*, **1994**, 27, 117.
- [18] P. J. Goodford, *J. Med. Chem.*, **1985**, 28, 849.
- [19] G. Cruciani and P. Goodford, *J. Mol. Graphics*, **1994**, 12, 116.
- [20] <http://www.moldiscovery.com/manual/index.html> (Chapter 4) GRID (version 20) manual.
- [21] <http://www.moldiscovery.com/manual/index.html> (Chapter 36) GRID (version 20) manual.
- [22] A. J. Hopfinger, *Conformational Properties of Macromolecules*, Academic Press, New York, chapter 2, **1973**.
- [23] D. N. A. Boobbyer, P. J. Goodford, P. M. McWhinnie, and R. C. Wade, *J. Med. Chem.*, **1989**, 28, 1083.
- [24] J. Bostrom, *J. Comp. Aid. Mol. Design*, **2002**, 15, 1137.

CHAPTER 4

CIRCULAR DICHROISM EXPERIMENTS SUGGESTED BY MOLECULAR MODELLING

4.1 Introduction

The Circular Dichroism experiments discussed in Chapter 2, provided very interesting information on DNA-surfactant interactions. Particularly, for zwitterionic surfactants as dodecyldimethylamine oxide, the pH of the solution seems to be a critical parameter for the interaction to occur. Previously reported CD experiments were performed in bidistilled water and the pH was adjusted by the addition of HCl or NaOH. The limit of this procedure, even if often used, [1] is that the ionic strength of the medium is poorly controlled due to the difficulty of preparing samples having the same ionic strength. To avoid this problem, other studies on DNA-surfactant interaction are often performed in Tris-HCl buffer, which is a commonly used buffer for biological systems. [2-3]

The structure of Tris (2-amino-2-hydroxymethyl-1,3-propane diol) is reported in Fig.1.

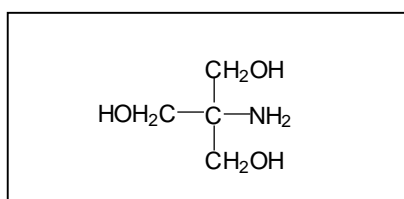


Fig. 2: Structure of Tris.

Tris has a $\text{pK}_a = 8.1$ at $25\text{ }^\circ\text{C}$, and its useful pH range as buffer is between 7 and 9. Tris, in the protonated form, is an ammonium salt and its utilisation as a buffer in studying DNA-surfactant interactions require

preliminary studies to control whether or not this compound can compete with surfactants for association to DNA.

Docking studies suggested that the energies and probabilities of interaction of Tris-HCl with DNA are very low. Thus, at least for cationic surfactants, an interference of Tris with DNA-CTABr interaction is unlikely. On the contrary, in the case of zwitterionic surfactants, whose energy of interaction with DNA is also very low, it was important to verify whether or not the presence of the buffer might introduce artifacts in the experimental data.

To evaluate the effect of the Tris-HCl buffer on DNA-surfactant interactions, additional Circular Dichroism experiments were performed using this buffer. Three different surfactants were used: CTABr, as a model of cationic surfactants, and two amine-oxides as DDAO and pDOAO. Comparison with previous results obtained in the absence of buffer for DDAO provides important information .

4.2 Effect of the Tris-HCl buffer on CD spectrum of DNA

As a preliminary approach to the problem, a CD spectrum of the Calf Thymus DNA in Tris-HCl buffer was recorded and compared to that obtained in distilled water at the same pH. Fig. 2 reports a comparison between the CD spectra of DNA both in bidistilled water and in 50 mM Tris-HCl buffer at pH= 7.5. As shown, the presence of Tris in solution induces a change in the DNA spectrum, and this effect is strongly related to the change in the ionic strength of the medium.

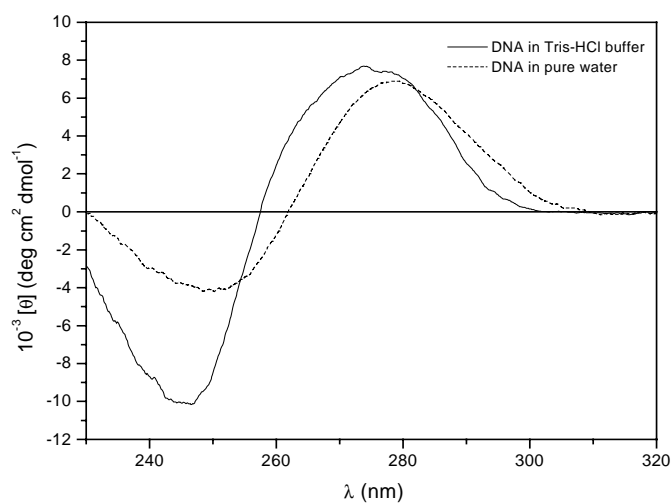


Fig. 2: CD spectra of CT-DNA in bidistilled water and in 50 mM Tris-HCl buffer at pH= 7.5. [DNA]= 2.0×10^{-5} M.

Since previous investigation on the interaction of zwitterionic surfactants and DNA were performed in bidistilled water in the range of pH between 5.5 and 7.5, CD spectra of DNA in 50mM Tris-HCl solution at pH= 5.8 and 7.5 were registered. As shown in Fig.3, identical spectra were obtained.

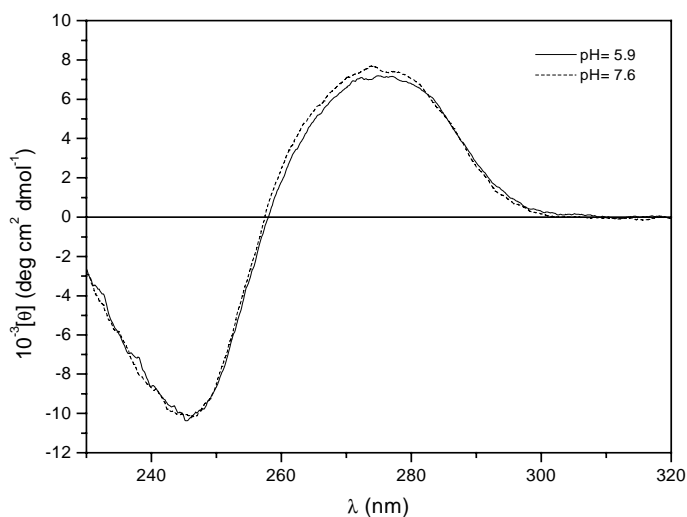


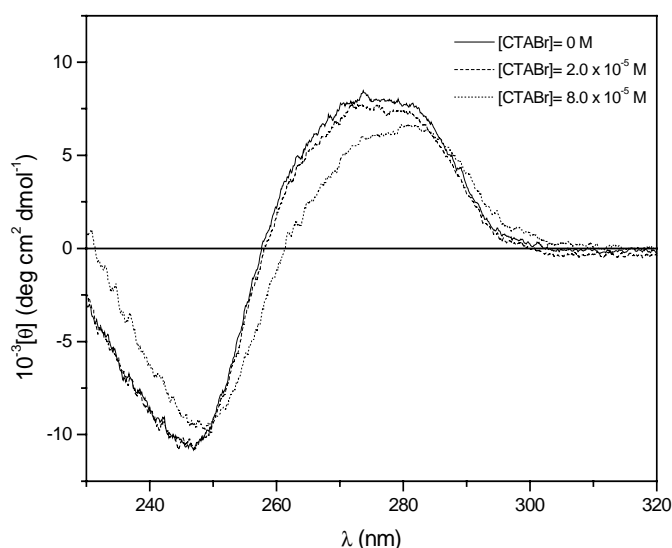
Fig. 3: CD spectra of CT-DNA at two different pH values in 50 mM Tris buffer solution. [DNA]= 2.0×10^{-5} M.

This indicates that, under these conditions, DNA conformation is not affected by pH, but by ionic strength. It is important to underline that, since

Tris pK_a is 8.1, the buffering capability of this compound at $pH= 5.8$ is practically lost, but it is useful in maintaining the ionic strength constant. On the basis of these results, it is possible to assume that changes of the CD spectra of DNA upon addition of surfactant are related only at an occurring DNA-surfactant interaction.

4.3 Circular Dichroism spectra of DNA in Tris-HCl upon addition of surfactants

Circular Dichroism experiments were performed to study the effect of the CTABr concentration on CT-DNA spectra in 50 mM Tris-HCl buffer, at $pH= 7.5$. The results of the experiments (Fig. 4) are very similar to those reported at Fig.6 - Chapter 2, obtained in bidistilled water having the pH adjusted at the same pH .



This result is in agreement with the predictions by molecular modelling studies. As mentioned above, cationic surfactants like CTABr have a higher

energy of interaction with DNA in comparison to protonated Tris, as well as a higher probability of interaction.

Circular Dichroism spectra of CT-DNA in 50 mM Tris-HCl solution were thus obtained upon addition of DDAO at two different pH values, in a range of surfactant concentration above and below the c.m.c. value (in analogy with the experiments performed in water, Fig 9-12, Chapter 2). The two pH values were 7.5 and 5.8, which did not affect the DNA structure in the absence of any other additive, as shown previously. The effects of DDAO concentration on CD spectra of CT-DNA in 50 mM Tris solution at pH 7.5 and 5.8 are reported in Figures 5 and 6.

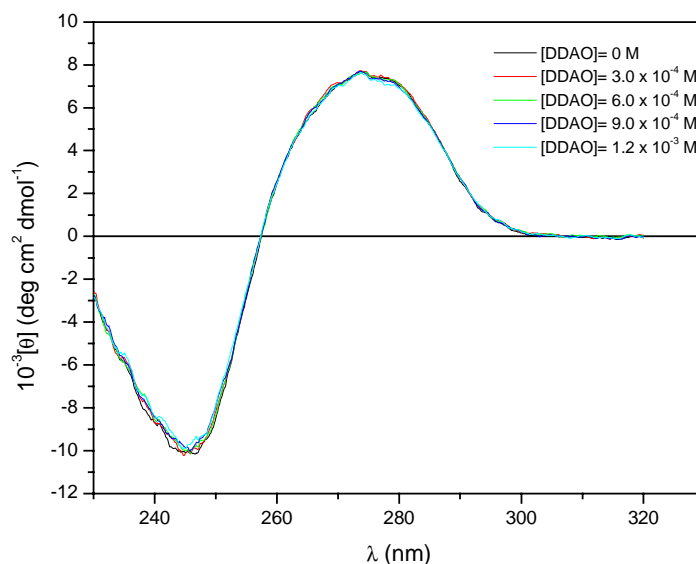


Fig. 5: CD spectra of CT-DNA upon addition of DDAO solution at pH=7.5. [DNA]= 2.0×10^{-5} M.

Under these conditions, the results are in agreement with those obtained in bidistilled water at the same pH values. In fact, at pH = 7.5 no changes in CD spectra of DNA were observed at concentration of DDAO above or below the c.m.c. value (7×10^{-4} M). This indicates that at pH= 7.5, no interactions between DDAO and DNA take place (Fig. 5).

On the contrary, changes of CD spectra were observed in similar experiments performed at pH= 5.8 at a concentration of DDAO higher than 6×10^{-4} M (Fig.6).

In this case also, the presence of Tris-HCl does not affect the DNA-DDAO interaction.

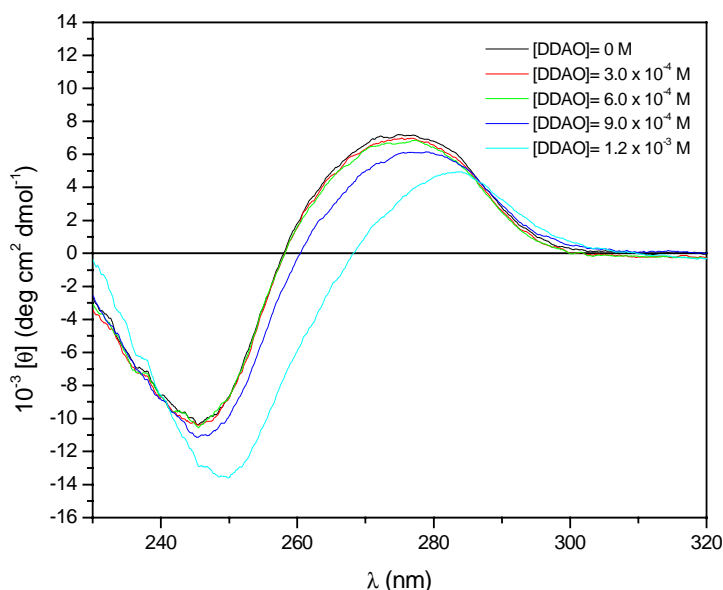


Fig. 6: CD spectra of CT-DNA upon addition of DDAO solution at pH=5.9. [DNA]= 2.0×10^{-5} M.

Finally, interactions between DNA and the zwitterionic surfactant pDOAO were studied by Circular Dichroism in Tris-HCl solution. The interaction of this surfactant with DNA was not previously studied by Circular Dichroism in bidistilled water. However, molecular modelling studies suggested that similar interactions to those obtained with DDAO should be expected.

The pDOAO was synthesised in our laboratory and differs from DDAO only in the nature of the hydrophobic moiety. Such structural modification greatly affects the c.m.c. value, which is significantly lower than that of DDAO (c.m.c. for DDAO and pDOAO in aqueous solutions are 7×10^{-4} M and 1.16×10^{-5} M respectively).

In our opinion, the comparison of the CD results obtained using the two compounds is very important to understand the nature of the interaction between zwitterionic surfactants and DNA. In fact, the interaction between DNA and DDAO at the appropriate pH value occurs only at concentration equal or higher than the c.m.c. of DDAO, as was shown by Circular Dichroism experiments performed both in bidistilled water and in Tris-HCl solution. On the basis of this experimental evidence two explanations are possible:

- 1) The DNA-DDAO interaction at pH lower than 7.1 is only dependent on the amount of protonated surfactant monomers; according to this hypothesis, the fact that such interaction occurs at high values of DDAO concentration is not directly related to the c.m.c. of the amine oxide surfactant.
- 2) The DNA-DDAO interaction at pH lower than 7.1 occurs between the biomolecule and the surfactant in the aggregated form (not necessarily spherical micelles), and in this case the observed phenomenon should be related to the c.m.c value.

Figures 7 and 8 report the CD spectra of DNA in Tris-HCl buffer upon addition of pDOAO in a range on concentration both above and below its c.m.c., at pH values of 5.8 and 7.5.

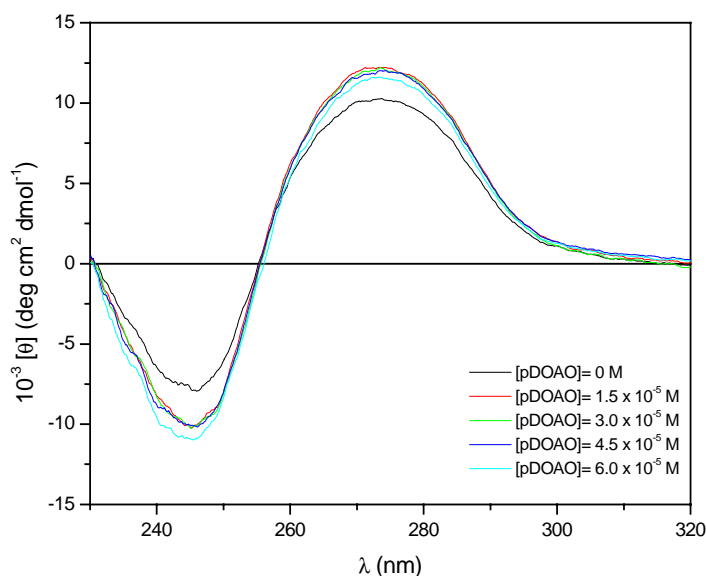


Fig. 7: CD spectra of CT-DNA upon addition of pDOAO solution at pH= 7.5. [DNA]= 2.0×10^{-5} M.

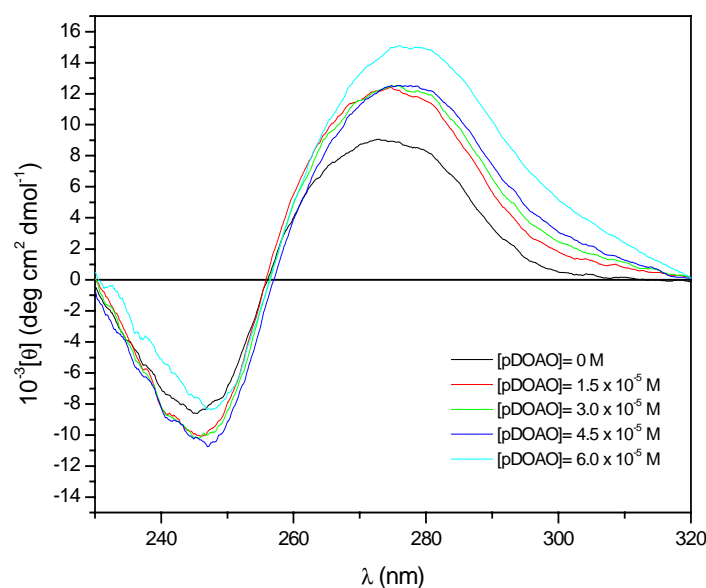


Fig. 8: CD spectra of CT-DNA upon addition of pDOAO solution at pH=5.8. [DNA]= 2.0×10^{-5} M.

As predicted by molecular modelling, results obtained for pDOAO are similar to those for DDAO. However, it is of interest to observe that, in the case of pDOAO, the interaction with DNA occurs at concentrations of surfactant 20-fold lower than that necessary when using DDAO. Considering the lower c.m.c. value for pDOAO, it seems that in the case of zwitterionic surfactants the interaction with DNA occurs only when surfactants monomers are able to self-aggregate, even if the nature of such aggregates should be influenced by the presence of DNA in solution. This hypothesis is in agreement with results reported by Mel'nikova and Lindman, where an interaction between DNA and rodlike-aggregates were proposed for DDAO. [1]

4.4 Concluding remarks

The results reported in this brief chapter are very important. Because the presence of Tris-HCl buffer does not affect the DNA-surfactant interaction, we can plan fluorescence experiments in this buffer, and thus benefit from the advantage of working in conditions where both the pH and the ionic strength

are controlled. Moreover, experiments performed using pDOAO allow to observe that the interaction between DNA and zwitterionic surfactants, unlike to cationic surfactants, is in some way related to the c.m.c. value. In our opinion, an interaction between DNA and simple micelles is improbable, due to the presence of an oppositely charged polyelectrolyte (the DNA) in solution which can affect the formation of the aggregate. This is agreement with the observation, reported by Mel'nikova and Lindman, that rodlike micelles of DDAO seem to form around DNA. [1]

Finally, studies reported in this Chapter are mostly in agreement with predictions by molecular modelling. It must be taken into account that docking studies performed can provide interesting information about the energy and the probability of the interaction between DNA and surfactant monomers, but they are not able to reproduce the effect of the surfactant concentration in this interaction. For this reason it is not possible for our model to predict the differences of concentration between DDAO and pDOAO in the interaction with DNA. Molecular dynamic studies could be useful for this purpose but, at the present, this approach presents limits on the system size and the time scale, which comport the use of significant approximations.

REFERENCES

- [1] Y. S. Mel'nikova and B. Lindman, *Langmuir*, **2000**, 16, 5871.
- [2] S.S. Bhattacharya and S.S. Mandal, *Biochemistry*, **1996**, 37, 7764.
- [3] S. Aktipis and A. Kindelis, *Biochemistry*, **1973**, 12, 1213.

CHAPTER 5

FLUORESCENCE SPECTROSCOPY

5.1 Introduction

5.1.1 Basic theory of fluorescence

The photophysical processes that occur from absorption to emission are often shown in a Jablónski diagram. Of course, all possible energy routes cannot be encompassed in a single figure, and different forms of the diagram can be found in different contexts. The diagram below (Fig.1) is a simple version, where intersystem crossing (from singlet to triplet states) leading to phosphorescence and delayed fluorescence as well as intermolecular processes (e.g. quenching, energy transfer, solvent interaction etc.) are omitted.

In the diagram, the electronic singlet states S_0 , S_1 and S_2 , along with three vibrational energy levels, are shown. In the ground state, the molecule will be in the lowest vibrational level of S_0 . At room temperature, the higher vibrational energy levels are in general not populated (less than 1% according to Boltzmann statistics). The magnitude of the absorbed photon energy ($h\nu_A$ in the figure) decides which vibrational level of S_1 (or S_2) becomes populated. This process is very fast and takes place within 10^{-15} s. In the next 10^{-12} s, the molecule relaxes to the lowest vibrational level of S_1 , a process called internal conversion. Since emission typically occurs after 10^{-9} s, the molecule is fully relaxed at the time of emission,. Hence, as a rule, emission occurs from the lowest vibrational level of S_1 (Kasha's rule) and the fluorescence spectrum is generally independent on the excitation wavelength. After emission ($h\nu_F$ in the figure), the molecule returns to the ground state, possibly after vibrational relaxation. This completes the simplest case of fluorescence: excitation, internal conversion, emission and relaxation. Energy losses between excitation

and emission are observed universally for fluorescing molecules in solution. One common cause of this Stokes shift is the rapid decay to the lowest vibrational level of S_1 . Furthermore, fluorophores generally decay to excited vibrational levels of S_0 (Fig.1), resulting in further loss of vibrational energy. In addition to these effects, fluorophores can display further Stokes shifts due to the solvent effects and excited state reactions.

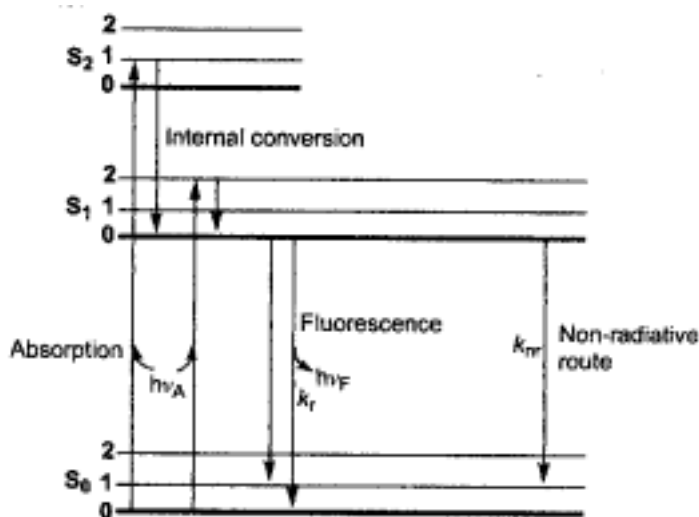


Fig. 4.: A simple Jablonski diagram. Three electronic levels are depicted along with three vibrational energy levels. $h\nu_A$ and $h\nu_F$ denotes absorption and fluorescence respectively. k_r is the rate constant for fluorescence and k_{nr} is the rate for the competing non-radiative route.

Identical fluorescence emission spectrum are generally observed irrespective of the excitation wavelength. Upon excitation into higher electronic and vibrational levels, excess energy is quickly dissipated, leaving the fluorophore in the lowest vibrational level of S_1 . This relaxation occurs in about 10^{-12} s. Generally, the fluorescence emission spectrum will appear as a mirror image of the absorption spectrum, specifically the absorption representing the S_0 to S_1 transition, provided little organisation occurs upon excitation. The generally symmetric nature of these spectra is a result of the same transitions being involved in both absorption and emission, and the similarities among the vibrational energy levels are not significantly altered by the different electronic distributions of S_0 and S_1 . According with the Franck-Condon principle, all electronic transitions are vertical, that is, they occur

without change the position of the nuclei. As a result, if a particular transition probability (Franck-Condon factor) between the 0 and the 2nd vibrational levels is largest in absorption, the reciprocal transition is also most probable in emission (Fig. 2).

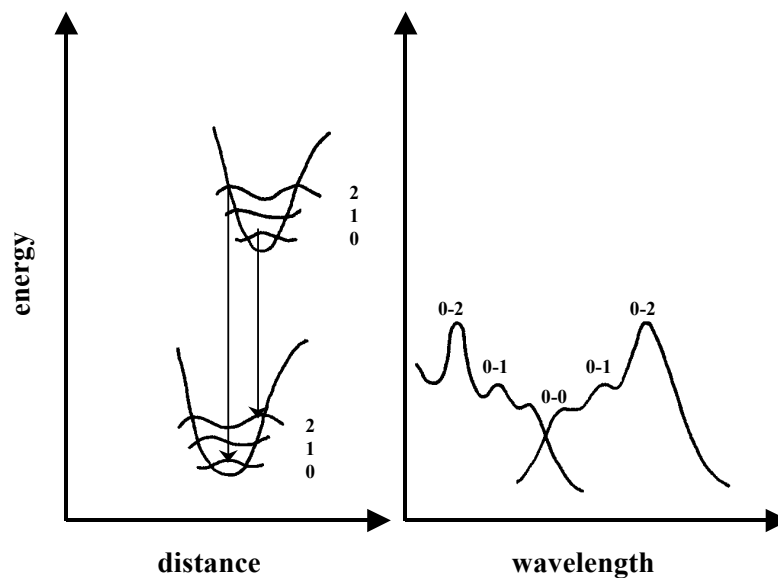


Fig. 5. Left: The mirror image rule: the absorption spectrum right is a mirror image of the emission spectrum left. Right: Franck-Condon principle: transitions are vertical. The 0-2 transition is the most probable.

While the relative peak intensity is governed by the Franck-Condon principle, the total fluorescence intensity I_F is related to the quantum yield (Φ_F), defined as the ratio of photons emitted to photons absorbed. I_F is given by the expression:

$$I_F = I_0 K \Phi \epsilon c l \quad (1)$$

where I_0 is the lamp intensity, K is an instrument constant, and $\epsilon c l$ is the amount of absorbed light (ϵ : extinction coefficient, c : concentration, l : length of light path.). The expression is valid for dilute solutions (optical density < 0.05). Returning to the Jabłoński diagram, two routes from S_1 to the ground state are

shown. Besides fluorescence, a molecule can typically choose between a number of non-radiative routes. The fluorescence quantum yield, Φ , can be expressed as the rate of photons emitted divided by the total rate of depopulation of the excited state:

$$\Phi_F = k_r / (k_r + k_{nr}) \quad (2)$$

If the non-radiative relaxation is fast compared to fluorescence ($k_{nr} > k_r$), Φ_F will be small, and the compound will fluoresce very little or not at all. Often different non-radiative events are limited in the solid phase, and long-lived luminescence (e.g. phosphorescence) is observed in frozen solution or other solid phases. Quenchers make non-radiative relaxation routes more favourable by intercepting the excited state. There is a simple relation between Φ_F and the quencher concentration, named as Stern-Volmer equation. The best-known quencher is probably O_2 , which quenches almost all fluorophores, other quenchers quench only a limited range of fluorophores. If a molecule is subjected to intramolecular quenching, Φ_F may yield information about the process. When an emission spectrum is obtained, data are typically collected for more than 0.1 sec. at each wavelength increment (typically 1 nm), but since fluorescence lifetimes typically is measured in nanoseconds, it follows that the obtained spectrum is a time-average of many events. The time-averaging loses much information, and time-resolved experiments are often more interesting when a system is investigated. The fluorescent lifetime of the excited state, τ , can be defined as the time required, after termination of the exciting radiation, for the fluorophore to decrease to 1/eth of its previous value and can be expressed as the inverse of the depopulation rate:

$$\tau = 1 / (k_r + k_{nr}) \quad (3)$$

Typical excited state lifetime values are in the pico- to the nano-second range. The above expression is related to the expression for Φ_F , in that they have a common denominator. Actually, an approximation of τ can be obtained by measuring Φ_F in aird and degassed solutions. Fluorescence spectra are registered by the use of a fluorimeter, and a simple scheme of the instrument is reported in Fig 3.

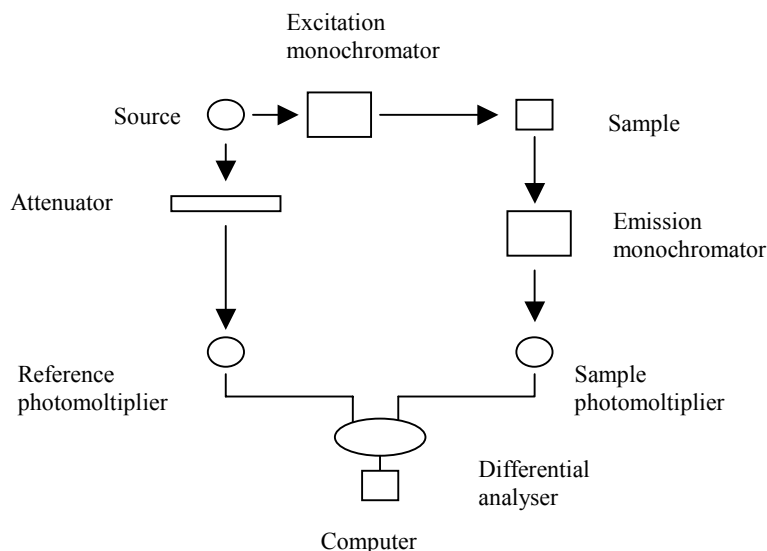


Fig. 3: Scheme of a spectrofluorimeter.

The components of spectrofluorimeters are analogous to those of a UV-Visible spectrophotometers. All instruments for fluorescence measurements are double beam to minimize the fluctuations in the light source. It is important to underline that, even if fluorescence emission is in every direction around the sample, it is more convenient to measure it at 90° with respect to the radiation of excitation. At other directions, the diffusion of the solution and of the cell increases the experimental error.

The complete description of all photophysical processes is beyond the purpose of this thesis. However, two other aspects: polarisation and quenching of fluorescence, will be discussed in detail in the next paragraphs. [1, 2]

5.1.2 Concepts of fluorescence polarisation

The measurement of polarised fluorescence emission allows the observation of rotational motion in fluorophores during the lifetime of the excited state. A group of similarly oriented molecules are chosen or photoselected using a polariser in the excitation beam. The polarised components of fluorescence emission are measured using polariser(s) in the emission path. The schematic representation of this technique is reported in Fig. 4. Measurement of polarisation or anisotropy are usually performed by measuring the vertically and horizontally polarised components of the emission. Polarisation is defined as the ratio of the linearly polarised component's intensity divided by the natural light component's intensity. Anisotropy is defined as the ratio of the linearly polarised component's intensity divided by the total light intensity. On the choice for using polarisation or anisotropy for a measurement depends the mathematical treatment required for results.

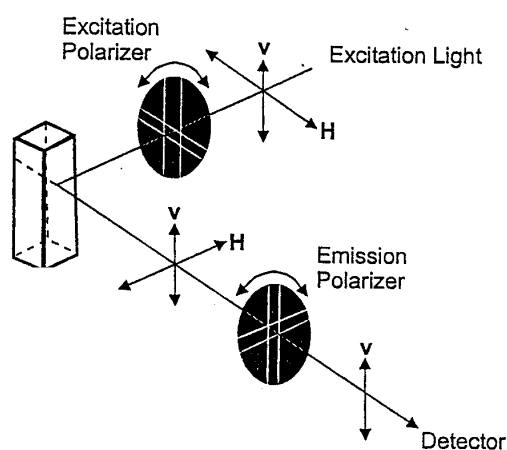


Fig.4: Scheme of the instrumentation for polarization measurements.

In an ideal system, polarisation (P) and anisotropy ($\langle r \rangle$) are measured using only the vertically polarised excitation with the horizontal and vertical emission components. These measurements can be designed I_{VV} and I_{VH} respectively. The first subscript indicates the position of the excitation

polariser, the second one that of the emission polariser. Vertically oriented polarisers (V) are said to be at 0° and horizontally oriented polarisers (H) are said to be at 90°. Polarisation and anisotropy can be expressed as follows:

$$P = \frac{(I_{VV} - I_{VH})}{(I_{VV} + I_{VH})} \quad (4)$$

$$\langle r \rangle = \frac{(I_{VV} - I_{VH})}{(I_{VV} + 2I_{VH})} \quad (5)$$

However, in a monochromator system, the grating factor G must be included to correct for the wavelength response to polarisation of the emission optics and detectors. The G factor is defined as:

$$G = G(\lambda_{EM}) = \frac{I_{HV}}{I_{HH}} \quad (6)$$

and the expression for P in a spectrophotometer becomes:

$$P = \frac{(I_{VV} - G \times I_{VH})}{(I_{VV} + G \times I_{VH})} = \frac{\frac{I_{VV} \times I_{HH}}{I_{VH} \times I_{HV}} - 1}{\frac{I_{VV} \times I_{HH}}{I_{VH} \times I_{HV}} + 1} \quad (7)$$

Note that both P and <r> are ratio quantities with no nominal dependence on dye concentration. [3]

5.1.3 Quenching of Fluorescence

Fluorescence quenching refers to any process which decreases the fluorescence intensity of a given substance. A variety of processes can result in

quenching. In this work, we consider only dynamic and static quenching. The former occurs when quenching results from collisional encounters between the fluorophore and the quencher, whereas the latter occurs when there is the formation of non emissive ground-state complexes. This is a frequent and complicated factor in the analysis of dynamic quenching.

In addition to the processes described above, apparent quenching can also occur due to a change in the optical properties of the sample. For example, high optical density or turbidity can result in decreased fluorescence intensity.

Fluorescence quenching has been widely studied both as a fundamental phenomenon and in the application of fluorescence to biochemical problems. Both static and dynamic quenching require molecular contact between the fluorophore and the quencher. In the case of collisional quenching, the quencher must diffuse to the fluorophore during the lifetime of the excited state. Upon contact, the fluorophore returns to the ground state without emission of a photon. In the case of static quenching, a ground state complex is formed between the fluorophore and the quencher, and this complex is non-fluorescent.

Collisional or dynamic quenching of fluorescence is described by the Stern-Volmer equation:

$$I_0/I = 1 + k_q\tau_0[Q] = 1 + K_D[Q] \quad (6)$$

In this equation I_0 e I are the fluorescence intensities in the absence and in presence of quencher, respectively, k_q is the apparent bimolecular quenching constant, τ_0 is the lifetime of the fluorophore in the absence of quencher, $[Q]$ is the concentration of the quencher, and $K_D = k_q\tau_0$ is the Stern-Volmer quenching constant.

This equation can be derived in several ways. For example, it can be obtained by considering the proportion of excited fluorophores which decay by

emission. This fraction (I/I_0) is given by the ratio of the decay rate Γ ($=\tau_0^{-1}$) to the total decay rate in the presence of quencher ($\Gamma + k_q[Q]$),

$$\frac{I}{I_0} = \frac{\Gamma}{\Gamma + k_q[Q]} = \frac{1}{1 + K_D[Q]} \quad (7)$$

which is another expression for equation (6).

Quenching data are frequently presented as a plot of I_0/I versus $[Q]$ because I_0/I is expected to be linearly dependent upon the concentration of the quencher. Such plot yields an intercept of 1 on the y axis and a slope equal to K_D . It is important to recognise that observation of a linear Stern-Volmer plot does not prove that collisional quenching of fluorescence has occurred. In fact a similar plot can be obtained for a static quenching.

In static quenching, the dependence of the fluorescence intensity upon the quencher concentration is easily derived by consideration of the association constant for ground state complex formation. This constant is given by:

$$K_S = \frac{[F-Q]}{[F][Q]} \quad (8)$$

Where $[F-Q]$ is the concentration of the complex and $[F]$ is the concentration of uncomplexed fluorophore. If the complexed species is non fluorescent, then the fraction of the fluorescence which remains (F/F_0) is given by the fraction of the total fluorophores which is not complexed (F). That is $f = F/F_0$. Recalling that the total concentration of the fluorophore $[F_0]$ is given by:

$$[F_0] = [F] + [F-Q] \quad (9)$$

after some arrangements we obtain:

$$\frac{F_o}{F} = 1 + K_s [Q] \quad (10)$$

Note that the dependence of F_o/F on $[Q]$ is identical to that observed for dynamic quenching, except that the quenching constant is now the association constant. In this case, if F_o/F vs. $[Q]$ is plotted, a linear dependence is found only at concentration values of the quencher that are lower than that at the saturation point. When all the fluorophore molecules are associated to the quencher a plateau is reached. Distinguishing between the two modes lifetimes, temperature or viscosity dependence of quenching can be very useful. [1]

5.2 Ethidium Bromide and Hoechst 33258: fluorescent probes for DNA

In studying DNA, the use of fluorescent probes is very common. Some compounds, even if they are not fluorescent in aqueous solution, become fluorescent when associated to DNA. This property is very useful for using fluorescence spectroscopy to obtain information regarding DNA structure or the interaction of DNA with other additives present in solution.

Ethidium bromide (EB), a fluorescent probe reported in Fig. 5, is one of the most used probes for DNA. It is generally agreed that strong fluorescence enhancement accompanies intercalation of the dye into the double helix of DNA. The intercalation process is not very specific, but a preference for A-T rich region is observed.

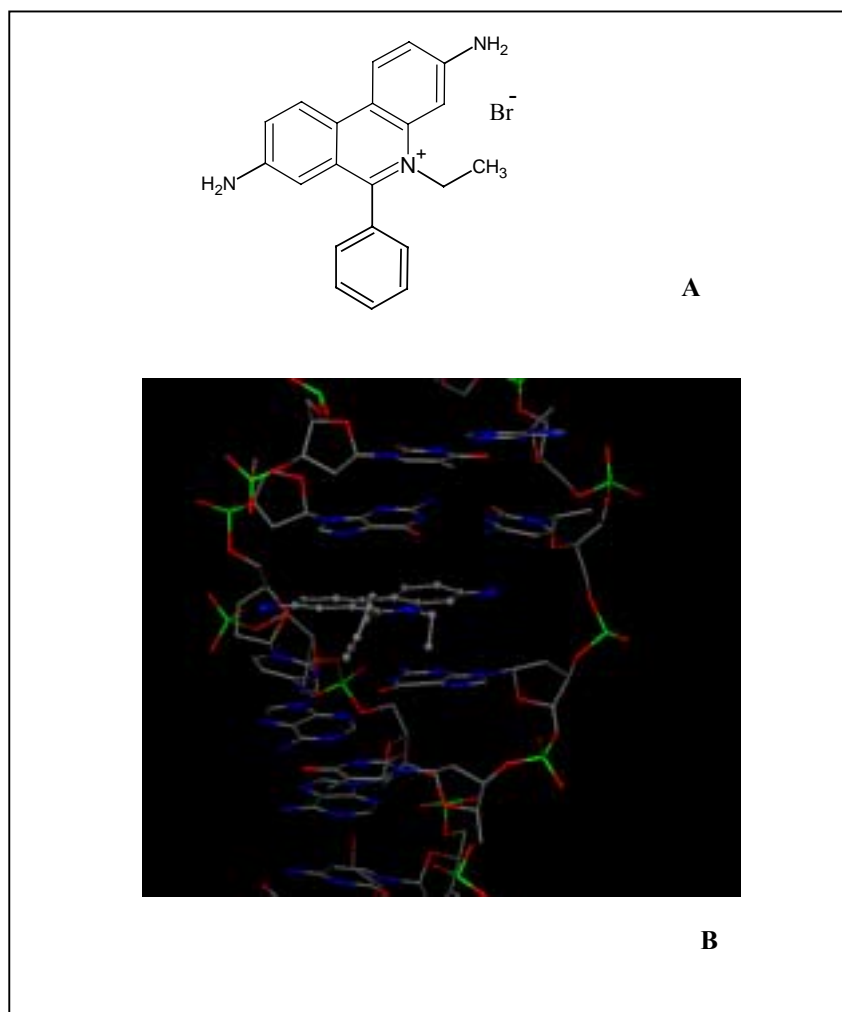


Fig. 5: A) Ethidium Bromide structure; B) Imagine of EB intercalated into a double helix DNA by molecular modelling.

Several attempts to explain the high degree of fluorescence enhancement for EB upon intercalation were proposed since the seventies, taking in account, for example, interchange of n , π^* and π , π^* states, or “base specific” interactions. Despite of this, the interaction of EB with the solvent seems to have a great effect in the fluorescence intensity. [4] The effect of different solvents on the fluorescence lifetime of EB is reported in Table 1.

Solvent	τ_0 (ns)	λ_{\max} (nm)
H ₂ O	1.8	480
Me ₂ SO	5.0	535
Pyridine	5.8	540
Glycerol	5.9	515
Methanol	6.0	520
Ethanol	6.9	532
Acetone	9.3	520

Table 1: Solvent effect on EB fluorescence

Data on the solvent effect and the observation of the quenching of fluorescence by proton acceptors, and substantial lengthening of lifetimes upon deuteration of the amino protons confirmed that proton transfer from the singlet excited state is the process primarily responsible for the low fluorescence yield in most polar solvents. Enhancement of fluorescence upon intercalation is attributed to a reduction in the rate of excited state proton transfer to solvent molecules. [5] In Fig. 6 the absorption and emission spectra for EB probe are reported.

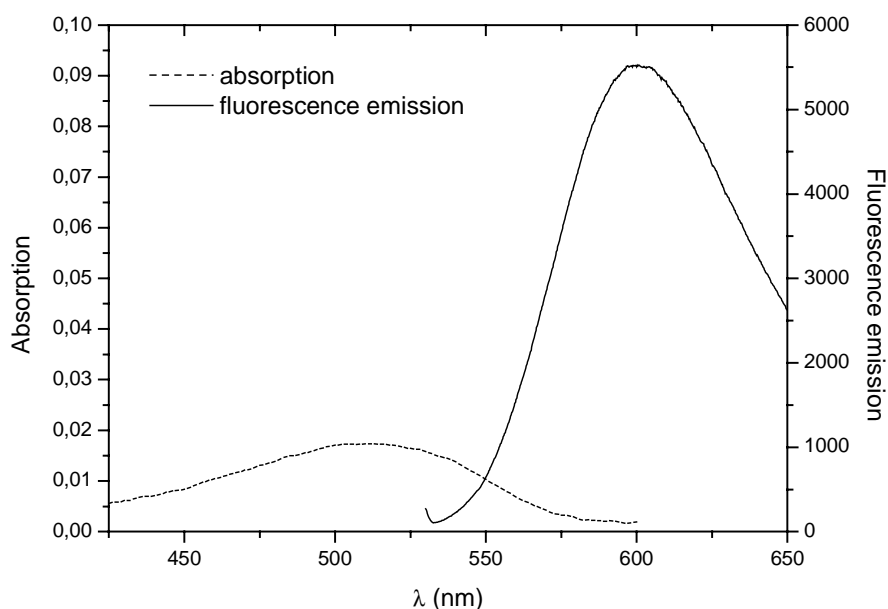


Fig. 6: Absorption and emission spectra for Ethidium Bromide in Tris-HCL buffer, pH= 5.9, [DNA]= 2.0×10^{-5} M, [EB]= 4.2×10^{-6} M.

Another probe used in the study of the interactions with double strand DNA and cells is Hoechst 33258. This dye has a benzimidazole structure and it is constituted by four rings, a phenol, two benzimidazole and a piperazine unit (see Fig. 7 for structure).

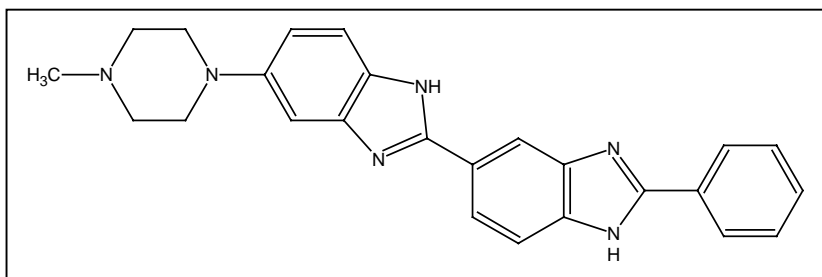


Fig. 7: Structure of Hoechst 33258.

Hoechst 33258, unlike ethidium bromide, does not intercalate into DNA, but binds the biomolecule in the minor groove at A-T rich sites. [7, 8] Two modes of association are possible and have been crystallised, where the molecule is only turned of 180° (Fig. 8). In both positions, H-bonding, electrostatic and van der Waals interactions play a significant role.

The quantum yield of fluorescence for this probe in neutral aqueous solution is 0.034 but it is strongly pH dependent. It decreases from a maximum of $\Phi_f = 0.4$ at pH=5 to 0.02 at pH 8. [6] In the presence of DNA in aqueous solution, its fluorescence intensity increases. The origin of this enhanced fluorescence upon increasing the ratio of base pairs to dye molecule is under discussion.

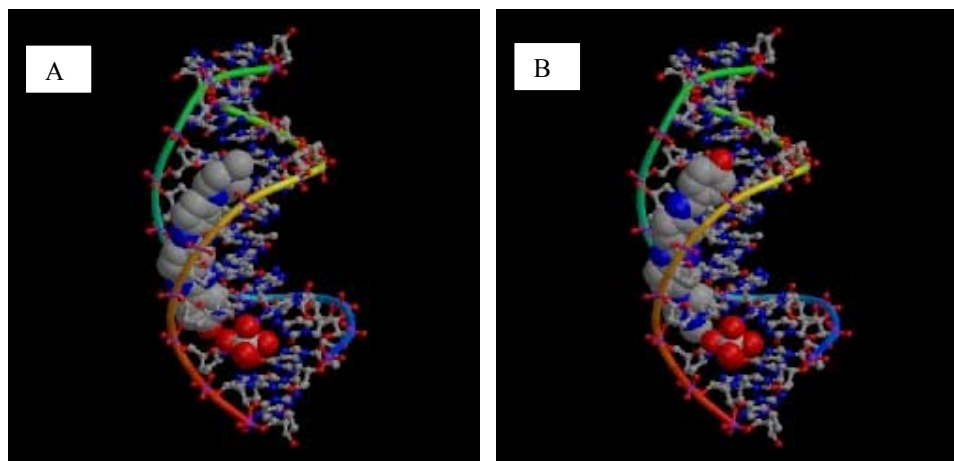


Fig. 8: Crystallographic structures of Hoechst 33258 bound to the DNA duplex C-G-C-G-A-A-T-T-C-G-C-G[8]A) piperazine down; B) piperazine up.

In Figure 9 the spectra of absorption and emission for Hoechst 33258.

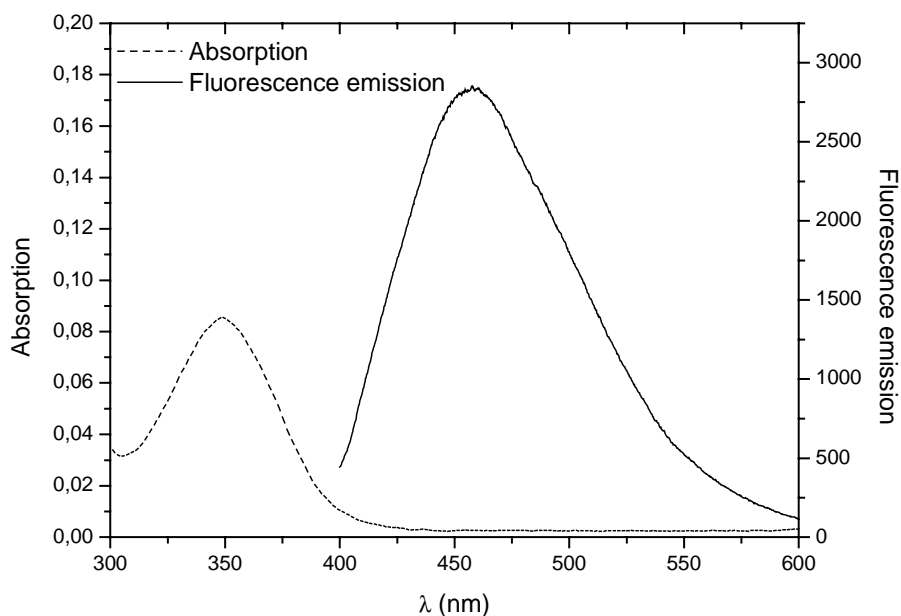


Fig. 9: Absorption and emission spectra for Hoechst 33258 in Tris-HCl buffer, pH= 7.4, [DNA]= 2.0×10^{-5} M, [Hoechst]= 2.0×10^{-6} M.

5.3 DNA-surfactant interaction: the use of fluorescence spectroscopy

The use of fluorescence spectroscopy to study the interaction between DNA and surfactants is quite common, since the technique is easy and inexpensive. This technique requires a fluorescent probe associated to DNA, and ethidium bromide is certainly the most utilised. As previously mentioned, the strong intercalative ability of ethidium bromide is well-known in literature. To study the possible interaction of surfactants or salts with DNA, the changes in the fluorescence emission spectra of the complexed ethidium bromide is followed by adding progressively increasing amounts of surfactants or salts solution, as reported in literature. [9-11]

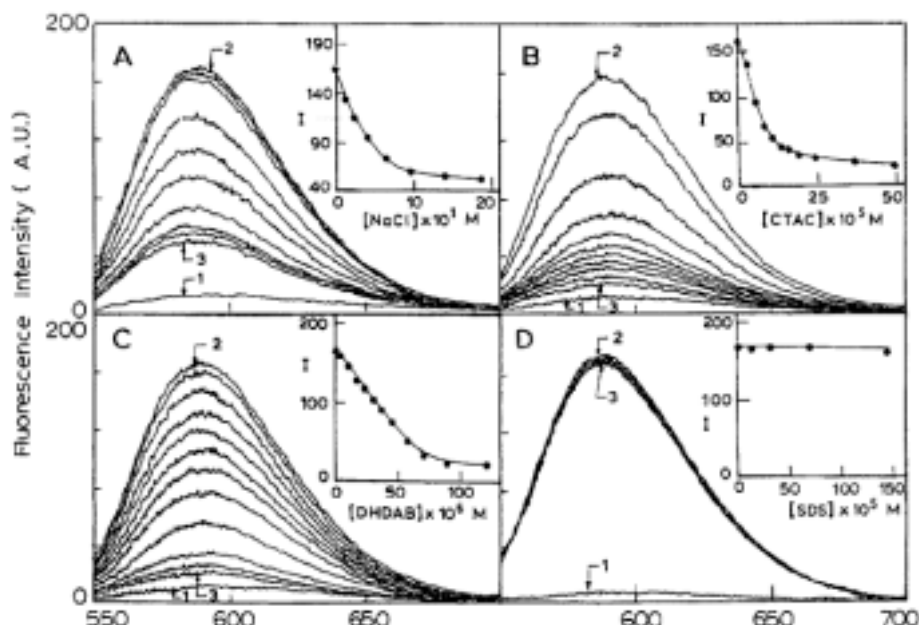


Fig. 10: Effect of addition of different additives on DNA-bound ethidium bromide. This experiment was carried out by adding increasing amounts of additives into the probe-DNA complex, and recording the fluorescence emission spectra after each addition. Panels A, B, C and D in this figure show the effect of NaCl, cetyl trimethylammonium chloride (CTAC), dihexadecyldimethylammonium bromide (DHDAB) and sodium dodecyl sulfate (SDS) respectively into the intercalated EB-DNA complex. [9]

It was found that the addition of single- or twin-chain cationic surfactants leads to a quenching of the fluorescence intensity at very low concentration of surfactants, whereas the addition of SDS (negative charged) to the DNA-EB solution does not decrease the fluorescence of the fluorophore. Salts like NaCl can equally quench the fluorescence, but only at very high concentration, as reported in the Fig. 10. [9] The hypothesis formulated by Bhattacharya et al. [10] is that the apparent quenching in the fluorescent emission intensity upon the addition of increasing amounts of salts or cationic surfactants could be due to a gradual release of the bound fluorescent probe (ethidium bromide) out of the probe-DNA complex. This would be due to salt- or cationic surfactant-induced perturbation of DNA organisation, leading to dissociation of the probe from the probe-DNA complex. Although the efficiency in affecting the destabilisation of the probe-DNA complex varies widely, all additives, salts,

organic cation or cationic surfactant could influence the probe-DNA complex stability. However, the addition of SDS could not affect the stability of DNA-bound ethidium bromide complex to any significant extent even at high concentration. This could be due to the lack of the interaction between anionic surfactant aggregates and the polyanionic DNA. It was also found that the quenching of fluorescence is a reversible process. [10] The addition of SDS in a solution containing already DNA-EB and CTAC, restores the fluorescent intensity of the EB-DNA complex. Other studies on the interactions between surfactants and the DNA-EB complex were performed by Eastman, [11] using liposomes. In this case it was shown that the DNA/ EB ratio is also very important for the interpretation of the experimental data. Indeed, if the saturation level of DNA with EB is reached, the fluorescence intensity becomes not dependent of variation in the DNA: EB ratio.

5.4 Results and discussion

5.4.1 Amphiphilic systems

For a better understanding of the driving forces involved in the interactions between DNA and surfactants, experiments similar to those reported by Bhattacharya were performed, using a larger number of surfactants with very different structures. As already reported in the first chapter of this thesis, it is known that small differences in the surfactant structure are often responsible for a great change in the physical properties of the aggregates. [12] The structures of the surfactants used for fluorescence studies are reported in Fig.11 and Fig. 12. We limited our study to cationic and zwitterionic surfactants, taking into account that anionic surfactants were not able to interact with DNA because the repulsion with phosphate groups. [13] Some of

the surfactants considered in this chapter were already investigated by Circular Dichroism (see Chapter 2).

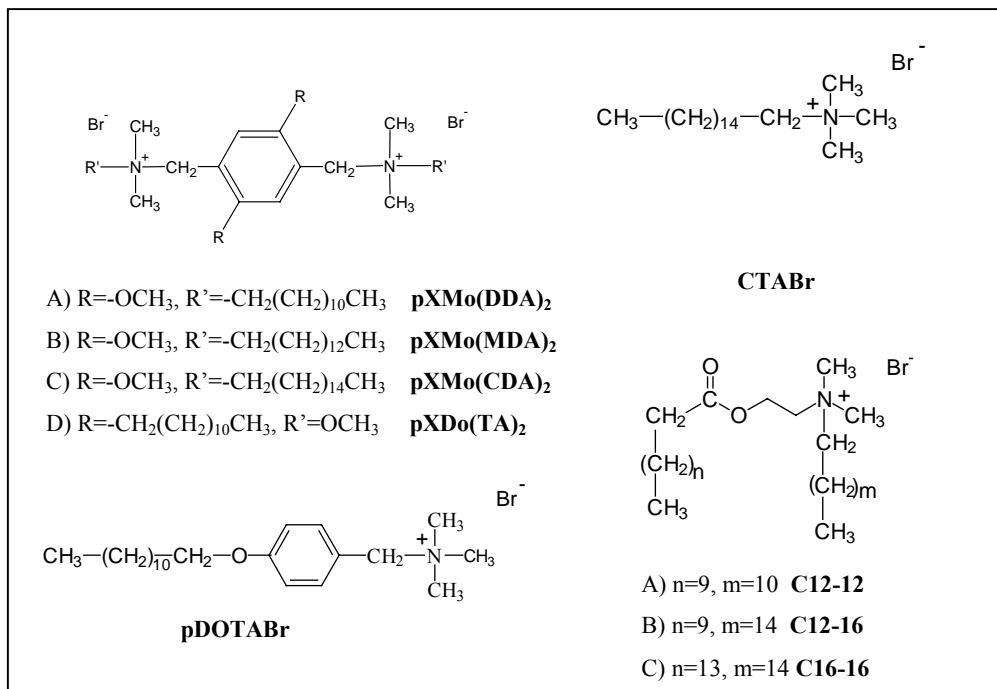


Fig. 11: Cationic surfactants studied by fluorescence spectroscopy.

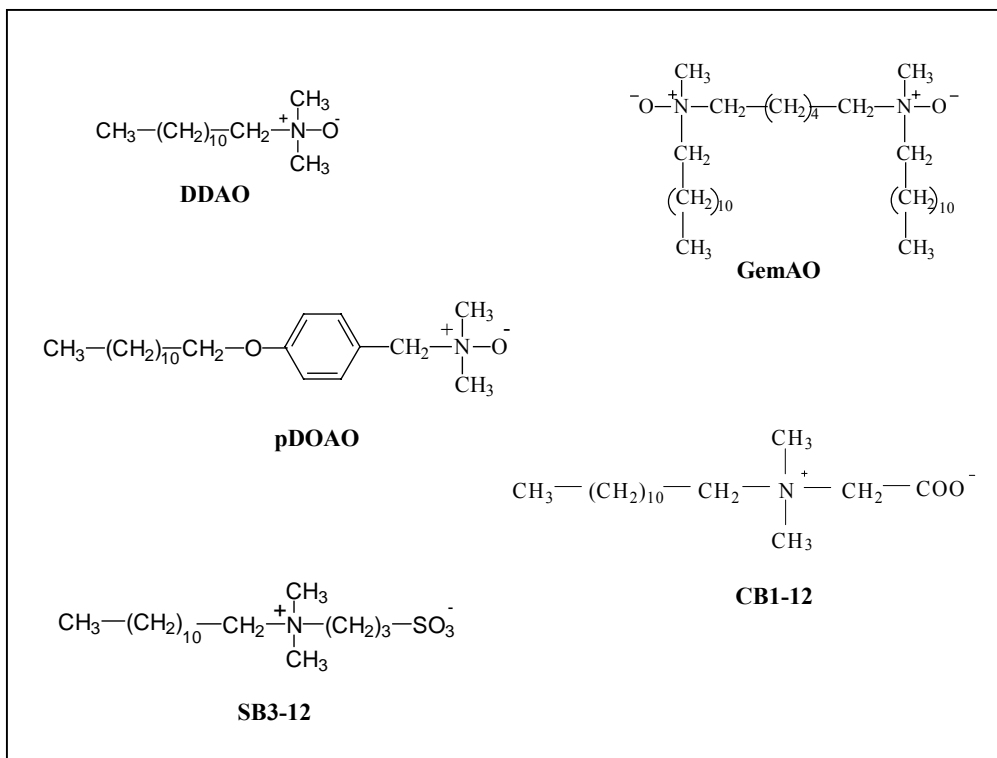


Fig. 12: Zwitterionic surfactants studied by fluorescence spectroscopy.

5.4.2 Preliminary investigation

To begin, we studied the fluorescence intensity of intercalated EB upon four additions of surfactant, to have a ratio $[\text{Surfactant}]/[\text{DNA}]$ equal to 1, 2, 3, 4. The results obtained are in agreement by those reported by Bhattacharya, and the polar moiety of the amphiphilic systems seems to be very essential in the decrease of EB fluorescence. In fact, cationic gemini surfactants lead to a greater quenching of fluorescence with respect to the monocharged cationic surfactants, whereas zwitterionic surfactants (both single chain and gemini), at least at pH 7.4, do not show any interaction with the DNA-EB complex. Fig. 13 reports the decrease of fluorescence obtained by three surfactants as an example (Table 1, Appendix IV).

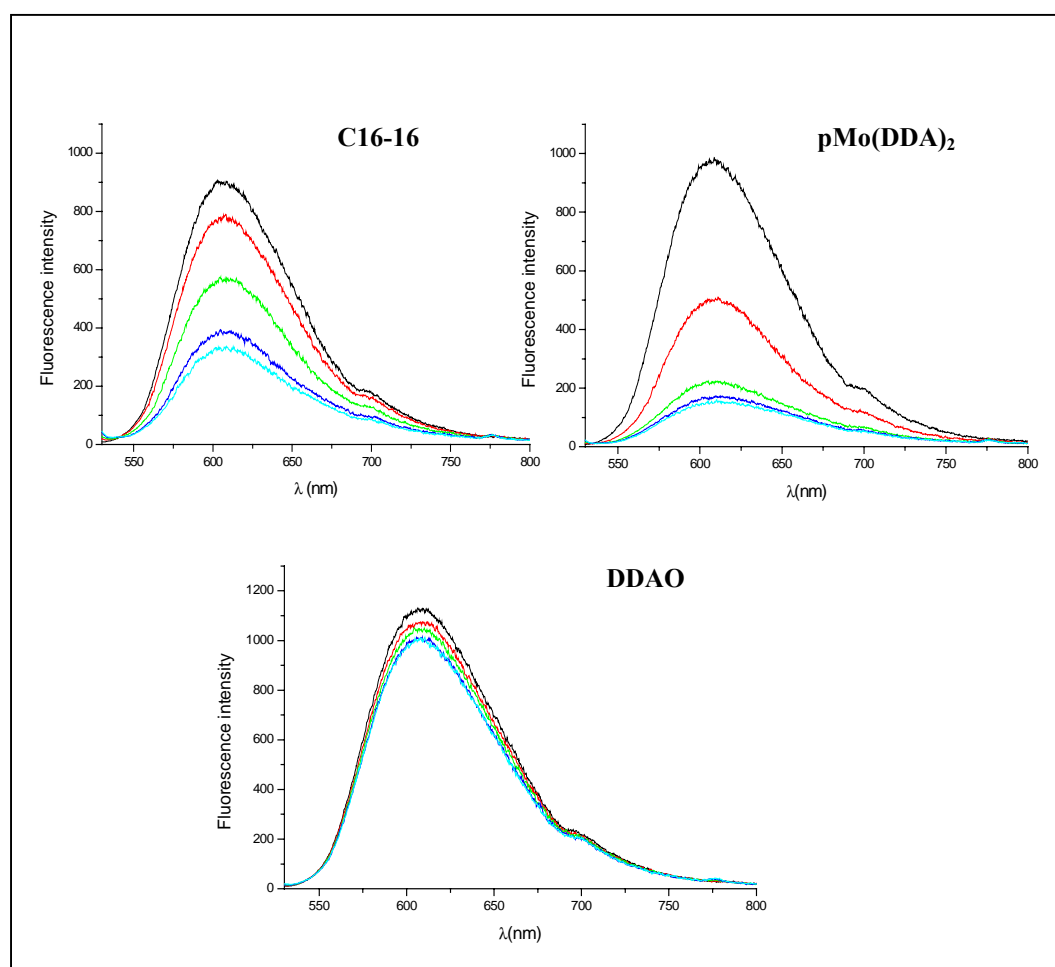


Fig. 13: Decrease of fluorescence intensity of the EB-DNA complex upon addition of surfactant solution. $[\text{surfactant}]/[\text{DNA}] = 1, 2, 3, 4$.

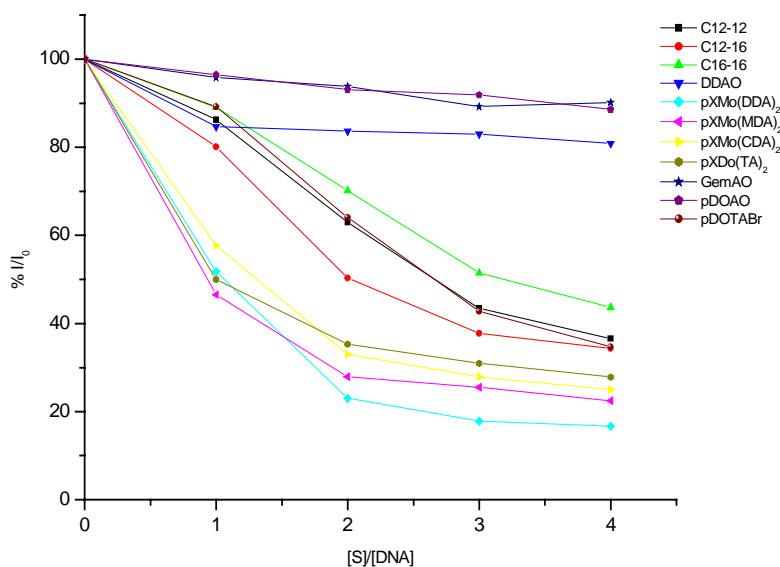


Fig. 14: Quenching of fluorescence upon addition of surfactant solution up to a final ratio [surfactant]/[DNA]=4. [DNA]= 2.0 x 10⁻⁵ M.

On the basis of these results, the following questions arose: 1) is the observed quenching of fluorescence really due to the exclusion of the ethidium bromide from DNA, due to the interactions of the surfactants with the biomolecule? 2) Might a specific interaction between the fluorescent probe and the amphiphile occur?

To better understand the reasons causing the quenching of EB fluorescence, studies on the interaction of the fluorescent probe with surfactants in the absence of DNA were performed. To this end, and considering that ethidium bromide has a very low fluorescence yield in water, we performed these experiments in acetonitrile: EB shows a good fluorescence intensity in this solvent and its dielectric constant is similar to that in water. Moreover, surfactants dissolved in acetonitrile are considered unable to aggregate into micelles, so that they can be considered in their monomeric form even at relatively high concentrations.

For estimating the origin of quenching caused by surfactants, three surfactants were investigated: we chose pXMo(DDA)₂ for its high quenching

effect on EB fluorescence, and two zwitterionic surfactants (pDOAO and DDAO) with different hydrophobic moieties (see Fig. 12 for structures). All of them are quite soluble in acetonitrile. To verify the Stern-Volmer equation, we operated as reported in the experimental section. Having plotted the I_0/I values versus $[Q]$, we measured the lifetime of the Ethidium Bromide in acetonitrile by the single photon counting technique (10,1 ns). The data obtained for pXMo(DDA)₂ and DDAO are reported in Table 1.

surfactant	K_{sv}	k_q ($M^{-1}s^{-1}$)
pXMo(DDA) ₂	170	1.7×10^{10}
DDAO	87	8.7×10^9

Table 1: Values of Stern-Volmer constant (K_{sv}) and of the bimolecular quenching constant (k_q) for surfactants pXMo(DDA)₂ and DDAO in acetonitrile.

These data indicate that dynamic quenching occurs for both surfactants; in fact, the dynamic quenching is limited only by the rate of diffusion of the reactives, and this value is $2,2 \times 10^{10} M^{-1} s^{-1}$ in acetonitrile. [14] Fig. 15 reports the plots used for the calculation of the Stern-Volmer constant (Tables 2 and 3, Appendix IV).

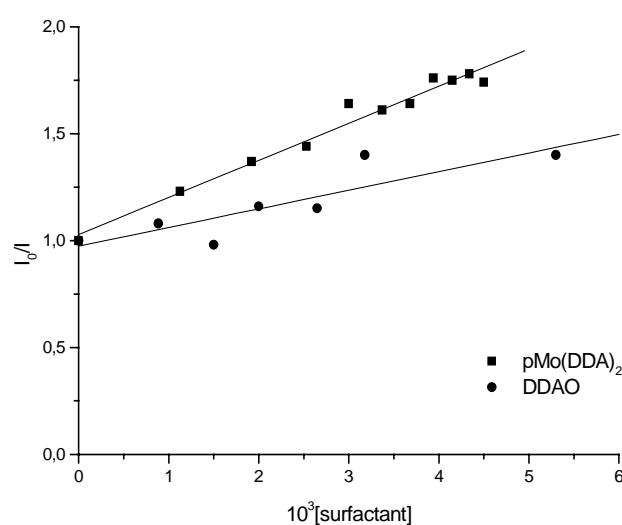


Fig. 15: Plot of I_0/I vs. $[\text{surfactant}]$ for pXMo(DDA)₂ and DDAO in acetonitrile.

Different results were obtained with pDOAO. A rapid loss of color of the solution after the addition of surfactant solution, clearly indicating an interaction at the ground state, as revealed also by absorption measurements (see Fig. 16).

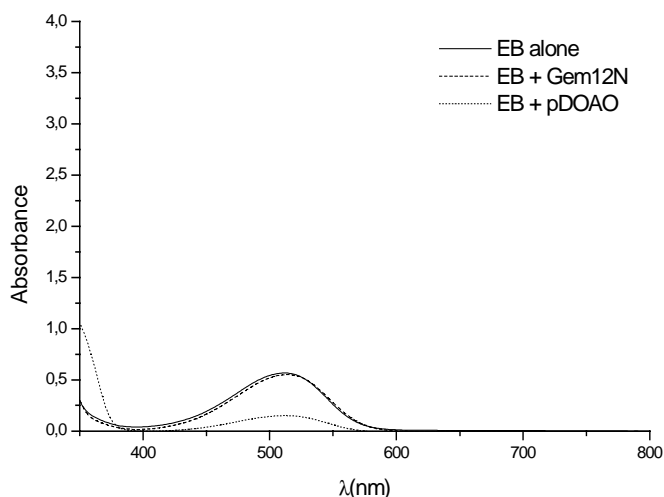


Fig. 16: Comparison of the absorption spectra for EB alone, EB upon addition of $pMo(DDA)_2$ and EB upon addition of pDOAO in acetonitrile.

The following step was to record the absorption spectra of the system DNA-EB-surfactant under the same conditions of the fluorescence experiment in aqueous solution. Because of the very low molar extinction coefficient of the ethidium bromide in water, cuvettes of 10 cm path length were used. Surprisingly, a scattering is observed for $pXMo(DDA)_2$ even at very low concentration of surfactant, as reported in Fig. 17. Because the solutions are well below the c.m.c. of the surfactants, it can be deduced that EB promotes the formation of aggregates.

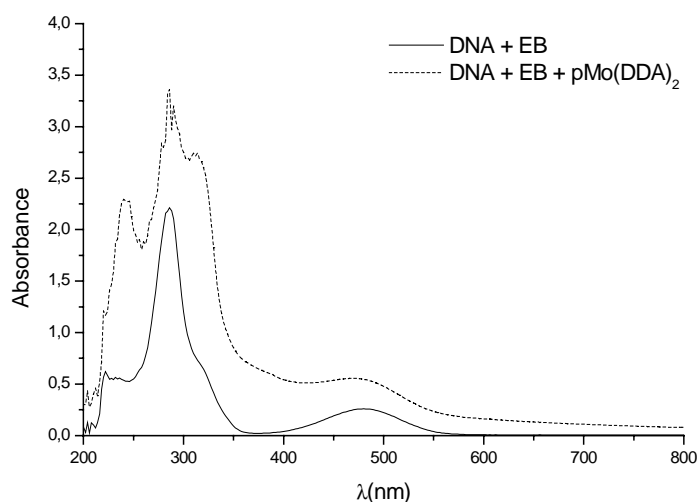


Fig. 17: Absorption spectra of EB-DNA complex alone and upon addition of gemini surfactant pXMo(DDA)₂ in aqueous solution.

5.4.3 The use of Hoechst 33258 probe in studying DNA-surfactants interaction.

To better understand the ground state behaviour ethidium bromide, we decided to use another fluorescence probe for comparison.

Hoechst 33258 (Fig. 7) was selected for the following reasons:

a) It does not intercalate into DNA, but the association with the biomolecule is at the minor groove level. The more superficial interaction, on the basis on the modelling results and of the hypothetical structures in literature, in principle allows a more sensitive investigation on what happens at the DNA-surfactant interface.

b) It is pH dependent, and information related to change of pH in the microenvironment of the DNA surface can be obtained.

Only one report on the use of this probe for studying surfactants has been published to date. [6] In this case, however, the interactions DNA-probe and probe-surfactants (in the absence of DNA) were considered separately.

We have already discussed on the pH dependence of Hoechst fluorescence in the probe-DNA complex. Moreover, results obtained for the Hoechst-surfactant systems showed that both for anionic (SDS) and cationic (CTABr) surfactants, an increase of the concentration of the surfactant results in an increase of the intensity of fluorescence. A sigmoid behaviour is obtained and the concentration value at the flex of the curves ($\text{conc}_{1/2}$) is often very close to the c.m.c. value of the surfactant.

In this work, two aspects were studied: first, the interaction between Hoechst 33258 and amphiphilic systems in the absence of DNA. Second, the interactions between DNA and surfactants using Hoechst on the basis of the results obtained for ethidium bromide. For a better description of the results, the experiments with cationic or zwitterionic surfactants will be reported separately.

5.4.5 Interaction between cationic surfactants and Hoechst 33258

5.4.5.a In the absence of DNA

Similarly to the studies reported by Gerner, [6] a preliminary investigation on the interactions between the fluorescent probe and cationic systems was performed. Each surfactant was investigated over the range of concentration that was near the c.m.c. value in water, to verify if changes in the fluorescence of the probe occur when micelles are formed.

Fluorescence emission obtained with various new cationic surfactants are shown in Fig. 18. The increase of probe emission in the presence of surfactant molecules can be explained with the insertion of the probe in a “micellar” environment, which is an environment of lower polarity with a reduced water content. (Tables 4-7, Appendix IV).

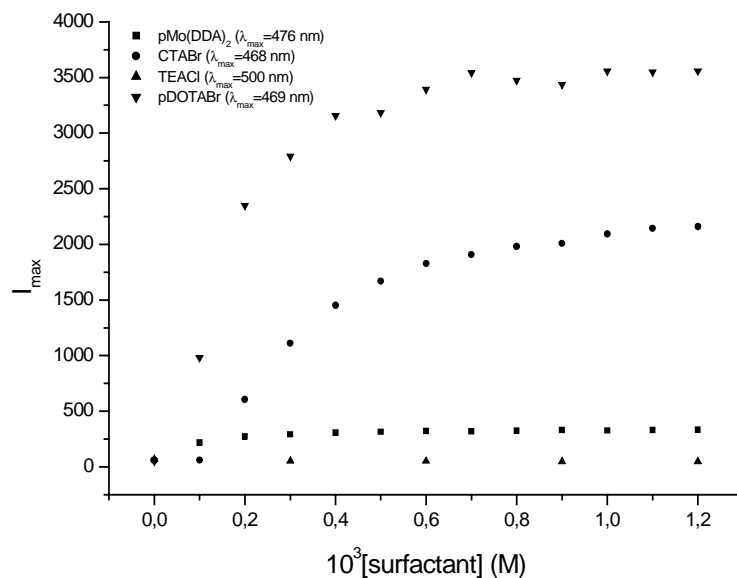


Fig. 18: Variation of I_{max} in function of the concentration of surfactant in 50 mM Tris-HCl buffer (pH= 7.5) in absence of DNA.

To verify if the only driving force in the process was the amount of water available to the probe, we compared these results with those previously obtained in our laboratory by kinetic studies. In fact, the decarboxilation of 6-nitrobenzoxazole-3-carboxilate (6-NBIC) performed in surfactant solutions allows to obtain information on the amount of water at the surface of the micellar system. [12]

By comparing the kinetic data at our disposal, [15-17] we found that for the case of the monocharged cationic surfactant, similar behaviour is obtained (pDOTABr seems to contain a lower amount of water at the microinterface in respect of CTABr). In contrast, for pMo(DDA)₂ we found lower values of fluorescence intensity, although we have already shown that such systems should be more “packed” at the microinterface. [17] If the amount of water is the only driving force in Hoechst’s fluorescence, a higher fluorescence value should be expected. Thus, this result suggests that in the case of gemini pMo(DDA)₂ other factors can be responsible for the fluorescence quenching.

5.4.5.b In the presence of DNA

For comparing data obtained using EB, similar experiments were performed with CTABr and pMo(DDA)₂ using Hoechst 33258. Results obtained with Hoechst are very similar to those obtained with the Ethidium Bromide, and cationic gemini surfactants show a larger effect in fluorescence quenching than CTABr. The experiments were conducted at a single pH value of 7.5, since cationic surfactants are not sensitive to a pH-change.

One of the main advantages in using Hoechst 33258 rather than EB is that the former can be followed also in absorption using a standard fluorescence cuvette of 1 cm optical path. This allows one to conduct experiments recording both the absorption and the fluorescence spectra for each addition of surfactant solution. Results obtained for CTABr are reported in Fig. 19 A and B.

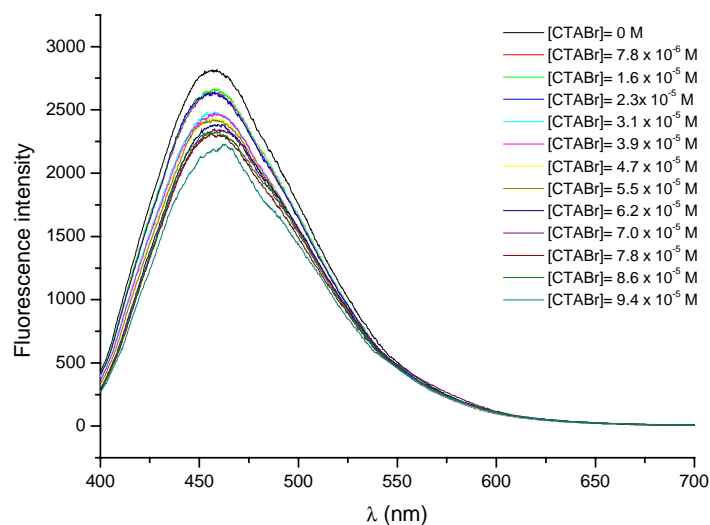


Fig. 19-A: Variation of fluorescence intensity of the Hoechst/DNA complex in 50 mM Tris-HCl buffer (pH= 7.5) upon addition of CTABr. [DNA]= 2.0 x 10⁻⁵ M; [Hoechst]= 2.0 x 10⁻⁶ M.

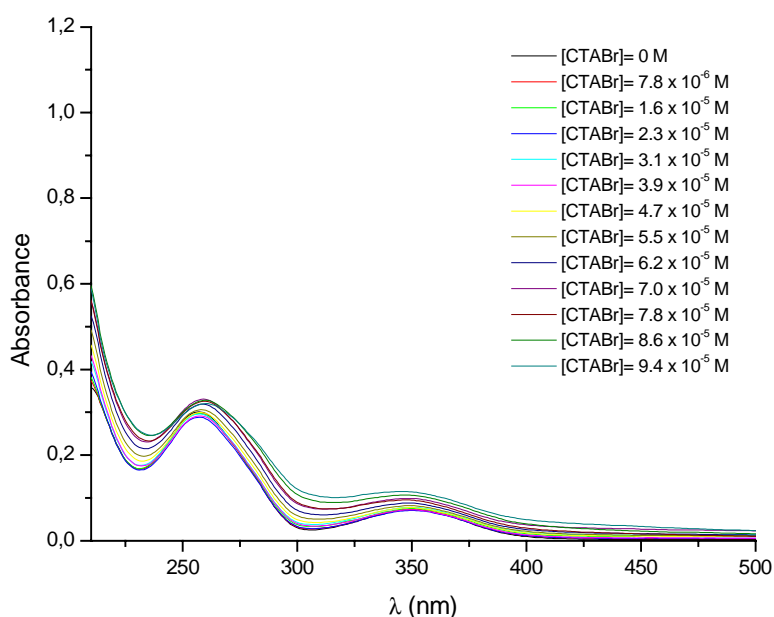


Fig. 19-B: Variation of absorbance of the Hoechst/DNA complex in 50 mM Tris-HCl buffer (pH= 7.5) upon addition of CTABr. [DNA]= 2.0×10^{-5} M; [Hoechst]= 2.0×10^{-6} M.

From these results, it is possible to see that, at $[CTABr] > 4 \times 10^{-5}$ M, scattering of the light appears, growing with the concentration of the surfactant. Considering that the concentration of DNA in cuvette is 4×10^{-5} M (expressed in base molar) it seems that scattering appears at a concentration of surfactant enough to neutralise the negative charges of phosphate groups, possibly leading to the precipitation of DNA-surfactant complexes. In fact, a careful inspection of the sample at the end of the additions evidences some precipitation.

In order to exclude that the precipitation could be related, for example, to a minor solubility of the surfactant in the buffer solution, or to some interactions between the probe and CTABr, we registered the absorption spectra of the surfactant alone in buffer solution at the same concentrations and such phenomenon did not occur. Then, we measured the absorption spectra of a buffer solution of DNA adding CTABr at increasing concentrations, in the absence of Hoechst. In these conditions the precipitation took place, growing at every addition of surfactant solution. The precipitation is thus related only to the neutralisation of the charge at the DNA surface.

It was thus hypothesised that by increasing the concentration of surfactant in cuvette at values above their c.m.c., the system could affect the organisation and could resolubilise the DNA. Experiments conducted with CTABr and pXMo(DDA)₂ did not support this hypothesis.

5.4.6 Interaction between zwitterionic surfactants and Hoechst 33258

5.4.6.a In the absence of DNA

Fig. 20 and 21 show the results obtained for the fluorescence intensity of the probe upon addition of zwitterionic surfactants, at concentrations both above and below to the c.m.c. values. For the pDOAO, the range of concentration considered is lower than those of other surfactants, because of its very low c.m.c. value (1.6×10^{-5} M in water).

In the case of SB3-12, a sigmoidal behaviour is obtained in agreement with results obtained by Gorner for sodium dodecylsulfate and CTABr.

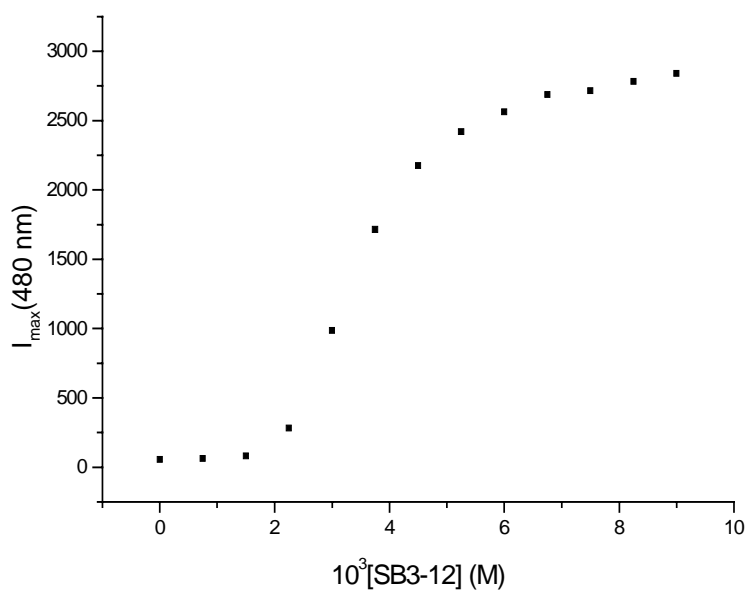


Fig. 20: Variation of I_{max} in function of the concentration of SB3-12 in 50 mM Tris-HCl buffer (pH= 7.5) in absence of DNA. [Hoechst]= 2.0×10^{-6} M.

For pDOAO, a rapid increase of fluorescence by increasing the surfactant concentration is also observed, even if at lower concentrations. However, because of problems in the viscosity of the systems, we could not perform measurements at higher concentrations of pDOAO. Surprisingly, at least in the range of concentration investigated, the amine-oxide DDAO does not induce any change in the Hoechst's fluorescence (Tables 8-11, Appendix IV).

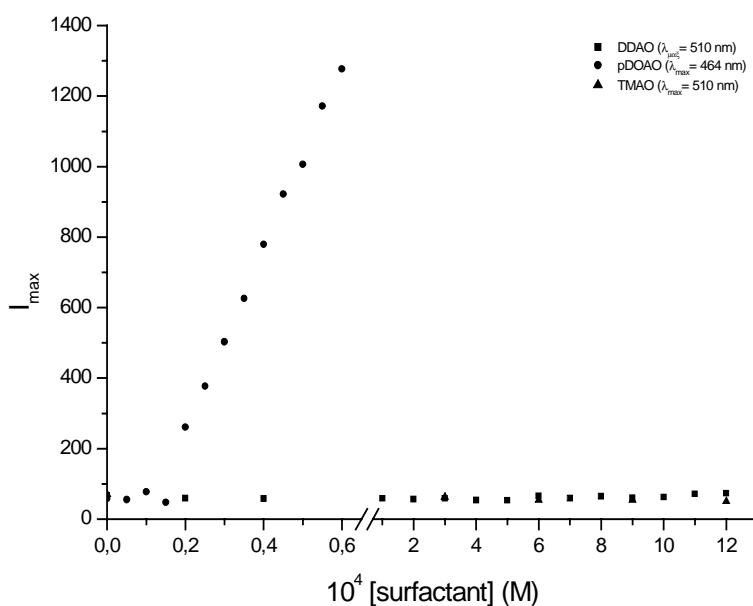


Fig. 21: Variation of I_{\max} in function of the concentration of surfactants in 50 mM Tris-HCl buffer (pH= 7.5) in the absence of DNA. [Hoechst]= 2.0×10^{-6} M.

5.4.6.b In the presence of DNA

In analogy with Circular Dichroism experiments, the zwitterionic surfactants were investigated in the range of concentration above and below the c.m.c. values and at two pH values: 7.5 and 5.8. We limited these studies to DDAO and pDOAO, to know if the variation in terms of the hydrophobic moiety could interfere with the interaction with DNA. Results obtained for DDAO are in agreement with those obtained by Circular Dichroism. In fact, at neutral pH we do not observe any interaction with DNA both above and below c.m.c. value (Fig. 22-A and B). On the contrary, repeating the experiments at

pH= 5.8, we found that the fluorescence decreases at concentrations of DDAO higher than c.m.c. value (Figures 23-A and B). This suggests that, in these conditions, DDAO can interact with DNA due probably to a partial protonation of the DDAO molecules. This hypothesis is confirmed by the fact that precipitation seems to occur at higher concentration of surfactant, as observed for cationic surfactants, even if the neutralisation process arrives at concentrations that are higher than 4×10^{-5} M (due to the fact that at this pH value only a fraction of the amine-oxide is protonated). Contrary to what observed for cationic surfactants, in the case of DDAO the decrease of fluorescence intensity for the probe is also accompanied by a shift of the maximum of intensity to lower wavelength, similar to that observed at pH=7.5. It can also be hypothesised that the decrease of fluorescence intensity can be due to the expulsion of the probe from DNA, but this hypothesis cannot explain the shift in the λ_{\max} of emission. Moreover, we have already reported that DDAO does not interact with Hoechst in absence of DNA, so that the hypothesis that Hoechst could go into a micellar aggregate can be excluded.

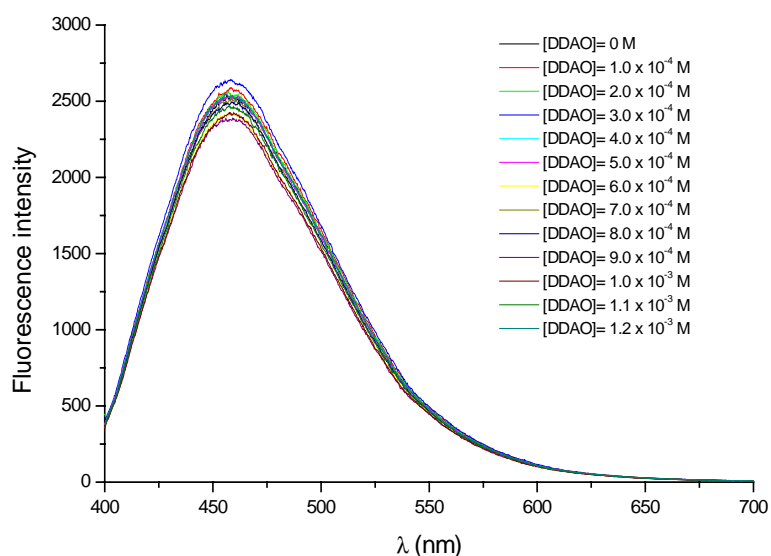


Fig. 22-A: Fluorescence intensity of Hoechst/DNA complex upon addition of DDAO in solution in 50 mM Tris-HCl buffer solution. [DNA]= 2.0×10^{-5} M, [Hoechst]= 2.0×10^{-6} M, pH= 7.5.

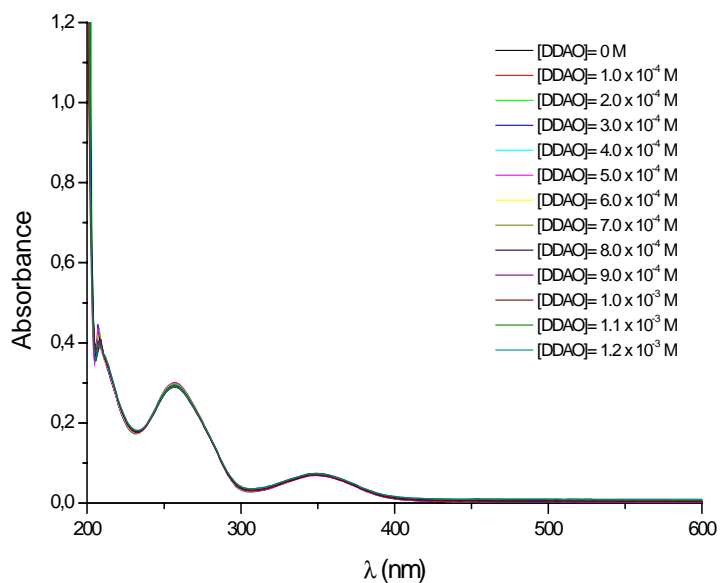


Fig. 22-B: Absorption of Hoechst/DNA complex upon addition of DDAO in solution in 50 mM Tris-HCl buffer solution. [DNA]= 2.0×10^{-5} M, [Hoechst]= 2.0×10^{-6} M, pH= 7.5.

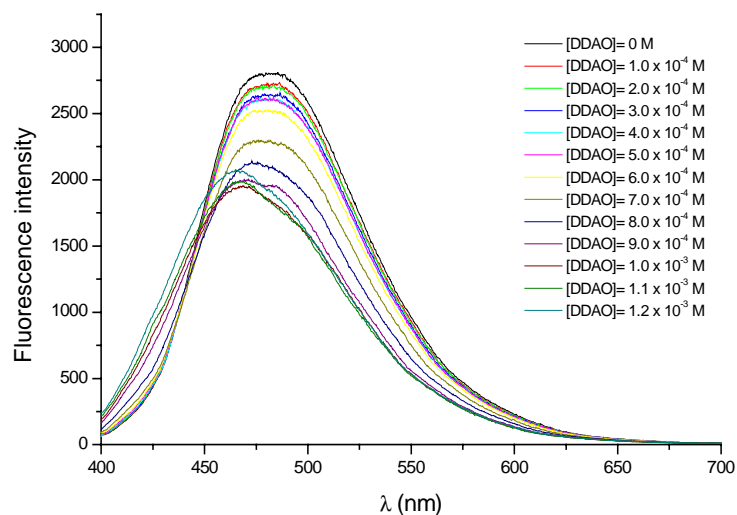


Fig. 23-A: Fluorescence intensity of Hoechst/DNA complex upon addition of DDAO in solution in 50 mM Tris-HCl solution. [DNA]= 2.0×10^{-5} M, [Hoechst]= 2.0×10^{-6} M, pH= 5.8.

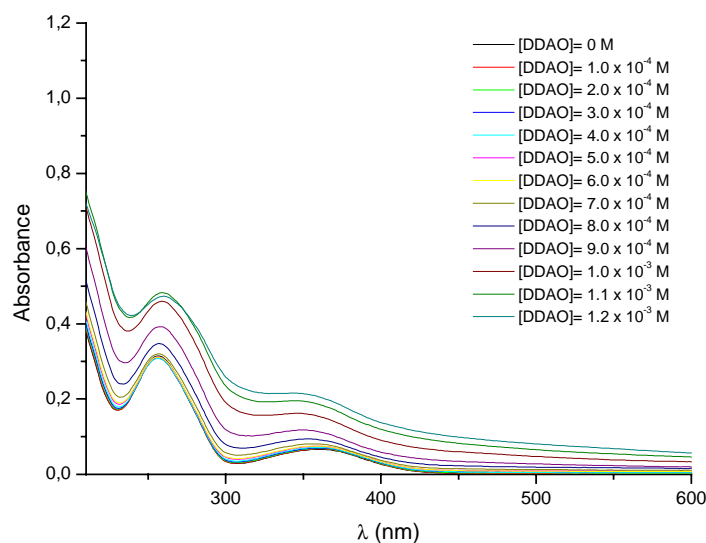


Fig. 23-B: Absorption of Hoechst/DNA complex upon addition of DDAO in solution in 50 mM Tris-HCl buffer solution. [DNA]= 2.0×10^{-5} M, [Hoechst]= 2.0×10^{-6} M, pH= 5.8.

We have also performed the same experiments using ethidium bromide instead of Hoechst, and no shift of the emission maximum was observed. A linear decrease of fluorescence intensity is found and only the measurement of the absorption spectra can evidence the presence of a scattering for higher concentration of surfactant (see Figures 24 A and B). These results cast serious doubts on the reliability of using simple Stern-Volmer kinetics to interpret complex surfactants-DNA interactions, as commonly done in the literature.

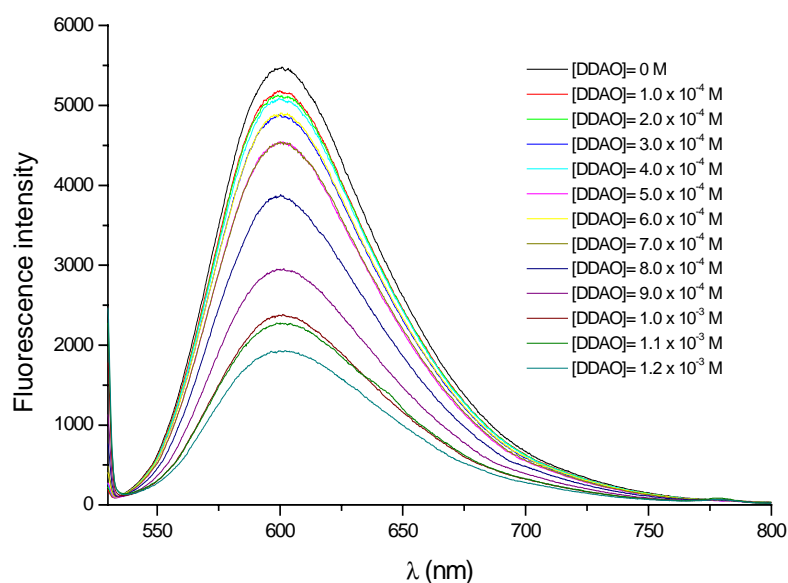


Fig. 24-A: Fluorescence intensity of EB/DNA complex upon addition of DDAO in solution in 50 mM Tris-HCl solution. [DNA]= 2.0×10^{-5} M, [EB]= 4.2×10^{-6} M, pH= 5.8.

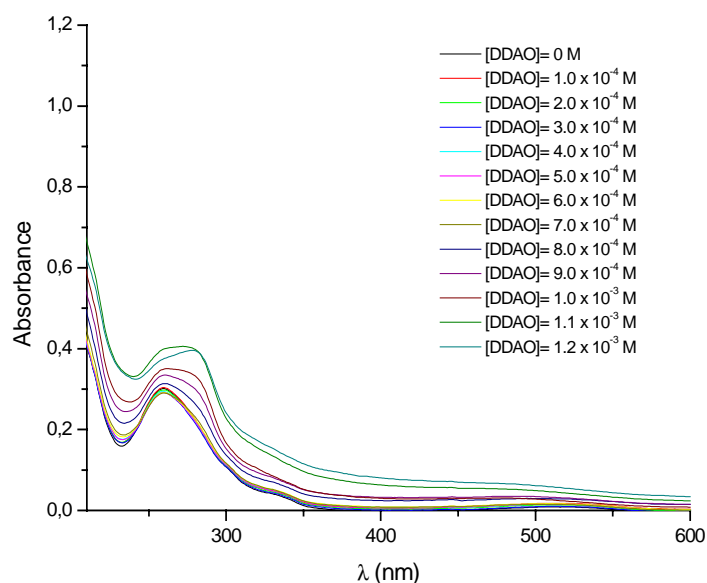


Fig. 24-B: Absorption of EB/DNA complex upon addition of DDAO in solution in 50 mM Tris-HCl solution. [DNA]= 2.0 x 10⁻⁵ M, [EB]= 4.2 x 10⁻⁶ M, pH= 5.8.

Analogues experiments were performed with pDOAO both with Hoechst 33258 and ethidium bromide. Similar results were obtained, at lower concentrations of surfactants because of the lower c.m.c. value of pDOAO (Figures 25- 27 A and B).

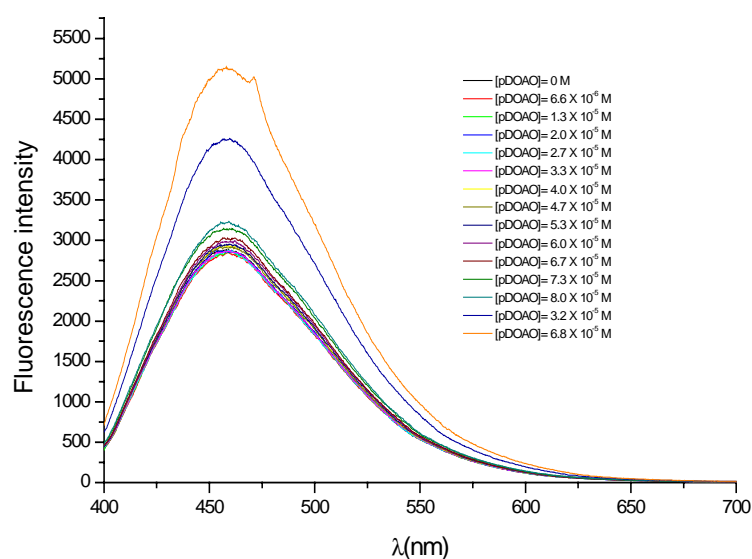


Fig. 25-A: Fluorescence intensity of Hoechst/DNA complex upon addition of pDOAO in solution in 50 mM Tris-HCl solution. [DNA]= 2.0 x 10⁻⁵ M, [Hoechst]= 2.0x 10⁻⁶ M, pH= 7.5.

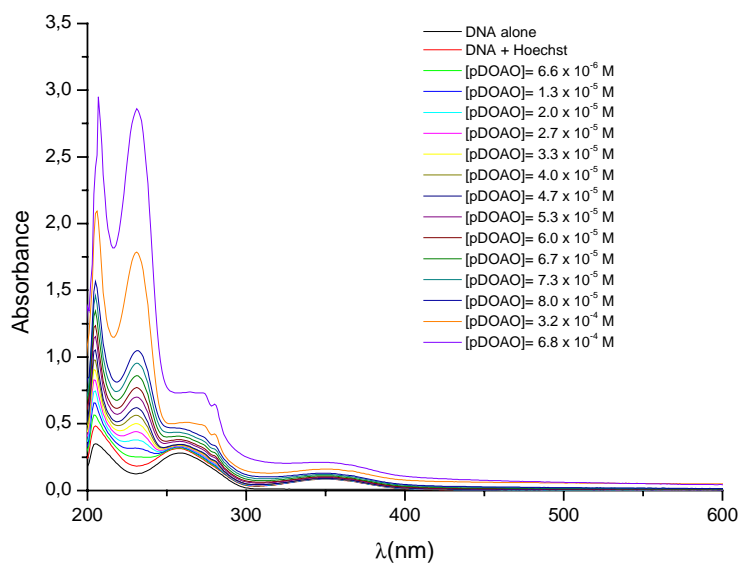


Fig. 25-B: Absorption of Hoechst/DNA complex upon addition of pDOAO in solution in 50 mM Tris-HCl buffer solution. [DNA]= 2.0×10^{-5} M, [Hoechst]= 2.0×10^{-6} M, pH= 7.5.

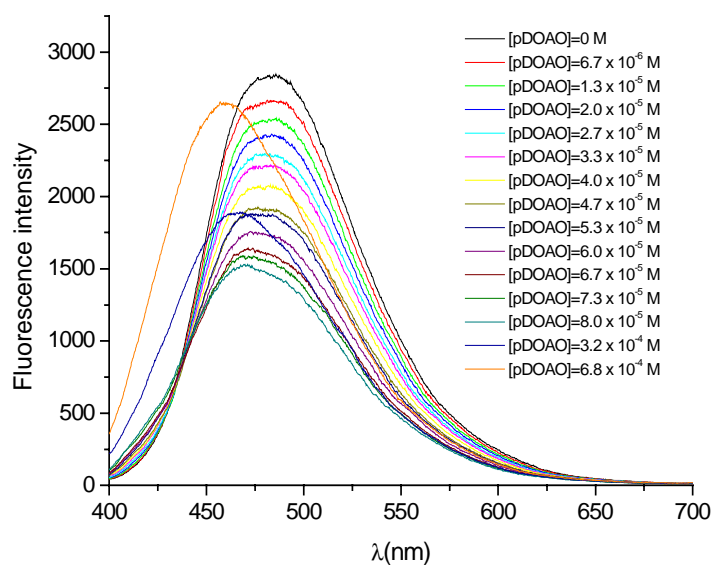


Fig. 26-A: Fluorescence intensity of Hoechst/DNA complex upon addition of pDOAO in solution in 50 mM Tris-HCl solution. [DNA]= 2.0×10^{-5} M, [Hoechst]= 2.0×10^{-6} M, pH= 5.8.

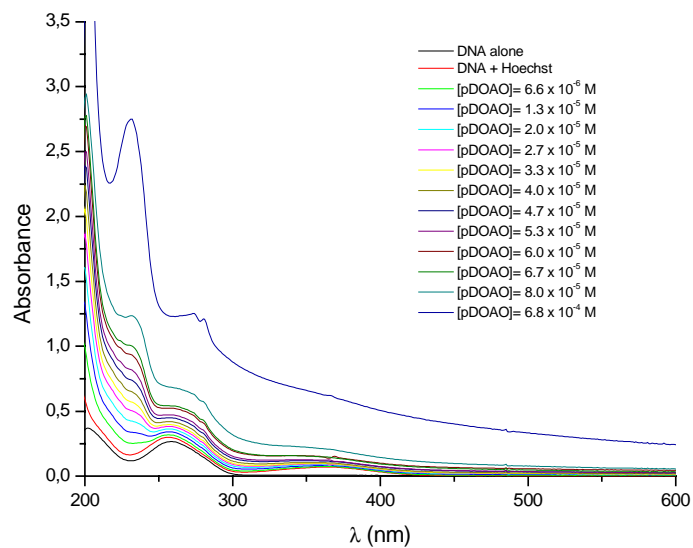


Fig. 26-B: Absorption of Hoechst/DNA complex upon addition of pDOAO in solution in 50 mM Tris-HCl solution. [DNA]= 2.0×10^{-5} M, [Hoechst]= 2.0×10^{-6} M, pH=5.8.

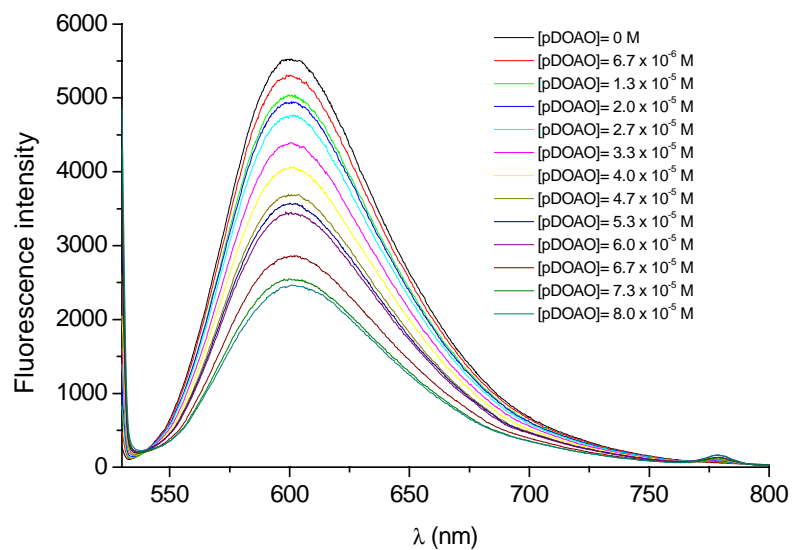


Fig. 27-A: Fluorescence intensity of EB/DNA complex upon addition of pDOAO in solution in 50 mM Tris-HCl solution. [DNA]= 2.0×10^{-5} M, [EB]= 4.2×10^{-6} M, pH= 5.8.

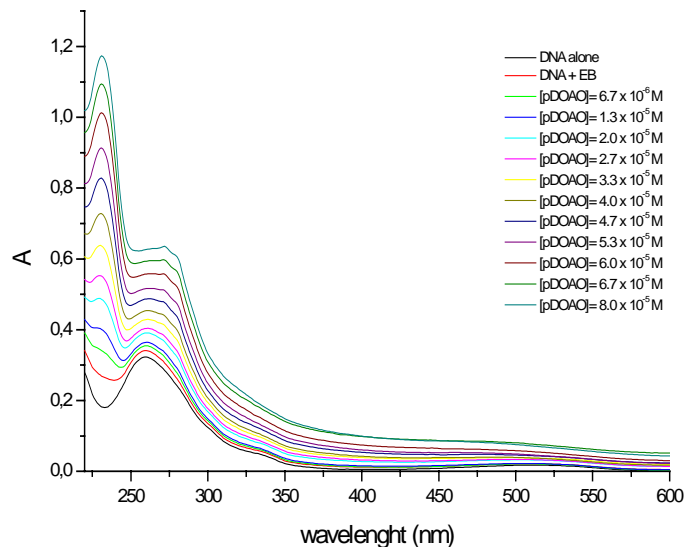


Fig. 27-B: Absorption of EB/DNA complex upon addition of pDOAO in solution in 50 mM Tris-HCl buffer solution. [DNA]= 2.0×10^{-5} M, [EB]= 4.2×10^{-6} M, pH= 5.8.

To completely exclude the possibility that the observed shift in emission maximum is due to the transfer of the probe from the minor groove of DNA to a micelle, we performed experiments using fluorescence depolarisation. In fact, as previously mentioned, fluorophores preferentially absorb photons whose electric vectors are aligned parallel to the transition moment of the fluorophore. The transition moment has a defined orientation in the fluorophore. In an isotropic solution, fluorophores are molecules oriented randomly. Upon excitation with polarised light, one selectively excites those fluorophore molecules whose absorption transition dipole is parallel to the electric vector of the excitation. This selective excitation of a partially oriented population of fluorophores (photoselection) results in partially polarised fluorescence emission. The application of fluorescence depolarisation to the elucidation of protein-guest aggregates is shown in Fig. 28.

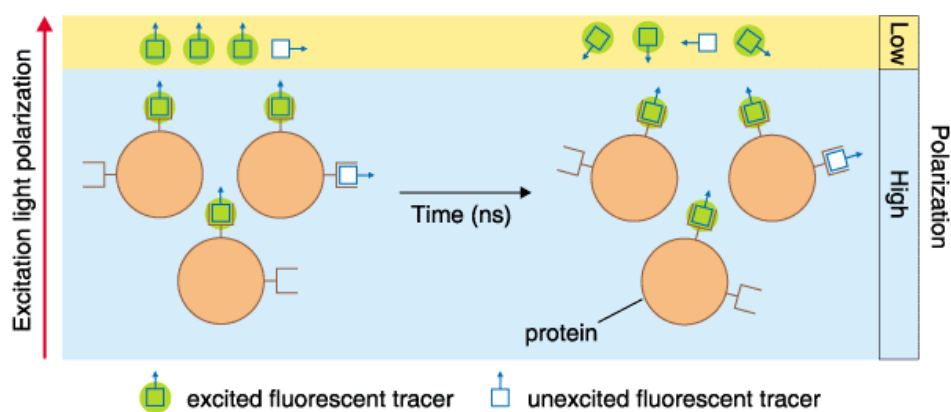


Fig. 28: Scheme of the polarization process.

Dye molecules with their absorption transition vectors (arrows) aligned parallel to the electric vector of linearly polarised light are selectively excited. For dyes that are free or attached to small, rapidly rotating molecules, the initially photoselected orientational distribution becomes randomised prior to emission, resulting in loss of fluorescence polarisation. Conversely, binding of the low molecular weight tracer to a large, slowly rotating molecule results in retention of fluorescence polarisation. Fluorescence polarisation therefore provides a direct readout of the extent of tracer binding to proteins, nucleic acids and other biopolymers. Because polarisation is a general property of fluorescent molecules, polarisation-based readouts are somewhat less dye-dependent and less susceptible to environmental interferences such as pH changes than assays based on fluorescence intensity measurements.

Thus, on the basis of these considerations, since the mobility of the two probes, Hoechst and ethidium bromide, should be very different in the two conditions (inserted in DNA or in micelles), such technique can be very sensitive to this change of environment. In Fig. 29 and 30, the curves of polarisation obtained for EB and Hoechst upon addition of DDAO are reported. Little changes of the polarisation are observed, indicating that the two probes remain associated to the biomolecule.

Similar results were obtained by using pDOAO, as reported in Appendix V.

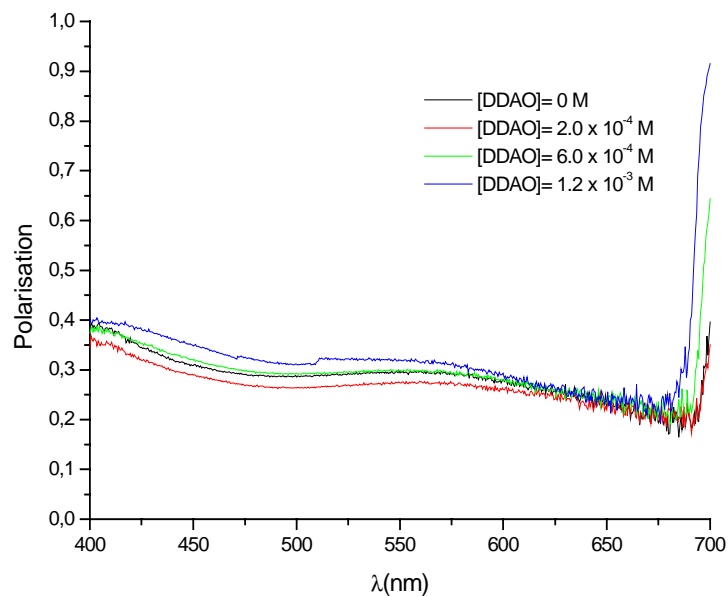


Fig. 29: Polarisation curves for Hoechst-DNA complex upon addition of DDAO at pH= 5.8. [DNA]= 2.0×10^{-5} M; [Hoechst]= 2.0×10^{-6} M.

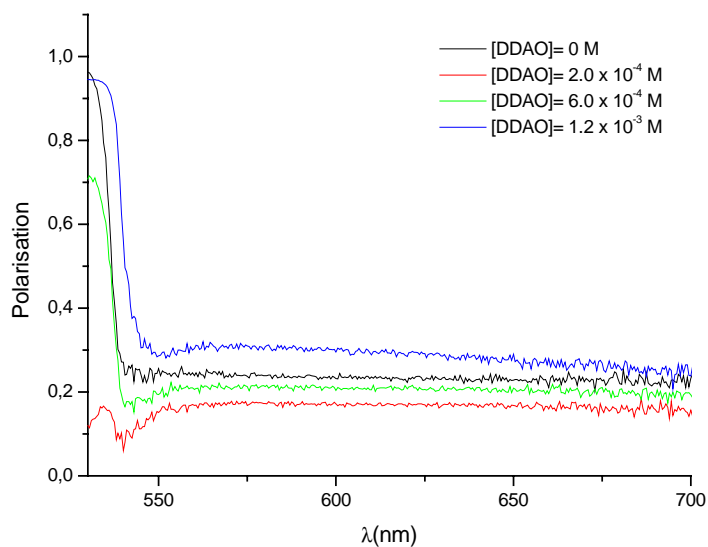


Fig. 30: Polarisation curves for EB-DNA complex upon addition of DDAO at pH= 5.8. [DNA]= 2.0×10^{-5} M; [EB]= 4.2×10^{-6} M.

5.5 Concluding remarks

In this Chapter the use of the fluorescent probe Hoechst 33258 to study DNA-surfactant interactions was discussed. We have found that ethidium bromide, frequently used as a probe for DNA studies, may provide information which could be wrongly interpreted in the absence of additional data. For example, from the fluorescence quenching of ethidium bromide alone, it is impossible to observe the precipitation phenomena that occurs upon increasing the surfactant concentration. On the basis of these and other considerations, we reasoned that a DNA binding agent with preference for binding to the surface of the double helix (in contrast to intercalating agents such as ethidium bromide) would be a more sensitive probe for the investigation of DNA-surfactant interactions. Experiments were thus undertaken using Hoechst 33258 as fluorescent probe, since it binds to DNA in the minor groove and is expected to show higher sensitivity towards nearby amphiphilic residues. To the best of our knowledge, this is the first time that Hoechst 33258 is used to study DNA-surfactant interactions. A comparison of the results obtained by using ethidium bromide and Hoechst 33258 in studying the interactions between cationic and zwitterionic surfactants with DNA, showed several advantages in the use of Hoechst 33258. First of all, it is possible to record contemporarily for each addition of surfactant both the absorption and the fluorescence spectra, and to control the eventual presence of a precipitate. This is more difficult using ethidium bromide, because its very low molar extinction coefficient in water requires the use of special cuvettes and a large volume of solution.

An unsuspected result was obtained when Hoechst 33258 was used to study the interaction of DDAO and pDOAO with DNA. A shift of the maximum of the fluorescence spectrum towards lower wavelength was observed at pH= 5.8 upon increasing the surfactant concentration, in addition to the quenching of fluorescence induced by the DNA-surfactant interaction. This behaviour is consistent with the fact that the spectrum of fluorescence of Hoechst/DNA complex assumes the features of the spectrum of fluorescence of the probe at higher pH. To exclude the possibility that the observed shift is due to the release of the probe from the minor groove of DNA to a micelle, fluorescence

depolarisation studies were performed. No changes in the polarisation curves were noted, indicating that the “solubilisation” of the probe by micellar aggregates is unlikely, and that the Hoechst 33258 probe is still bound to the DNA.

Therefore, it can be concluded that the probe is responding to a local change of pH, induced by the presence of additional surfactant molecules. If this is indeed the case, the use of Hoechst 33258 as a fluorescent probe of DNA-surfactant interactions holds great promise as it can provide information on the geometry of the DNA (presence of minor groove), the extent of interaction of the DNA with amphiphiles (fluorescence quenching) and of the local pH (shift in the emission spectrum).

Fluorescence spectroscopy results were also useful to verify the predictivity of the model built by molecular modelling. In fact, fluorescence experiments were performed to study the interaction of previously modelled surfactants and DNA, and the experimental data are in agreement with results obtained by docking studies.

REFERENCES

- [1] J.R. Lakowicz, “*Principles of Fluorescence Spectroscopy*”, Plenum Press, New York, **1984**.
- [2] *Analytical instrumentation Handbook*, ed. by Galen Wood Ewing, Marcel Dekker, Inc., New York, 1990.
- [3] Spex polarizers hardware manual, Jobin Yvon-SPEX, Edison, New Jersey (USA)
- [4] J.H. Sommer, T.M. Nordlun, M. McGuire and G. McLendon, *J. Phys. Chem.*, **1986**, 90, 5173.
- [5] J. Olmsted III and D.R. Kearns, *Biochemistry*, 16(16), **1977**, 3647.
- [6] H. Görner, *Photochemistry and Photobiology*, **2001**, 73(4), 339.
- [7] A. Czarny, D. W. Boykin, A. A. Wood, C. M. Nunn, S. Neidle, M. Zhao, W. D. Wilson; *J. Am. Chem. Soc.*, **1995**; 117(16); 4716.
- [8] J. R. Quintana, A. A. Lipanov, R. E. Dickerson; *Biochemistry* ; **1991**; 30(42); 10294.
- [9] S. Batthacharya and S.S. Mandal , *Biochimica et Biophysica Acta*, **1997**, 1323(1), 29.
- [10] S. Bhattacharya and S.S. Mandal, *Biochemistry*, **1998**; 37(21); 7764.
- [11] S.J. Eastman, C. Siegel, J. Tousignant, A.E. Smith, S.H. Cheng, R.K. Scheule, *Biochimica et Biophysica Acta*, **1997**, 1325(1), 41.
- [12] G. Savelli; R. Germani; L. Brinchi “*Reactivity Control by Aqueous Amphiphilic Self-Assembling Systems*” in “*Reactions and Synthesis in Surfactant Systems*”, J. Texter ed., Surfactant Science Series; M. Dekker: New York, **2001**, 175.
- [13] Y. S. Mel’nikova and B. Lindmam, *Langmuir*, **2000**, 16, 5871.
- [14] T. H. Lowry, K. S. Richardson "Mechanism and Theory in Organic Chemistry", 2nd Ed., Harper & Row, N. Y., **1981**, p. 195.
- [15] C.A. Bunton, M.J. Minch, J. Hidalgo and L. Sepulveda, *J. Am. Chem. Soc.*, **1973**, 95, 3262.
- [16] L. Brinchi, R. Germani, G. Savelli and L. Marte, *J. Colloid and Interface Science*, **2003**, 262, 290.

[17] L. Brinchi ; R. Germani; L. Goracci; G. Savelli; C.A. Bunton, *Langmuir* **2002**, *18*, 7821.

CHAPTER 6

CONCLUSIONS AND PERSPECTIVES

The aim of this work is to investigate the driving forces responsible for the formation of DNA-surfactants complexes, whose use may provide an alternative to viral vectors in DNA transfection processes. In this study, cationic and zwitterionic surfactants were studied, taking into account that anionic surfactants do not generally interact with DNA because the electrostatic repulsion with the phosphate groups. In order to study the relationship between the structure of the amphiphiles and their ability to interact with DNA, new synthetic surfactants were synthesised to obtain a series of amphiphilic systems that is heterogeneous in structures and properties. The investigation of these systems was performed by combining three different techniques: Circular Dichroism, Molecular Modelling and Fluorescence Spectroscopy. The comparison of the results obtained by each of these techniques contributed to the understanding of the bases of the DNA-surfactant interaction.

For both cationic and zwitterionic surfactants, it was found that, in addition to the electrostatic forces, the hydrophobic interactions between DNA and the non-polar moiety of the amphiphiles are of crucial importance. All three different experimental approaches showed that non-micellisable analogues of the tested surfactants do not interact with DNA when assayed at the same concentrations.

Particularly interesting results were found for the amine oxide zwitterionic surfactants. A previous study on the interaction of the dodecyldimethyl amine oxide (DDAO) with DNA [1] indicated that such interactions were dependent on the concentration of DDAO and on pH. Our Circular Dichroism studies led us to emphasise that the DNA-DDAO interaction is switched “on” and “off” within a very narrow pH range of 7.1-7.5. This effect can be explained with the

protonation of DDAO at pH lower than 7.1. In fact, as showed by Lindman with fluorescence microscopy studies, [1] the presence of DNA in solution is able to increase the degree of ionisation of DDAO, as compared to the free surfactant in aqueous solution. It was proposed that this effect is due to the cooperative electrostatic interactions. Molecular modelling studies performed on DNA-DDAO system led us to hypothesise that both DDAO and DDAOH may interact with DNA, but the energy of such interaction is significant only for the cationic form of DDAO.

A more accurate description of the DNA-DDAO system is, however, very complex, due to the possibility of DNA interacting both with monomers and micelles, and taking into account that the presence of DNA in solution can dramatically shift the acid-base equilibrium for DDAO toward the cationic form, and its propensity to aggregate.

Using cationic surfactants, the condensation of DNA occurred at very low surfactant concentrations, well below their c.m.c. values. This is likely due to the interaction of the monomers with the oppositely charged polyelectrolyte. The precipitation of DNA upon addition of cetyltrimethylammonium bromide (CTABr) at a concentration of surfactant coincident with the concentration of the phosphate groups (4×10^{-5} M), as revealed by the absorption measurements reported in this work, are in agreement with this assumption.

On the contrary, the interaction between DNA and DDAO at pH values lower than 7.1 occurs only at concentrations equal to or higher than the c.m.c., as shown both by fluorescence spectroscopy and circular dichroism. On the basis of this experimental evidence two hypotheses are possible:

- 3) the DNA-DDAO interaction at pH lower than 7.1 is only dependent on the amount of protonated surfactant monomers. According to this hypothesis, the fact that such interaction occurs at high values of DDAO concentration is not directly related to the c.m.c.
- 4) the DNA-DDAO interaction at pH lower than 7.1 occurs between the biomolecule and the surfactant in the aggregated form (not necessarily spherical micelles). In this case the observed phenomenon should be correlated to the c.m.c value.

The importance of the amphiphilic nature of the additive was proved by using the non-micellising trimethylamine oxide (TMAO), which does not show any DNA condensing properties.

This ambiguity was lifted by investigating a new surfactant, paradodecyloxybenzildimethylamine oxide (pDOAO). The c.m.c. value for DDAO in aqueous solution is 7×10^{-4} M, c.m.c. for pDOAO in aqueous solution is 1.16×10^{-5} M.

If the interaction between amine oxides and DNA is controlled by the ability of aggregation of the surfactant, we expect that pDOAO should induce a DNA condensation at lower surfactant concentration with respect to DDAO, due to its lower c.m.c. value.

The studies performed by Circular Dichroism and Fluorescence spectroscopy indicate that pDOAO induces structural modifications of DNA at concentrations of surfactant ca. 20-fold lower than DDAO. This result supports the second hypothesis, in which it is proposed that, in the case of the amine oxides, DNA interacts with aggregated surfactant molecules;

In addition to the results discussed so far, a new approach in the use of fluorescence spectroscopy for studying DNA-surfactant interactions has been proposed in this study. Our investigation of DNA-surfactant interactions by the combination of various spectroscopic techniques (absorption and fluorescence spectroscopy, circular Dichroism), has shown that ethidium bromide, frequently used as a probe, may provide information which could be wrongly interpreted due to the precipitation of DNA-probe-surfactant aggregate. We showed that a DNA binding agent with preference for binding to the surface of the double helix is a more sensitive probe for the investigation of DNA-surfactant interactions. To the best of our knowledge, this is the first time that Hoechst 33258 is used to study DNA-surfactant interactions. The use of Hoechst 33258 allows one to record contemporarily both the absorption and the fluorescence spectra, and to control the eventual presence of a precipitate.

The use of Hoechst 33258 confirmed previous results obtained using Circular Dichroism, even if fluorescence studies were performed in Tris-HCl buffer.

Particularly, the dependence of amine oxide –DNA interaction on the pH and surfactant concentration was confirmed with this technique. Additionally, it was evidenced that Hoechst 33258 is sensitive to changes in the local pH environment induced by the presence of surfactants bound in the vicinity.

Using fluorescence depolarisation, it was verified that the probe remained bound to the DNA over the entire surfactant concentration range investigated.

The mechanism by which the presence of zwitterionic surfactants bound to the DNA surface (that should be mostly in their protonated form) could induce deprotonation of Hoechst 33258 is still under investigation. However, it can be hypothesised that electrostatic and/or aggregation effects may be responsible for the change in pH.

The results obtained by molecular modelling studies complement the experimental work described above. Molecular modelling allows a different approach to the experimental results, leading us to analyse the data from an energetic and probabilistic point of view. Moreover, the model built by the use of docking procedures showed predictive ability: this is very important because on one hand this validates the model and, on the other hand, this property is very useful to assess the binding ability of new surfactants towards DNA.

As future developments of this study, the basic research on DNA-surfactants interaction will be continued by using the techniques described in this thesis and other techniques that might be helpful for obtaining further information. Particularly, we have already started a further investigation by the use of Dynamic Light Scattering to get data on the changes in aggregate structures of amine-oxide surfactants in the presence of DNA. In addition, in order to test the possibility of using these systems in DNA transfection, experiments on the interaction of surfactants with plasmid DNA will be also performed, using similar procedures adopted in this thesis with Calf Thymus DNA. These studies will allow selecting the amphiphilic systems that might be more suitable for in vitro transfection. Preliminary experiments on this aspect have been already planned with the research group of Dott. Servillo (Faculty of Medicine, University of Perugia), as planned in the research project of the CEMIN (Centro di Eccellenza in Materiali Innovativi Nanostrutturati per

applicazioni chimiche, fisiche e biomediche) coordinated by Prof. Savelli, and recently financed by MIUR (Ministero dell'Istruzione, dell'Università e della Ricerca).

Particularly, our attention will be focused on the amine-oxide surfactants for the possibility to modulate their interaction with DNA by changing pH and carrier concentration. On the basis of the preliminary transfection results we would like to design, synthesise and test new amphiphilic systems, using also predictions by molecular modelling.

REFERENCES

- [1] Y. S. Mel'nikova, B. Lindman, *Langmuir*, 2000, 16, 5871.

CHAPTER 7

EXPERIMENTAL SECTION

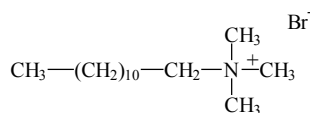
7.1 Materials

7.1.1 Commercially available compounds

Type I Calf Thymus DNA (i.e. purified and dried to have Na 6.2 %, H₂O 13 %) was purchased from Sigma-Aldrich (USA), and has been used without further purification. DNA solutions were prepared by using deionised and bidistilled water. Trimethyldimethylamine oxide (TMAO), tetrabutylammonium bromide (TBABr), trimethylammonium-propane sulfonate (SB3-1), dodecyldimethylammonium-propane sulfonate (SB3-12), and cetyltributylammonium bromide (CTABr) were purchased from Aldrich (Germany), and purified as described below

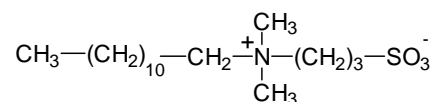
7.1.2 Purification of commercially available compounds

A) Purification of CTABr



Commercially available CTABr was refluxed in Et₂O for 4 hours. After filtration, the solid was dried and then crystallised from ethanol-Et₂O (1/1, v/v). The value of c.m.c. is 8.3×10^{-4} M.

B) Purification of the sulfobetaine SB3-12



Commercially available SB3-12 (Fluka) was recrystallized from acetone and then dried at 60°C. m.p. 257-260 °C; c.m.c.= 2.96 x 10⁻³ M at 25 °C. Because no minima were observed in the surface tension vs. log [SB3-12] plot, the surfactant was considered pure.

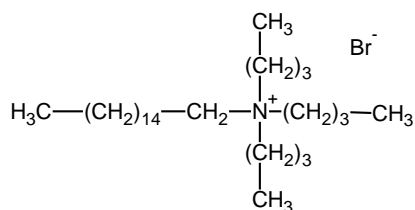
C) Purification of TMAO, SB3-1 and TBABr

TMAO, SB3-1 and TBABr were purified by crystallisation from acetone/ethanol solution and dried prior to use.

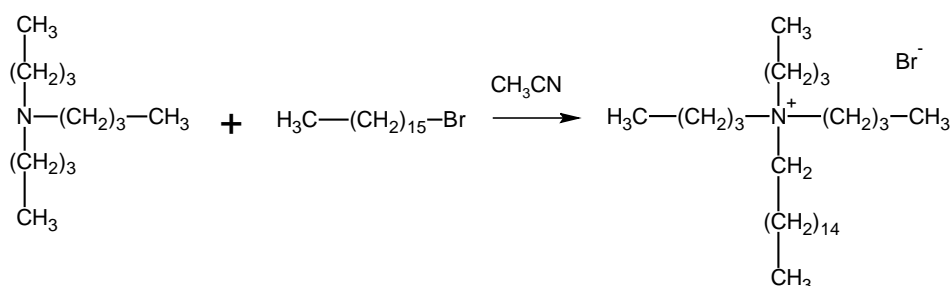
7.1.3 Synthesis and purification of cationic surfactants

Test of purity of the surfactants that have been synthesised were made by means of ¹H-NMR, conductivity, and melting points (when possible); plots of surface tension against -log[surfactant] are also useful in that the absence of minima implies the absence of surface active reagents (or other surface active compounds). Moreover, c.m.c. values are reported, with an exception for C12-12, C12-16 and C16-16 that give spontaneously vesicles. Finally, the purity of cationic surfactants having Br⁻ as counterion was confirmed by potentiometric titration with AgNO₃ at known concentration, after precipitation of the surfactant with NaClO₄ and acidification to pH = 1.

A) Synthesis and purification of cetyltributylammonium bromide (CTBABr)



The scheme of synthesis for this surfactant is the following:



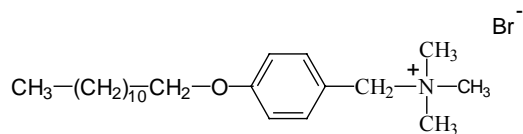
Tributylamine (18.3 gr, 0.1 mol) and cetyl bromide (30.5 gr, 0.1 mol) were added to 200 ml of CH_3CN in a 500 ml round-bottom flask. The biphasic mixture was refluxed for 5 days, by when the mixture was monophasic and yellowish. After slowly cooling to room temperature the reaction mixture was washed with n-hexane. After elimination of the $\frac{3}{4}$ of the total CH_3CN and addition of 1 l of Et_2O , a white solid precipitated. This was collected and washed several times with Et_2O , recrystallised from acetone- Et_2O , and then from ethylacetate. After filtration, the solid was washed with petroleum ether and dried at 60°C *in vacuo*.

M.W. = 490.70

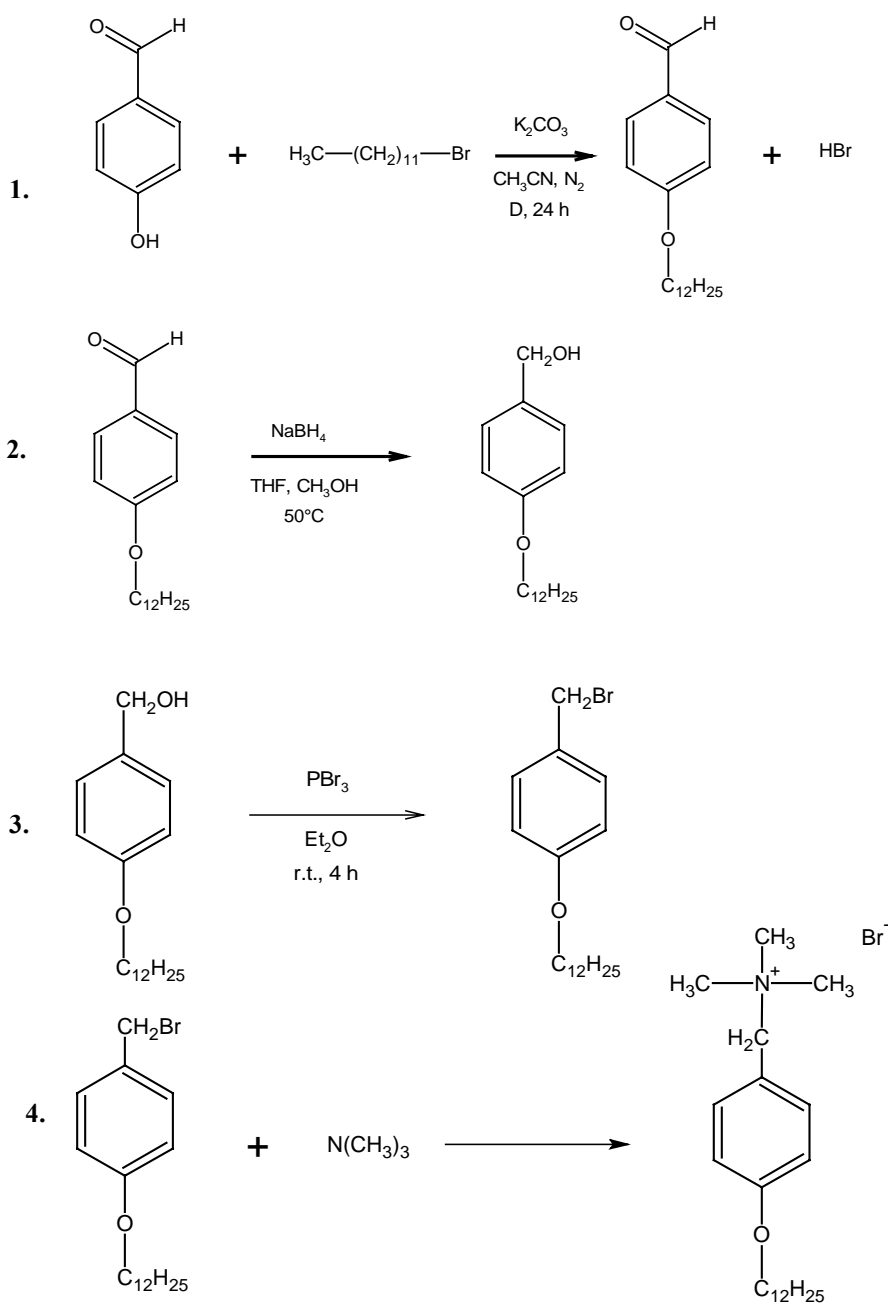
c.m.c. (surface tension) = 2.81×10^{-4} M.

$^1\text{H-NMR}$ (200 MHz) CDCl_3 δ : 0.80-0.90 (t, 3H, CH_3); 0.90-1.05 (t, 9H, CH_3); 1.20-1.60 (m, 32 H, CH_2); 1.60-1.75 (m, 8H, CH_2); 3.27-3.47 (m, 8H, CH_3).

B) Synthesis and Purification of *p*-dodecyloxybenzyltrimethylammonium bromide Surfactant (*p*DOTABr)



The four-step synthesis of the cationic *p*DOTABr surfactant was carried out according to the following scheme:



1. Synthesis of p-dodecyloxybenzaldehyde

In a 3-necked 1 l round-bottom flask equipped with a mechanical stirrer, p-hydroxybenzaldehyde (purified using activated carbon and crystallised from water) (30.0 gr, 0.264 mol) and anhydrous K_2CO_3 (37.0 gr, 0.267 mol) were refluxed in 400 ml of CH_3CN under N_2 atmosphere. To this heterogeneous mixture dodecylbromide (59.4 gr, 0.238 mol) was added over 1 hour, and the reaction was allowed to proceed for 24 hours under reflux. The reaction mixture was cooled and 500 ml of water were added. Extraction with petroleum ether of the organic phase, which was washed twice with 100 ml of 10% NaOH and then with water until neutrality was reached, dried over anhydrous Na_2SO_4 and evaporated under reduced pressure, yielded a pale yellow oil. This was converted into a crystalline white solid by crystallisation from CH_3OH at $-20^\circ C$, and washed with cold petroleum ether.

M.W. = 290.44

Yield = 98 %

m.p. = $< 30^\circ C$.

2. Synthesis of p-dodecyloxybenzylalcohol

In a 1 l flask equipped with a mechanical stirrer, p-dodecyloxybenzaldehyde (step 1) (30.0 gr, 0.264 mol) were dissolved in 400 ml of THF and 6 ml of CH_3OH , then $NaBH_4$ (9.4 gr, 0.249 mol) was carefully added. After 1 g of $NaBH_4$ was added, the mixture was warmed to $50^\circ C$ and hand shaken until the reaction started, then the remaining $NaBH_4$ was gradually added, always shaking (about 15 minutes). After the reaction mixture was cooled (water and ice), the excess of hydride was neutralised by carefully adding 10 % H_2SO_4 until no more hydrogen development was observed. The reaction mixture was put in a 2 l separatory funnel containing 500 ml of water and extracted twice: first using petroleum ether, then ethyl acetate. The organic phases were combined and washed with water until neutrality, dried over anhydrous Na_2SO_4 and the volume was reduced to 500 ml. The product crystallised from

this solution at $-20\text{ }^{\circ}\text{C}$. The white solid thus obtained was filtered and washed with cold petroleum ether and ethyl acetate.

M.W. = 292.47

Yield = 98 %

m.p. = $68\text{-}70\text{ }^{\circ}\text{C}$.

3. Synthesis of p-dodecyloxybenzylbromide

In a 500 ml flask p-dodecyloxybenzylalcohol (step 2) (37.7 gr, 0.129 mol) was dissolved in 200 ml of ethyl ether, and PBr_3 (12.14 ml, 0.129 mol dissolved in 50 ml of ethyl ether) was added with stirring over 30 minutes at room temperature. The reaction was allowed to proceed for other 4 hours, then the reaction mixture was carefully added to cold water in a 1 l separatory funnel and washed until neutrality. The organic phase was dried over anhydrous Na_2SO_4 and evaporated to yield a white solid, which was used in the following step without further purification.

M.W. = 355.35

Yield = 97 %

m.p. = $< 49\text{-}50\text{ }^{\circ}\text{C}$.

4. Synthesis of the p-dodecyloxybenzyltrimethylammonium bromide (pDOTABr)

Cationic p-dodecyloxybenzyltrimethylammonium bromide surfactant was prepared by quaternisation of trimethylamine (5.9 gr, 0.1 mol) using p-dodecyloxybenzylbromides (step 3) (17.8, 0.05 mol) in 250 ml of CH_3CN . The reaction was conducted at room temperature by hand-shaking the flask. As the reaction proceeded, the initially heterogeneous mixtures became homogeneous. Afterwards, the liquid phase was evaporated and the raw material was washed 3-4 times with ethyl ether to eliminate the residual amine, to give a white solid

or semisolid was obtained. The raw material was recrystallised from anhydrous THF at -20°C , washed with cold ethyl ether and dried in a drying tube for 24 hour.

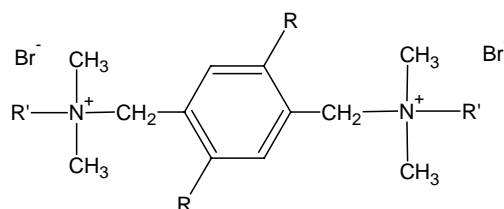
M.W. = 414.47.

Yield = 98 %.

c.m.c. = 5.9×10^{-4} M (Surface tension); 4.9×10^{-4} M (Conductivity); α : 0.22 (Conductivity). As no minima were observed in the surface tension vs. log [pDOTABr] plot, the surfactant is considered pure.

$^1\text{H-NMR}$ (CD_3OD , 200 MHz) δ , ppm: 0.93 (t, CH_3); 1.25–1.60 (m, 9 CH_2); 1.70–1.95 (m, CH_2); 3.1 (s, 3 CH_3); 4.06 (t, CH_2); 4.4 (s, CH_2); 7.08 (d, 2 H); 7.49 (d, 2 H).

C) Synthesis and purification of $\text{pXMo}(\text{R}'\text{DA})_2$ and $\text{pXDo}(\text{TA})_2$ gemini surfactants



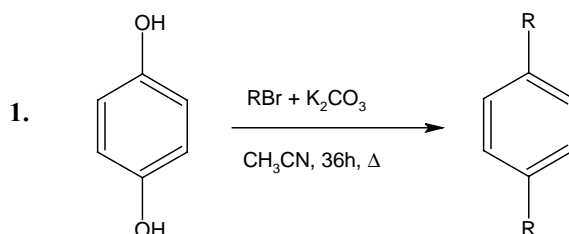
a. $\text{pXMo}(\text{DDA})_2$: $\text{R} = \text{OCH}_3$, $\text{R}' = (\text{CH}_2)_{11}\text{CH}_3$;

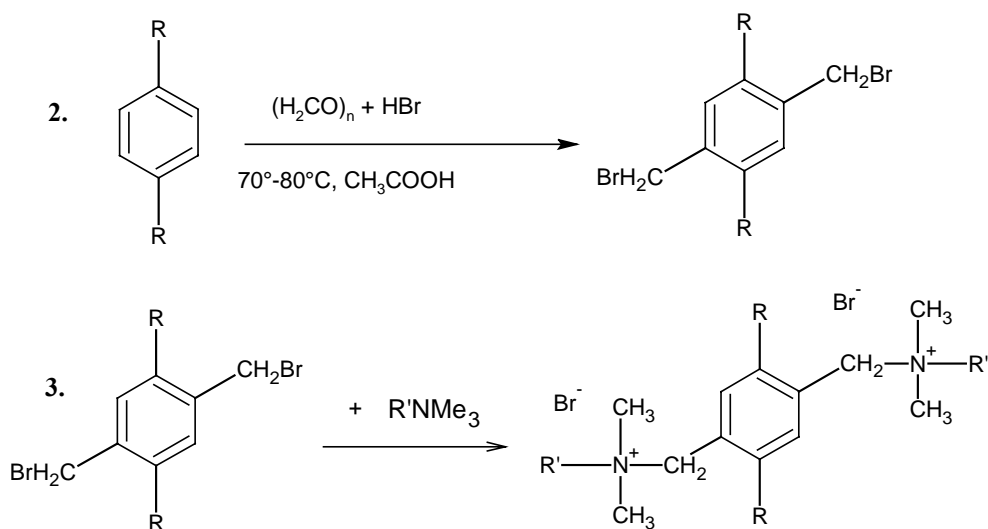
b. $\text{pXMo}(\text{MDA})_2$: $\text{R} = \text{OCH}_3$, $\text{R}' = (\text{CH}_2)_{13}\text{CH}_3$;

c. $\text{pXMo}(\text{CDA})_2$: $\text{R} = \text{OCH}_3$, $\text{R}' = (\text{CH}_2)_{15}\text{CH}_3$;

d. $\text{pXDo}(\text{TA})_2$: $\text{R} = \text{O}(\text{CH}_2)_{11}\text{CH}_3$, $\text{R}' = \text{CH}_3$.

The synthesis of gemini surfactants **1-4** can be illustrated as follows:





Synthesis of gemini surfactants a-c

To synthesise surfactants a-c step 1 was not necessary, by using commercial 1,4-dimethoxy-benzene (Aldrich).

2. Preparation of 1,4-dibromomethyl-2,5-dimethoxy-benzene

A solution of HBr in acetic acid (74.0 ml, 30%) was added to a well-stirred suspension of 1,4-dimethoxybenzene (20.0 gr, 0.144 mol) and paraformaldehyde (8.9 gr, 0.296 mol) in 200 ml of glacial acetic acid. The heterogeneous mixture turned homogeneous and pale yellow after a few minutes at 70-80 °C. After ca. 10-20 minutes, a solid started to form increasing with time. The mixture was stirred at 70-80 °C for 2 hours, after which it was cooled to r.t. and 150 ml of MeOH was added. After cooling the mixture in ice-water for few minutes, the solid was filtered off and recrystallised from Et₂O.

M.W. = 423.78.

Yield = 71 %.

m.p. = 204-206 °C.

¹H-NMR (200 MHz CDCl₃) δ: 3.87 (s, 6H, 2 OCH₃); 4.53 (s, 4H, 2 CH₂Br); 6.87 (s, 2H, Ar).

3. Preparation of gemini a

Dimethyldodecylamine (16.2 gr, 0.067 mol) was added to 1,4-dibromomethyl-2,5-dimethoxybenzene (10.0 gr, 0.030 mol) in 200 ml of CH₃CN. The mixture became homogeneous and pale yellow after 20 minutes under reflux. After 4 h under reflux the mixture was cooled to r.t and a white and microcrystalline solid formed. 250 ml of acetone were added to the suspension and the mixture was cooled in ice- water for several minutes. After cooling the solid was filtered off and recrystallised from CH₃CN/CH₃OCH₃ (1/1 v/v) and dried *in vacuo* at room temperature over P₂O₅.

M.W. = 750.84

Yield = 95 %.

m.p. = 186-188 °C.

c.m.c. = 6.6×10^{-4} M (conductivity); 6.4×10^{-4} M (surface tension).

¹H-NMR (200 MHz CDCl₃) δ: 0.87 (t, 6H, 2CH₃); 1.25-1.40 (m, 36 H, 18 CH₂), 1.75-1.88 (m, 4H, 2CH₂); 3.24 (s, 12H, 4CH₃N⁺); 3.98 (s, 6H, 2OCH₃); 5.09 (s, 4H, 2ArCH₂N⁺); 8.18 (s, 2H, Ar).

Preparation of gemini b

Dimethyltetradecylamine (14.5 g, 0.067 mol) was added to 1,4-dibromomethyl-2,5-dimethoxybenzene (10.0 g, 0.030 mol) in 200 ml of CH₃CN. Subsequent steps were as for pMo(DDA)₂, and pMo(MDA)₂. A white solid was obtained.

M.W. = 806.94

Yield = 96 %

m.p. = 195-197 °C

c.m.c. = 1.2×10^{-4} M (conductivity); 1.1×10^{-4} M (surface tension).

¹H-NMR (200 MHz CDCl₃) δ: 0.87 (t, 6H, 2CH₃); 1.16-1.40 (m, 36 H, 18 CH₂), 1.75-1.88 (m, 4H, 2CH₂); 3.24 (s, 12H, 4CH₃N⁺); 3.97 (s, 6H, 2OCH₃); 5.02 (s, 4H, 2ArCH₂N⁺); 8.11 (s, 2H, Ar).

Preparation of gemini c

Dimethylesadecylamine (6.6 gr, 0.022 mol) was added to 1,4-dibromomethyl-2,5-dimethoxybenzene (3.6 gr, 0.011 mol) in 200 ml of CH₃CN. Subsequent steps were as for pMo(DDA)₂, but only 2 h at reflux were

necessary. The solid was recrystallised from CH₃OCH₃/CH₃OH (95/5 v/v) to obtain a white solid

M.W. = 863.05

Yield = 95%

m.p. = 195-196 °C.

c.m.c. = 0.35×10^{-4} M (conductivity); 0.36×10^{-4} M (surface tension).

¹H-NMR (200 MHz CDCl₃) δ: 0.86 (t, 6H, 2CH₃); 1.20-1.40 (m, 36 H, 18 CH₂), 1.75-1.88 (m, 4H, 2CH₂); 3.24 (s, 12H, 4CH₃N⁺); 3.97 (s, 6H, 2OCH₃); 5.02 (s, 4H, 2ArCH₂N⁺); 8.12 (s, 2H, Ar).

Synthesis of gemini d

1. Preparation of 1,4-Bis(dodecyloxy)benzene

It was prepared as described Wasielewsky et al. (J. Am. Chem. Soc., Vol. 119, No. 1, 1997).

M.W.= 446.76

Yield = 92%

m.p. = 77-78°C.

¹H-NMR (200 MHz CDCl₃) δ: 0.88 (t, 6H, 2CH₃); 1.20-1.49 (m, 36 H, 18 CH₂); 1.68-1.78 (m, 4H, 2CH₂), 3.90 (t, 4H, 2CH₂O), 6.81 (s, 4H, Ar).

2. Preparation of 1,4-bis- bromomethyl-2,5-bisdodecyloxybenzene.

The same procedure as for a was used to prepare 1,4-dibromomethyl-2,5-dimethoxybenzene, starting from HBr in acetic acid (22.0 ml, 30%), 1,4-Bis(dodecyloxy)benzene (20.0 gr, 0.044 mol) and paraformaldehyde (2.75 gr, 0.091 mol) in 200 ml of glacial acetic acid. 1,4-Bis-bromomethyl-2,5-bisdodecyloxybenzene was obtained as a white solid.

M.W. = 634.62.

Yield= 77 %.

m.p. = 96-97 °C.

$^1\text{H-NMR}$ (200 MHz CDCl_3) δ : 0.88 (t, 6H, $J = 6.90$ Hz, 2 CH_3); 1.18-1.55 (m, 36H, 18 CH_2); 1.70-1.96 (m, 4H, 2 CH_2); 3.98 (t, 4H, $J = 6.38$ Hz, 2 OCH_2); 4.53 (s, 4H, 2 CH_2Br); 6.85 (s, 2H, Ar).

3. Synthesis of gemini 4

A solution of trimethylamine in MeOH (30 ml, 25%) was added to 1,4-bis-bromomethyl-2,5-bisdodecyloxybenzene (16.6 gr, 0.026 mol) in 200 ml of CH_3OH . The mixture was stirred for ca. two hours and refluxed for one hour to obtain a homogeneous solution. After cooling to r.t., the solvent was taken off under reduced pressure. The residue was dissolved in small amount of Et_2O and dried twice, and the solid thus obtained was recrystallised from CH_3OCH_3 plus few drops of CH_3OH . The white solid was filtered off and dried *in vacuo* over P_2O_5 .

M.W. = 750.84.

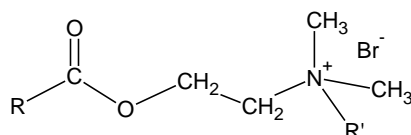
Yield= 95%.

m.p. 209-210 $^\circ\text{C}$.

c.m.c. = 4.4×10^{-4} M (conductivity); 4.2×10^{-4} M (surface tension).

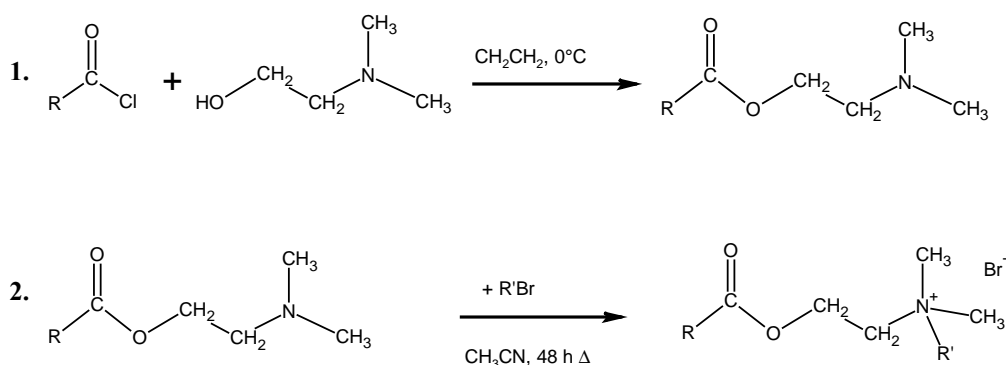
$^1\text{H-NMR}$ (400 MHz CDCl_3) δ : 0.88 (t, 6H, $J = 6.90$ Hz, 2 CH_3); 1.18-1.45 (m, 36H, 18 CH_2); 1.70-1.76 (m, 4H, 2 CH_2); 3.41 (s, 18 H, 6 CH_3); 4.12 (t, 4H, $J = 6.38$ Hz, 2 OCH_2); 4.96 (s, 4H, 2 CH_2Ar); 7.79 (s, 2H, Ar).

D) Synthesis and purification of C12-12, C12-16 and C16-16 surfactants



- a. R = CH₂-(CH₂)₉-CH₃; R' = CH₂-(CH₂)₁₀-CH₃ **C12-12**
b. R = CH₂-(CH₂)₉-CH₃; R' = CH₂-(CH₂)₁₄-CH₃ **C12-16**
c. R = CH₂-(CH₂)₁₃-CH₃; R' = CH₂-(CH₂)₁₄-CH₃ **C16-16**

The synthetic scheme used is as follows:



1. Synthesis of 2-(dimethylamino)ethyl-carboxylate

In a dry round-bottom flask containing anhydrous CH₂Cl₂, the acylchloride was added under stirring, keeping the flask at 0°C. One equivalent of dimethylaminoethanol dissolved in CH₂Cl₂, was added dropwise. At the end of the addition, the mixture was stirred at room temperature for 4 h. Upon cooling to 0°C, a white solid precipitated. The work up was different depending on using lauroylchloride or palmitoylchloride (see below).

2-(dimethylamino)ethyl laurate: The solvent was removed, giving an oil + solid mixture. This was dissolved in petroleum ether and the precipitated solid was filtered off. The organic phase was then washed with water until neutrality. After drying with anhydrous Na_2SO_4 , removing the petroleum ether gave an oil.

M.W. = 271.45.

Yield= 82%

$^1\text{H-NMR}$ (200 MHz) CDCl_3 δ : 0.84-0.91 (t, 3H, CH_3); 1.20-1.27 (m, 16 H, CH_2); 1.58-1.65 (m, 2H, CH_2); 2.29-2.36 (m, 8H, $2\text{CH}_3 + \text{CH}_2$); 2.53-2.61 (m, 2H, CH_2); 4.14-4.20 (m, 2H, CH_2).

2-(dimethylamino)ethyl palmytate: water and KH_2CO_3 were added and the mixture was washed with water until the neutrality of the aqueous phase. The organic phase was then dried with anhydrous Na_2SO_4 and the solvent removed *in vacuo* to obtain an oil. This was dissolved in petroleum ether and after cooling at -20°C the white solid that precipitated was filtered off. The petroleum ether was removed under reduced pressure to give an oil.

M.W. = 327.55.

Yield= 80%

$^1\text{H-NMR}$ (200 MHz) CDCl_3 δ : 0.81-0.88 (t, 3H, CH_3); 1.18-1.27 (m, 24H, CH_2); 1.55-1.62 (m, 2H, CH_2); 2.31-2.38 (m, 8H, $2\text{CH}_3 + \text{CH}_2$); 2.50-2.58 (m, 2H, CH_2); 4.11-4.17 (m, 2H, CH_2).

2. Synthesis of surfactants 1-3

In a 500 ml round-bottom flask, product 1 and the corresponding alkylbromide in ratio 1:1 in mole were dissolved in ca. 220 ml of CH_3CN . The mixture was refluxed for 48 h. The mixture was concentrated under reduced pressure and the solid was crystallised by heating to complete solubilisation

and by addition of few drops of Et₂O to the solution. After cooling at 0°C the solid was filtered off *in vacuo* and washed with Et₂O.

1. C12-12: A white solid is obtained.

M.W. = 576.78.

Yield = 82 %.

¹H-NMR(200 MHz) CDCl₃ δ: 0.78-0.88 (tr, 6H, CH₃); 1.16-1.36 (m, 34 H, CH₂); 1.58-1.65 (m, 2H, CH₂); 1.67-1.80 (m, 2H, CH₂); 2.31-2.38 (tr, 2H, CH₂); 3.30 (s, 6H, CH₃); 3.55-3.63 (m, 2H, CH₂); 4.07-4.11 (m, 2H, CH₂); 4.54-4.59 (m, 2H, CH₂).

This surfactant seems to self-aggregate spontaneously to form vesicles by Dynamic light scattering measurements. It was impossible to determinate the c.m.c. value.

2. C16-16: A white solid is obtained.

M.W.= 632.28.

Yield = 80 %

¹H-NMR(200 MHz) CDCl₃ δ: 0.78-0.88 (tr, 6H, CH₃); 1.16-1.36 (m, 38 H, CH₂); 1.58-1.65 (m, 2H, CH₂); 1.67-1.80 (m, 2H, CH₂); 2.31-2.38 (tr, 2H, CH₂); 3.30 (s, 6H, CH₃); 3.55-3.63 (m, 2H, CH₂); 4.07-4.11 (m, 2H, CH₂); 4.54-4.59 (m, 2H, CH₂).

This surfactant seems to self-aggregate spontaneously afford vesicles by Dynamic light scattering measurements. It was impossible to determinate the c.m.c. value.

3. Colin12-16: A white solid is obtained.

M.W. = 576.79.

Yield= 83%

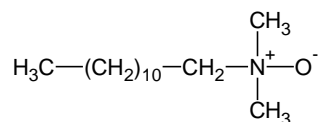
¹H-NMR(200 MHz) CDCl₃ δ: 0.78-0.88 (tr, 6H, CH₃); 1.16-1.36 (m, 36 H, CH₂); 1.58-1.65 (m, 2H, CH₂); 1.67-1.80 (m, 2H, CH₂); 2.31-2.38 (tr, 2H,

CH₂); 3.30 (s, 6H, CH₃); 3.55-3.63 (m, 2H, CH₂); 4.07-4.11 (m, 2H, CH₂); 4.54-4.59 (m, 2H, CH₂).

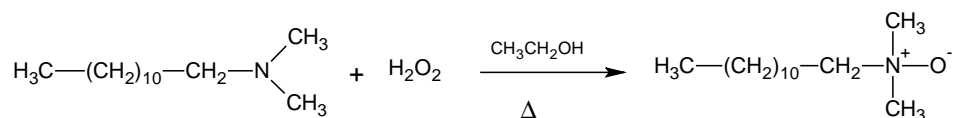
This surfactant seems to self-aggregate to spontaneously afford vesicles by Dynamic light scattering measurements. It was impossible to determinate the c.m.c. value.

7.1.4 Synthesis and purification of zwitterionic surfactants

A) Synthesis and purification of the dodecylamine oxide (DDAO)



The synthesis can be schematised as following:



In a 1 l round-bottom flask dodecyl dimethylamine (43.1 gr, 0.1 mol) and 45 ml of ethanol were added, and the mixture was heated to reflux. Hydrogen peroxide (33%, 16.5 gr, 0.50 mol) were added over 1 hour to the refluxing mixture, then the reaction was allowed to proceed for 9 hours. Excess peroxide was removed by carefully adding solid MnO₂ to the hot mixture, until no more oxygen evolution was observed. The reaction mixture was then brought to room temperature, filtered on a paper filter (washing more than once with anhydrous EtOH) and evaporated to obtain a white solid. The solid was crystallised from an acetone/Et₂O mixture and dried *in vacuo* over P₂O₅.

Surface tension measurements confirm the purity of the product.

M.W. = 229.46.

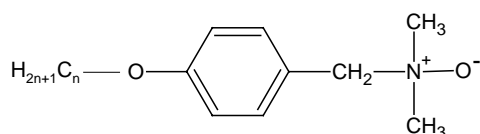
Yield = 90 %

c.m.c. = 7.0×10^{-4} M

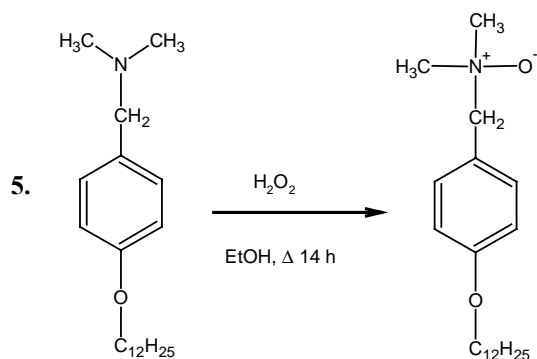
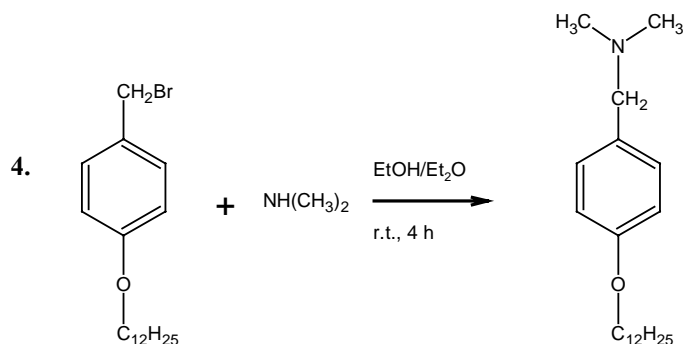
$^1\text{H-NMR}$ (200 MHz) CDCl_3 δ : 0.88 (t, 3H, CH_3); 1.22-1.40 (m, 18H, CH_2);

1.78-1.96 (m, 2H, CH_2); 3.18 (s, 6H, CH_3); 3.19-3.30 (m, 2H, CH_2).

B) Synthesis and Purification of p-dodecyloxybenzyl-dimethylamine oxide Surfactant (pDOAO)



The five-steps synthesis of the zwitterionic p-dodecyloxybenzyltrimethylamine oxide was conducted according to the general scheme for pDOTABr, for **1**, **2** and **3**, where the starting reactant is the bromide derivative of step **3**:



4. Synthesis of p-dodecyloxybenzyl dimethylamine

In a 500 ml flask p-dodecyloxybenzyl bromide (step 3) (18.5 gr, 0.052 mol) was dissolved in 30 ml of absolute EtOH. Then NHMe_2 (33% w/w in EtOH) (42 ml, 0.234 mol) was slowly added while stirring at room temperature, and the reaction was worked up for 4 hours. The reaction mixture was elaborated by adding 100 ml of 10% NaOH, and extracted with ethyl ether. The organic phase was washed with water until neutral and evaporated; the yellow oil was separated from a fine white solid impurity by filtration on a short neutral alumina column (petroleum ether).

M.W. = 319.51.

$^1\text{H-NMR}$ (CD_3OD , 200 MHz) δ , ppm: 0.88 (t, CH_3); 1.23-1.45 (m, (n-3) CH_2); 1.73-1.80 (m, CH_2); 2.37 (s, 2 CH_3); 3.47 (s, CH_2); 3.94 (t, CH_2); 6.87 (d, 2 H); 7.28 (d, 2 H).

5. Synthesis of p-dodecyloxybenzyl dimethylamine oxide

In a 100 ml flask p-alkyloxybenzyl dimethylamine (step 5) (6.7 gr, 0.021 mol) was dissolved in 15 ml of anhydrous EtOH and a 33% H_2O_2 solution (3.4 ml, 0.033 mol) was added over 1 hour to the refluxing mixture, and the reaction was carried on for 14 hours. Excess peroxide was removed by carefully adding solid MnO_2 to the hot mixture, until no more oxygen evolution was observed. The reaction mixture was then brought to room temperature, filtered on a paper filter (washing more than once with anhydrous EtOH) and evaporated. The yellow oil was treated 3-4 times with ethyl ether and evaporated until a white solid was obtained. The solid was dispersed in ethyl ether, sonicated, cooled to 0°C , filtered, rinsed with cold ethyl ether and dried over P_2O_5 in vacuum.

As no minima were observed in the surface tension vs. $\log [\text{pDOAO}]$ plot, the surfactant was considered pure.

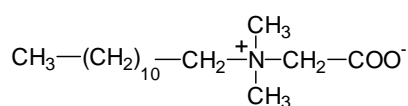
M.W. = 335.59.

Yield = 98 %.

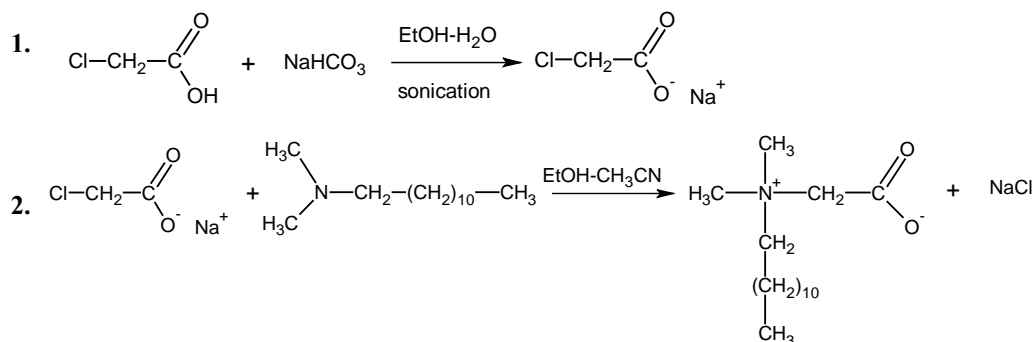
c.m.c. = $1.6 \cdot 10^{-5}$ M (Surface tension).

$^1\text{H-NMR}$ (CD_3OD , 200 MHz) δ : 0.78 (t, 3 H, CH_3); 1.18–1.30 (m, 18 H, 9 CH_2); 1.58–1.70 (m, 2 H, CH_2); 2.95 (s, 6 H, 2 CH_3); 3.87 (t, 2 H, CH_2); 4.23 (s, 2 H, CH_2); 6.84 (d, 2 H, Ar); 7.33 (d, 2 H, Ar).

C) Synthesis and purification of dodecyl dimethyl carboxybetaine (CB1-12)



The scheme of synthesis is as following:



1. Preparation of sodium chloroacetate

In a 250 ml round-bottom flask the monochloroacetic acid (20,3 gr. 0.214 mol) was dissolved in a mixture of EtOH/ H_2O 80:20. Sodium bicarbonate (18.05 gr, 0.214 mol) was then added to the solution, and the solution was stirred until the end of the development of CO_2 . A small amount of acid was then added to the solution, to be sure that all the sodium bicarbonate was consumed. The solution obtained was poured in acetone while stirring, and a white solid formed. This solid was filtered, washed with acetone, dried over P_2O_5 *in vacuo*, and then dried at 110°C for 6-8 h.

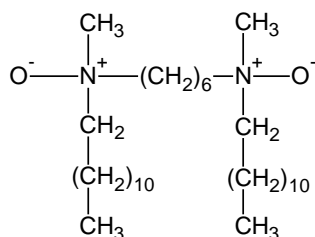
2. Synthesis of the dodecyldimethylcarboxybetaine (CB1-12)

In a 250 ml round-bottom flask, sodium chloroacetate (10 gr, 0.085 mol) and dimethyldodecylamine (18,32 gr, 0.085 mol) were dissolved in 100 ml EtOH and 100 ml CH₃CN. The mixture was refluxed for 40 h under stirring. After that, it was cooled to -20 °C, and the NaCl formed was filtered off on Watman filter paper. The solution was concentrated and the solid was dissolved in Et₂O and refluxed for 1 h. After cooling to room temperature, the solid was filtered under nitrogen using a büchner. An easily-filtered fine white solid was obtained. This solid was again refluxed after addition of Et₂O, and after filtration the solid was kept *in vacuo* in the presence of P₂O₅ for several days. Since the solid is quite hygroscopic all operations were conducted under N₂. Finally, it was crystallised from ethylacetate/EtOH (99/1).

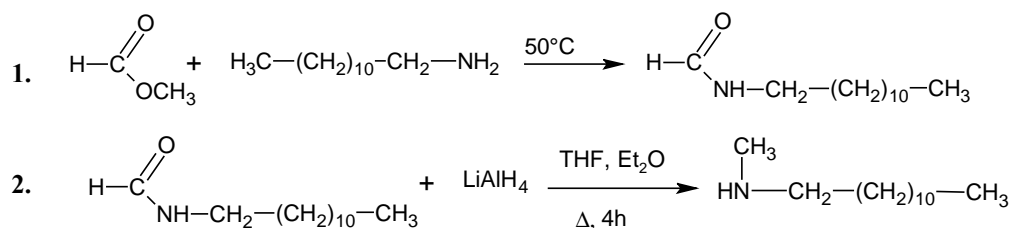
Yield = 80%

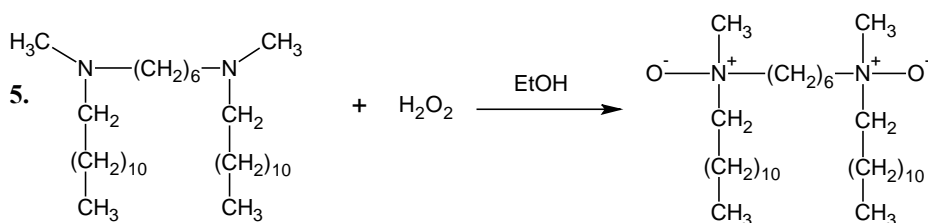
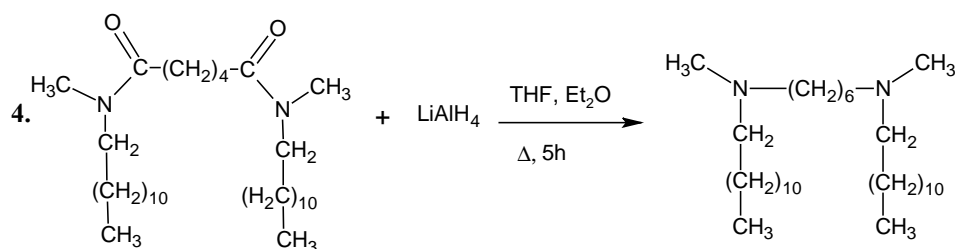
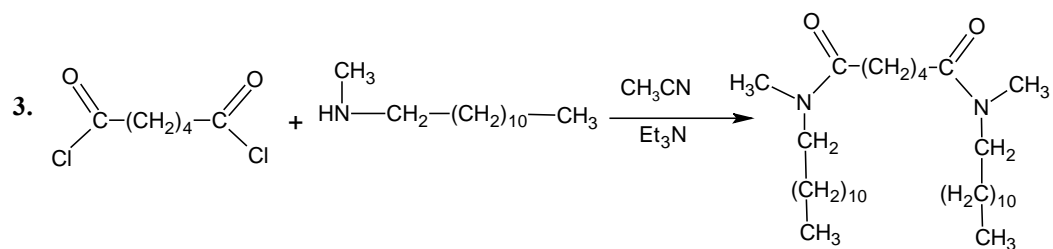
¹H-NMR (CDCl₃, 400 MHz) δ: 0.88 (t, 3H, CH₃); 1.26–1.34 (m, 18H, 9CH₂); 1.70–1.73 (m, 2H, CH₂); 3.18 (s, 6H, 2 CH₃); 3.23-3.27 (m, 2H, CH₂); 3.77-3.82 (m, 2H, CH₂).

D) Synthesis and purification of gemini GemAO



The scheme of synthesis is as following:





1. Synthesis of dodecylformamide

In a 250 ml glass bottle with screw cap, equipped with a magnetic stirring bar, dodecylamine (40.0 gr, 0.216 mol) and methyl formate (48.7 g, 0.811 mol) were added without any solvent, and the system was kept for one night in a oil bath at 50 °C under stirring. A pale yellow mixture is obtained. Then, the bottle was left for 3h at room temperature, and after few minutes a white solid was formed. The solid was filtered and dissolved in ethyl ether by heating, and was crystallised at 4 °C. The filtered white solid was washed with ethyl ether and dried *in vacuo*.

M.W. = 213.36.

Yield = 96 %.

m.p. = 39-40 °C

¹H-NMR(200 MHz CDCl₃) δ: 0.78-0.98 (m, 3H, 1CH₃); 1.16-1.46 (m, 18H, 9CH₂); 1.49-1.61 (m, 2H, 1CH₂); 3.16-3.38 (m, 2H, 1CH₂); 5.53 (s, 1H, NH); 8.05 (d, 1H, HCO); 8.16 (s, 1H, HCO).

2. Synthesis of the N-methyl-N-dodecyl amine

In a dry round-bottom flask formildodecyl amine (44.3 gr, 0.208 mol) was dissolved in 400 ml of anhydrous THF under nitrogen. Maintaining the system under nitrogen atmosphere and under vigorous stirring LiAlH₄ (208 ml of a 1 M solution in diethyl ether, 0.218 mol) was added dropwise. At the end of the addition the mixture of reaction was refluxed for 4h and a white solid was obtained. After cooling the flask to room temperature, excess LiAlH₄ was eliminated by addition of ice into the mixture, keeping the flask at 0 °C. Then, the mixture was made basic upon addition of some pellets of NaOH. The reaction mixture was then filtered to remove the aluminium hydroxide formed, washed with diethyl ether, and extracted to remove the aqueous phase. The organic phase was dried adding anhydrous Na₂SO₄, and after removing the solvent, a pale yellow oil was obtained.

M.W. = 198.36.

Yield = 89 %.

¹H-NMR(200 MHz CDCl₃) δ: 0.84 (t, 3H, 1CH₃); 1.17-1.37 (m, 18H, 9CH₂); 1.37-1.47 (m, 2H, 1CH₂); 2.43 (s, 3H, CH₃N); 2.52-2.59 (t, 1H, NH).

3. Synthesis of N,N'-didodecyl-N,N'-dimethyl-adipoyldiamide

In a dry 1l three neck round-bottom flask methyldodecylamine (27.2 gr, 0.137 mol) was dissolved in 350 ml of dry CHCl₃. Trimethylamine (13.66 gr, 0.136 mol) was thus added. Then, adipoyldichloride (12.5 gr, 0.0683 mol) dissolved in CHCl₃ was added dropwise under nitrogen, maintaining the flask at 0°C. After 3h, from the end of the addition, the yellow solution obtained was warmed to room temperature and then at 40°C for 1h. At the end, ice and water were added to the solution and the organic phase was extracted and washed with water until neutrality. After drying over anhydrous Na₂SO₄, the chloroform was removed, to give a yellow oil that become a solid at 0 °C. The solid was recrystallised from methanol at -20 °C. An amorpheous white solid was obtained.

M.W. = 508.86.

Yield = 76 %

m.p. = 47-48 °C.

¹H-NMR (200 MHz CDCl₃) δ: 0.88 (t, 6H, 2CH₃); 1.17-1.35 (m, 18H, 9CH₂); 1.50-1.60 (m, 4H, 2CH₂); 1.65-1.70 (m, 4H, 2CH₂); 2.32-2.40 (m, 4H, 2CH₂); 2.90 (d, 6H, 2CH₃); 2.86 (s, 3H, 1CH₃); 2.96 (s, 3H, 1CH₃); 3.24 e 3.33 (2t, 4H, 2CH₂).

4. Synthesis of the N,N'-didodecyl-N,N'-dimethyl-hexane-1,6-diamine

In a dry 1l round-bottom flask N,N'-didodecyl-N,N'-dimethyl-adipoyldiamide (26.2 gr, 0.0052 mol) was dissolved in 400 ml of THF under nitrogen. Maintaining the system under nitrogen atmosphere and under vigorous stirring, LiAlH₄ (115 ml of a 1 M solution in diethyl ether, 0.115 mol) was added dropwise. At the end of the addition the reaction mixture was refluxed for 5h and a white solid was obtained. After cooling the flask to room temperature, excess LiAlH₄ was eliminated by addition of ice into the mixture, keeping the flask at 0°C. Then, the mixture was made basic upon addition of some pellets of NaOH. The mixture of reaction was thus filtered to take off the aluminium hydroxide formed, washed with diethyl ether, and extracted to remove the aqueous phase. The organic phase was dried adding anhydrous Na₂SO₄, and after having removed the solvent a pale yellow oil was obtained.

M.W. = 480.89.

Yield = 94 %

¹H-NMR (200 MHz CDCl₃) δ: 0.88 (t, 6H, 2CH₃); 1.1-1.5 (m, 48H, 24CH₂); 2.19 (s, 6H, 2CH₃N); 2.26-2.43 (t, 8H, 4CH₂).

5. Synthesis of the N,N'-didodecyl-N,N'-dimethyl-hexane-1,6-diamine oxide

In a 500 ml round-bottom flask N,N'-didodecyl-N,N'-dimethyl-hexane-1,6-diamine oxide (11,4 gr, 0.024 mol) was dissolved in 200 ml of ethanol and the system was heated to reflux. As the reflux began, a 30% solution of H₂O₂

(7.8 ml, 0.0768 mol) was added. After about 16h of reflux, the reaction mixture was cooled to room temperature. Excess peroxide was removed by carefully adding solid MnO₂, until no more oxygen development was observed. The reaction mixture was then brought to room temperature, filtered on a paper filter and evaporated. It was washed 3-4 times with ethyl ether and evaporated until a white solid was obtained. The solid was dissolved in ethyl ether and one drop of methanol by heating the solution, and it was crystallised at 4°C. After filtration it was dried over P₂O₅ in vacuum.

M.W. = 512.89.

Yield = 63 %

m.p. = 128-130 °C

¹H-NMR (200 MHz CDCl₃) δ: 0,90 (t, 6H, 2CH₃); 1,19-1,5 (m, 40H, 20CH₂); 1,75-2,00 (m, 8H, 4CH₂); 3,09 (s, 6H, 2CH₃); 3,10-3,27 (m, 8H, 4CH₂).

7.2 Methods

7.2.1 Determination of DNA concentration

The DNA concentration in solution was determined by spectrophotometric measurements, using a Hitachi U-3300 spectrophotometer. The wavelength of reference is 260 nm. The Lambert-Beer equation was used:

$$A = \varepsilon [DNA] l$$

where:

$l = 1$ cm (optical path)

ε = Molar extinction coefficient. An $\varepsilon = 13000 \text{ M}^{-1}\text{cm}^{-1}$ was used to have a DNA concentration expressed in base pair molar.

The measurement was registered at the following conditions: medium response, band width 2 nm, scan speed of 40 nm/min, 220-320 range, T= 25 °C.

7.2.2 Circular dichroism measurements

A JASCO J-810 spectropolarimeter was used, covering the range between 210 and 320 nm. For some systems such as CTABr, CTBABr and TBABr too high a voltage for the instrument was registered, due to the high absorption of the solution in this wavelength range. For this reason these compounds were studied over a narrower range, between 230 and 320 nm.

The CD spectra obtained were converted to molar ellipticity with a specific program, by inserting the values of the optical path, the molar weight of DNA (that, referred to the single nucleotide is 400), and the concentration of the DNA solution that was analysed.

Experimental procedure in water solution

In order to better control the pH in the absence of buffer, a DNA solution in concentration 2.37×10^{-4} M was prepared by adjusting the pH with additions of HCl or NaOH solutions to have the desired value. Then, the surfactant solution at the desired concentration was prepared similarly. Aliquots of the two solutions were then mixed to obtain a solution having $[\text{DNA}] = 2.0 \times 10^{-5}$ M (base pairs) at the desired surfactant concentration. The pH of this solution was readjusted where necessary. Finally, 2.4 ml of the solution were put in a 3 ml cuvette of a 1 cm path and CD spectrum were registered. Analogue solutions without DNA were prepared as blanks.

The instrument was set as following: optical path = 1 cm; band width = 10 nm; response 2 sec; standard sensitivity = 1000 mdeg, scan speed = 20 nm/min, accumulation = 3, T = 25°C.

The maximal λ value was determined by using a Jasco programme, which calculates this value after a smoothing of the curve and was verified by using the Origin programme. No differences were found.

Experimental procedure in Tris-HCl

In a 3 ml cuvette (1 cm optical path) 2,4 ml of Tris-HCl solution of the desired pH value was measured as blank value. In the same cuvette, about 2 μl of a concentrated DNA solution was added to the buffer, to give a concentration of DNA of 2×10^{-5} M. The CD spectra of the DNA in buffer solution was thus registered. Subsequently, four additions of 30 μl of a surfactant solution gave the required concentrations of surfactant. After each addition a new CD spectrum was recorded. The instrumental conditions where in this case optimised to avoid the use of smoothing programmes.

Instrumental conditions: sensitivity = standard; range of measurement = 320-230 nm; Data pitch = 0.1; scanning mod = continuous; scan speed = 5 nm/min; response= 8 sec; band width =: 1 nm; accumulation: 4.

7.2.3 Fluorescence measurements

A Hitachi F-4500 fluorimeter was used. The spectra were registered with a scan speed of 240 nm/min and a response of 0.5.

The other instrumental parameters for Hoechst 33258 were: range of measurement= 400 - 700 nm; excitation wavelength: 360 nm; excitation slit: 2.5; emission slit: 5.0.

In the case of Ethidium Bromide: range of measurement= 530 - 800 nm; excitation wavelength: 520 nm; excitation slit: 10; emission slit: 5.0.

Experimental procedure

In a 3 ml (1 cm path) cuvette, 2 ml of Tris-HCl buffer at the desired pH value was measured as blank. In the same cuvette, about 2 μ l of a concentrated DNA solution was added to the buffer, giving a concentration of DNA of 2×10^{-5} M. The fluorescence spectra of the DNA in buffer solution was thus registered. Subsequently, 10-12 additions of 10 μ l of the surfactant solution were effectuated into the same cuvette, to have the required concentration of surfactant. After each addition a new fluorescence spectrum was registered.

7.2.4 Absorption measurements

The absorption spectra were registered after each addition of surfactant, along with the fluorescence measurements. A Hitachi U-3300 spectrophotometer was used with 1 cm optical path cuvettes.

The instrumental parameters were: scan speed. 600 nm/min; sampling interval: 1nm; wavelength range: 200-700 nm

For the measurements performed using a 10 cm optical path cuvette, a Hewlett Packard 8452 diode array spectrophotometer was used.

7.2.5 Polarization measurements

A SPEX FLUOROLOG 2.1.2 instrument was used for polarization measurements.

In the case of Hoechst 33258, the instrumental parameters were: range of measurement= 400-700 nm; excitation wavelength= 360 nm; increment= 0.5 nm; integration= 0.5 sec; excitation slit= 10 nm; emission slit= 10 nm.

In the case of Ethidium Bromide the instrumental parameters were: range of measurement= 530-800 nm, excitation wavelength= 520 nm; increment=0.5 nm; integration= 0.5 sec; excitation slit= 10 nm; emission slit= 10 nm.

Experimental procedure

A procedure analogous to that for other fluorescence measurement was followed.

7.2.6 Surface tension measurements

Surface tension measurements were carried out with a Du Nouy tensiometer (Fisher) using a 6.015 cm circumference platinum-iridium ring, flamed before each run. Surface tension of water was used to test the cleanness of the equipment. Each measurement was repeated at least three times, and average values were calculated. Solutions were prepared using deionised bidistilled water. C.m.c. values were calculated as the intersections points of the two straight lines in surface tension vs. $-\log$ [surfactant] plots. Tensidic impurities - free surfactants give profiles with no minima in correspondence of the c.m.c..

7.2.7 Conductivity measurements

Conductivity was measured in a conductimeter Orion Research, equipped with a platinum electrode, of cell constant 1.1 cm^{-1} . Solutions were at $25.0 \text{ }^\circ\text{C}$ ($\pm 0.1 \text{ }^\circ\text{C}$) and continuously stirred.

7.2.8 Molecular modelling studies

All molecular modelling calculations were performed using the software packages Sybyl and GRID running on a Silicon Graphics O2 R12000, Intel Pentium IV 1.4 GHz workstation. For the conformational analysis and minimisation, the Confort and Omega methods were adopted. The 3D structure of DNA was obtained from the DNA builder in Sybyl. DNA counterions were added by the programme GRIN. This programme adds a potassium counterion for each phosphate in the middle of the nucleic acid sequence, and a magnesium ion for the 5' terminus. The counterions are placed by GRIN at 10.0 \AA distance from each phosphorus atom of DNA. They are normally located in the water phase, well “off-shore” from the regular Target atoms. Finally, GRID programme was set to give the maximal mobility to the counterions.

The binding mode of the ligands was extensively analysed by the mean of the docking procedure. A family of 100 conformations of each ligand was generated using the following procedure: the initial conformation of the ligand obtained from the reported minimum conformation was arbitrarily rotated. By filtering out all of the conformers showing high internal energy, the final conformation family of 100 conformers was achieved. Each conformer was then docked into the DNA tridecamer and the binding results were associated with the most stable complexes. The procedure was then repeated for all the remaining conformers. The atom charges automatically assigned by GRID module were retained on all docking calculations. An alternative docking procedure was used to explore the binding conformation of the ligand as before, but generating the conformers upon docking. No significant differences

were obtained. To compute interaction energies a 3D grid of 0.2 Å, resolution was centred on DNA automatically. The size of the grid box was chosen to enclose all selected atoms with an extra margin of 5 Å. The grid had a size of about 36 × 31 × 33 Å and was composed of about 1 400 000 grid points. Energy scoring were obtained by using an all-atom model and a distance-dependent dielectric function with a 10 Å cut-off. GRID atomic charges were assigned to all DNA atoms. The ligand was then docked into the DNA active site by matching Molecular Interaction Fields minima with ligand atoms.

APPENDIX I

Circular Dichroism

Table 1: Variation of the λ_{\max} in function of the concentration of CTABr at pH = 7.1 and at 25°C.^a

10^4 [CTABr] (M)	λ_{\max} (nm)
0	273.8
0.003	273.8
0.01	273.8
0.03	274.8
0.06	275.5
0.10	276.3
0.32	276.9
1.00	277.3
10.0	277.4
83.0	277.4
160.0	277.4

^a [DNA] = 2.0×10^{-5} M.

Table 2: Variation of the λ_{\max} in function of the concentration of CTBABr at pH = 7.1 and at 25°C.^a

10^4 [CTBABr] (M)	λ_{\max} (nm)
0	273.8
0.003	273.8
0.01	273.8
0.03	274.4
0.10	275.6
0.32	276.6
1.00	276.7
10.0	276.7
50.0	276.7
100.0	276.7

^a [DNA] = 2.0×10^{-5} M.

Table 3: Variation of the λ_{\max} in function of the concentration of TBABr at pH = 7.1 and at 25°C.^a

10^4 [TBABr] (M)	λ_{\max} (nm)
0	273.8
0.003	274.0
0.01	274.0
0.10	274.0
1.00	274.1
5.00	274.2
10.0	274.1
50.0	274.2
100.0	274.2
200.0	274.0

^a [DNA] = 2.0×10^{-5} M.

Table 4: Variation of the λ_{\max} in function of the concentration of CTABr at pH = 7.5 and at 25°C.^a

10^4 [CTABr] (M)	λ_{\max} (nm)
0	273.8
0.003	273.8
0.01	273.8
0.03	274.2
0.06	274.6
0.10	275.4
0.30	276.5
1.00	277.1
10.0	277.3
100.0	277.3
200.0	277.3

^a [DNA] = 2.0×10^{-5} M.

Table 5: Variation of the λ_{\max} in function of the concentration of CTBABr at pH = 7.5 and at 25°C.

10^4 [CTBABr] (M)	λ_{\max} (nm)
0	273.8
0.003	273.8
0.01	273.8
0.03	274.7
0.10	275.5
0.30	276.4
0.94	276.7
10.0	276.7
50.0	276.6
200.0	276.5

^a [DNA] = 2.0×10^{-5} M

Table 6: Variation of the λ_{\max} in function of the concentration of TBABr at pH = 7.5 and at 25°C.^a

10^4 [TBABr] (M)	λ_{\max} (nm)
0	273.8
0.01	273.6
1.0	274.4
5.0	274.5
10.0	274.3
50.0	274.4
100.0	274.4
200.0	274.8

^a [DNA] = 2.0×10^{-5} M.

Table 7: Variation of the λ_{\max} in function of the pH for the DNA + DDAO system at 25.0°C.^a

pH	λ_{\max} (nm)
5.55	285.5
5.84	285.8
6.11	286.2
6.41	285.5
6.97	283.7
7.38	274.9
7.58	275.5

^a [DNA] = 2.0×10^{-5} M; [DDAO] = 1×10^{-2} M.

Table 8: Variation of the λ_{\max} in function of the concentration of DDAO at pH = 6.5 and at 25°C.^a

10^3 [DDAO] (M)	λ_{\max} (nm)
0	273.8
0.10	274.4
0.32	274.8
1.00	276.2
2.00	279.8
3.20	281.8
6.00	281.5
10.0	282.0
20.0	280.8

^a [DNA] = 2.0×10^{-5} M.

Table 9: Variation of the λ_{\max} in function of the concentration of DDAO at pH = 7.1 and at 25°C.^a

10^3 [DDAO] (M)	λ_{\max} (nm)
0	273.8
0.10	273.4
0.12	273.4
0.20	273.9
0.32	273.6
0.40	274.2
0.50	275.6
0.60	276.6
1.00	278.6
1.90	278.0
3.50	281.0
5.00	282.4
6.00	281.1
10.20	284.6
20.00	284.3
32.00	282.6

^a [DNA] = 2.0×10^{-5} M.

Table 10: Variation of the λ_{max} in function of the concentration of DDAO at pH = 7.5 and at 25°C.^a

10^3 [DDAO] (M)	λ_{max} (nm)
0	273.8
0.32	274.8
3.20	273.8
20.0	273.4
32.0	273.6

^a [DNA] = 2.0×10^{-5} M.

Table 11: Variation of the λ_{max} in function of the pH for the DNA + DDAO system at 25.0°C.^a

pH	λ_{max} (nm)
7.10	284.7
7.15	284.8
7.20	283.6
7.25	277.1
7.30	273.9
7.35	273.5
7.40	274.0
7.45	274.0
7.50	274.2

^a [DNA] = 2.0×10^{-5} M; [DDAO] = 2×10^{-2} M.

Table 12: Variation of the λ_{max} in function of the pH for the DNA + DDAO system at 25.0°C.^a

pH	λ_{max} (nm)
5.05	277.8
5.30	277.7
5.56	276.6
5.74	276.0
6.10	274.9
6.50	274.4
6.75	274.0
7.10	273.8
7.30	274.0
7.50	274.1

^a [DNA] = 2.0×10^{-5} M; [DDAO] = 8×10^{-5} M.

Table 13: Variation of the λ_{max} in function of the pH for the DNA + SB3-12 system at 25.0°C.^a

pH	λ_{max} (nm)
6.07	274.5
6.54	274.3
7.08	274.5
7.52	274.2

^a [DNA] = 2.0×10^{-5} M; [SB3-12] = 2×10^{-2} M.

Table 14: Variation of the λ_{max} in function of the pH for the DNA + SB3-12 system at 25.0°C.^a

pH	λ_{max} (nm)
7.10	274.2
7.21	274.0
7.32	274.3
7.41	273.8
7.52	274.2

^a [DNA] = 2.0×10^{-5} M; [SB3-12] = 2×10^{-2} M.

Tabella 15: Variation of the λ_{max} in function of the concentration of SB3-12 at pH = 7.1 and at 25°C.^a

10^3 [SB3-12] (M)	λ_{max} (nm)
0	273.8
0.10	274.1
0.50	274.2
1.00	274.0
5.00	274.3
10.0	274.2
20.0	274.2

^a [DNA] = 2.0×10^{-5} M.

Tabella 16: Variation of the λ_{max} in function of the concentration of SB3-12 at $pH = 7.5$ and at $25^{\circ}C$.^a

10^3 [SB3-12] (M)	λ_{max} (nm)
0	273.8
0.10	274.1
0.50	274.2
1.00	274.1
5.00	274.1
10.0	274.0
20.0	274.2

^a [DNA] = 2.0×10^{-5} M.

Table 17: Variation of the λ_{max} in function of the pH for the DNA + TMAO system at $25.0^{\circ}C$.^a

pH	λ_{max} (nm)
6.06	274.0
6.55	274.0
7.05	274.4
7.50	273.8

^a [DNA] = 2.0×10^{-5} M; [TMAO] = 2×10^{-2} M.

Table 18: Variation of the λ_{max} in function of the concentration of TMAO at $pH = 7.1$ and at $25^{\circ}C$.^a

10^3 [TMAO] (M)	λ_{max} (nm)
0	273.8
0.10	273.8
5.00	273.6
10.0	274.7
20.0	273.6

^a [DNA] = 2.0×10^{-5} M.

Table 19: Variation of the λ_{\max} in function of the concentration of TMAO at pH = 7.5 and at 25°C.^a

10^3 [TMAO] (M)	λ_{\max} (nm)
0	273.8
0.10	273.8
5.00	273.6
10.0	274.7
20.0	273.6

^a [DNA] = 2.0×10^{-5} M.

Table 20: Variation of the λ_{\max} in function of the concentration of SB3-1 at pH = 7.1 and at 25°C.^a

10^3 [SB3-1] (M)	λ_{\max} (nm)
0	273.8
0.10	274.1
1.00	274.0
10.0	274.1
20.0	274.1

^a [DNA] = 2.0×10^{-5} M.

Table 21: Variation of the λ_{\max} in function of the concentration of TMAO at pH = 7.5 and at 25°C.^a

10^3 [SB3-1] (M)	λ_{\max} (nm)
0	273.8
0.10	273.9
1.02	274.0
9.94	274.0
20.0	273.9

^a [DNA] = 2.0×10^{-5} M

APPENDIX II

Surface Tension

Table 1: Variation of the surface tension in function of the concentration of CTABr in H₂O at 25.0°C.

10^3 [CTABr] (M)	$-\log$ [CTABr]	γ (10^{-3} N/m)
0		72.42
0.08	4.10	47.46
1.00	4.00	44.46
0.12	3.92	42.27
0.20	3.70	39.43
0.25	3.61	38.05
0.37	3.43	35.60
0.48	3.32	34.34
0.72	3.14	33.47
1.17	2.93	32.95
1.69	2.77	33.18
2.16	2.67	32.73
3.97	2.40	32.97
8.28	2.08	32.89

Table 2: Variation of the surface tension in function of the concentration of CTABr in the presence of DNA at 25.0°C.

10^3 [CTABr] (M)	$-\log$ [CTABr]	γ (10^{-3} N/m)
0		58.24
0.08	4.10	41.93
0.01	4.00	40.38
0.12	3.92	38.26
0.20	3.70	36.83
0.25	3.61	35.61
0.37	3.43	34.66
0.48	3.32	33.98
0.72	3.14	33.41
1.17	2.93	33.23
1.69	2.77	33.18
2.16	2.67	33.21
3.97	2.40	33.24
8.28	2.08	32.82

^a [DNA] = 2.0×10^{-5} M.

Table 3: Variation of the surface tension in function of the concentration of DDAO in H₂O at pH = 7.1 and at 25.0°C.

10^3 [DDAO] (M)	$-\log$ [DDAO]	γ (10^{-3} N/m)
0		70.66
0.05	4.30	41.17
0.10	4.00	38.18
0.13	3.89	37.34
0.18	3.74	36.55
0.26	3.59	35.30
0.39	3.41	34.12
0.51	3.29	33.57
0.76	3.12	32.69
1.00	3.00	32.64
1.49	2.83	32.60
2.42	2.62	32.60
4.63	2.33	32.61
8.50	2.07	32.72
17.6	1.75	32.77

Table 4: Variation of the surface tension in function of the concentration of DDAO in the presence of DNA at pH = 7.1 and at 25.0°C.^a

10^3 [DDAO] (M)	$-\log$ [DDAO]	γ (10^{-3} N/m)
0		53.59
0.05	4.30	44.67
0.10	4.00	38.88
0.13	3.89	36.79
0.18	3.74	34.02
0.26	3.59	32.59
0.39	3.41	32.09
0.51	3.29	32.10
0.76	3.12	32.17
1.00	3.00	32.00
1.49	2.83	32.04
2.42	2.62	32.23
4.63	2.33	32.47
8.50	2.07	32.00
17.6	1.75	31.95

^a [DNA] = 2.0×10^{-5} M.

Table 5: Variation of the surface tension in function of the concentration of DDAO in the presence of DNA at pH = 5.0 and at 25°C.^a

10^3 [DDAO] (M)	$-\log$ [DDAO]	γ (10^{-3} N/m)
0		53.50
0.08	4.10	42.34
0.10	4.00	40.22
0.12	3.92	39.33
0.20	3.70	38.42
0.25	3.61	37.05
0.37	3.43	35.99
0.48	3.32	35.23
0.72	3.14	34.08
1.17	2.93	33.89
1.69	2.77	33.82
2.16	2.67	33.81
3.97	2.40	33.64
8.28	2.08	33.55

^a [DNA] = 2.0×10^{-5} M.

APPENDIX III

Molecular Modelling

Table 1: GRID probes. Multi-atom probes are the marked with the symbol (M).

Probe name	Brief description	Probe name	Brief description
C3	Methyl CH ₃ group	C1=	sp ² CH aromatic or vinyl
N:#	sp N with lone pair	N:=	sp ² N with lone pair
N:	sp ³ N with lone pair	N:-	Anionic tetrazole N
N1	Neutral flat NH eg amide	N1+	sp ³ amine NH cation
N1=	sp ² Amine NH cation	N1:	sp ³ NH with lone pair
NH=	sp ² NH with lone pair	N1#	sp NH with one hydrogen
N2	Neutral flat NH ₂ eg amide	N2+	sp ³ amine NH ₂ cation
N2=	sp ² Amine NH ₂ cation	N2:	sp ³ NH ₂ with lone pair
N3+	sp ³ amine NH ₃ cation	NM3	Trimethyl ammonium cation
O1	Alkyl hydroxy OH group	OH	Phenol or carboxy OH
O-	sp ² phenolate oxygen	O	sp ² carbonyl oxygen
O::	sp ² carboxy oxygen atom	COO-	Multi-atom carboxy
OES	sp ³ ester oxygen atom	OC2	Ether or furan oxygen
OS	O of sulphone / sulphoxide	ON	Oxygen of nitro group
O=	O of sulphate or sulphonamide	OH2	Water
PO4	PO ₄ phosphate dianion	PO4H	PO ₄ H phosphate anion
S1	Neutral SH group		
F	Organic fluorine atom	F-	Fluoride anion
CL	Organic chlorine atom	CL-	Chloride anion
BR	Organic bromine atom	BR-	Bromide anion
I	Organic iodine atom	I-	Iodide anion
LI+	Lithium cation	NA+	Sodium cation
K+	Potassium cation	RB+	Rubidium cation
CS+	Caesium cation	MG+2	Magnesium cation
CA+2	Calcium cation	SR+2	Strontium cation
ZN+2	Zinc cation	CU+2	Cupric copper cation
FE+2	Ferrous iron cation	FE+3	Ferric iron cation
BOTH	The Amphipatic Probe	DRY	Hydrophobic Probe
COO-	Aliphatic anionic carboxy group ^(M)	AR.COO-	Aromatic anionic carboxy group ^(M)
CONH2	Aliphatic neutral amide group ^(M)	AR.CONH2	Aromatic neutral amide group ^(M)
CONHR	Aliphatic neutral amide group ^(M)	AR.CONHR	Aromatic neutral amide group ^(M)
AMIDINE	Aliphatic cationic amidine group ^(M)	AR.	Aromatic cationic amidine group ^(M)
M-DIAMINE	Meta-diamino-benzene ^(M)	AMIDINE	group ^(M)

Fig.1: comparison of the energy values of the docking solutions of pDOAO and pDOAOH.

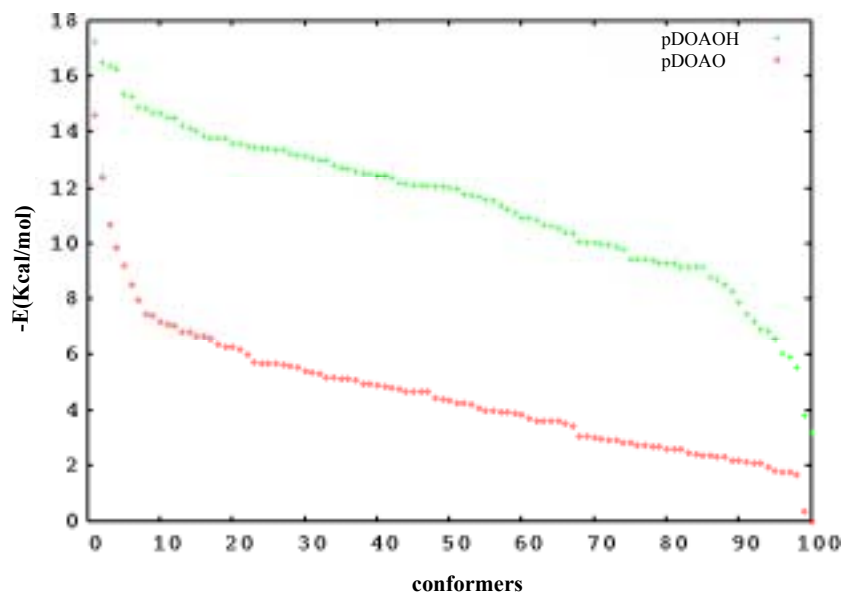
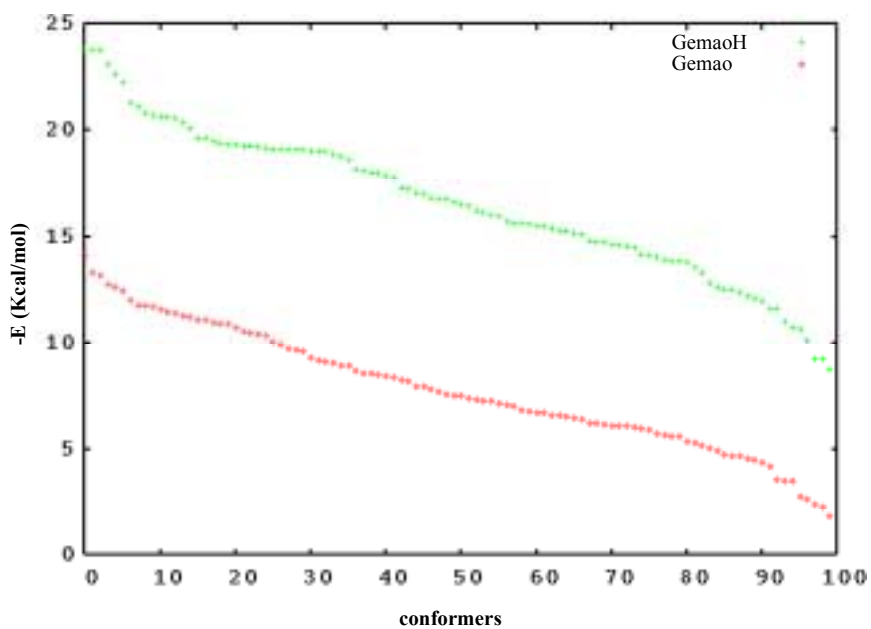


Fig.2: comparison of the energy values of the docking solutions of GemAO and GemAOH.



APPENDIX IV

Fluorescence Spectroscopy

Table 1: Quenching of fluorescence of EB intercalated into DNA in Tris-HCl buffer upon addition of surfactant solution up to a final ratio $[surfactant]/[DNA] = 4$. $[DNA] = 2.0 \times 10^{-5} M$; $[EB] = 4.2 \times 10^{-6} M$, $pH = 7.5$

Surfactant (S)	I/I ₀				
	Without S	[S]/[DNA]= 1	[S]/[DNA]= 2	[S]/[DNA]= 3	[S]/[DNA]= 4
C12-12	100	86.26	62.99	43.48	36.61
C12-16	100	80.13	50.29	37.78	34.30
C16-16	100	89.08	70.17	51.47	43.62
DDAO	100	84.67	83.66	82.99	80.88
pXMo(DDA) ₂	100	51.78	23.05	17.85	16.67
pXMo(MDA) ₂	100	46.57	27.89	25.54	22.44
pXMo(CDA) ₂	100	57.68	33.02	27.92	25.00
pXDo(TA) ₂	100	49.98	35.33	30.98	27.88
GemAO	100	95.88	93.86	89.22	90.18
pDOAO	100	96.49	93.11	91.87	88.62
pDOTABr	100	89.22	64.10	42.79	34.71

Table 2: Quenching of fluorescence of EB intercalated into DNA in acetonitrile upon additions of pXMo(DDA)₂; $[DNA] = 2.0 \times 10^{-5} M$.

$10^3 [pXMo(DDA)_2] (M)$	I ₀ /I
0	1.00
1.12	1.23
1.92	1.37
2.53	1.44
3.00	1.64
3.37	1.61
3.68	1.64
3.94	1.76
4.15	1.75
4.34	1.78
4.50	1.74

Table 3: Quenching of fluorescence of EB intercalated into DNA in acetonitrile upon additions of DDAO; $[DNA] = 2.0 \times 10^{-5} M$.

$10^3 [DDAO] (M)$	I_0/I
0	1.00
0.88	1.08
1.50	0.98
2.00	1.16
2.65	1.15
3.18	1.40
5.30	1.40

Table 4: Maximal values of the fluorescence intensity at $\lambda = 476 \text{ nm}$ for Hoechst 33258 in Tris-HCl 50 mM buffer upon addition of $pXMo(DDA)_2$ in the absence of DNA. $[Hoechst] = 2 \times 10^{-6} M$, $pH = 7.5$.

$10^4 [pXMo(DDA)_2] (M)$	$I_{max} (\lambda_{max} = 476)$
0	58.91
1.0	218.21
2.0	273.36
3.0	291.75
4.0	308.23
5.0	315.42
6.0	321.34
7.0	320.40
8.0	324.75
9.0	332.03
10.0	326.98
11.0	330.69
12.0	332.47

Table 5: Maximal values of the fluorescence intensity at $\lambda = 468$ nm for Hoechst 33258 in Tris-HCl 50 mM buffer upon addition of CTABr in the absence of DNA. $[Hoechst] = 2.0 \times 10^{-6}$ M, pH = 7.5.

$10^4[CTABr]$ (M)	$I_{max}(\lambda_{max} = 468)$
0	59.86
1.0	60.51
2.0	605.86
3.0	1111.08
4.0	1451.73
5.0	1668.01
6.0	1828.30
7.0	1906.78
8.0	1981.44
9.0	2008.37
10.0	2093.32
11.0	2143.72
12.0	2159.23

Table 6: Maximal values of the fluorescence intensity at $\lambda = 500$ nm for Hoechst 33258 in Tris-HCl 50 mM buffer upon addition of TEACl in the absence of DNA. $[Hoechst] = 2.0 \times 10^{-6}$ M, pH = 7.5.

$10^4[TEACl]$ (M)	$I_{max}(\lambda_{max} = 500)$
0	67.81
3.0	55.47
6.0	52.73
9.0	46.94
12.0	47.04

Table 7: Maximal values of the fluorescence intensity at $\lambda = 469$ nm for Hoechst 33258 in Tris-HCl 50 mM buffer upon addition of pDOTABr in the absence of DNA. [Hoechst] = 2.0×10^{-6} M, pH = 7.5.

10^4 [pDOTABr] (M)	I_{\max} ($\lambda_{\max} = 469$)
0	49.96
1.0	980.64
2.0	2347.70
3.0	2790.94
4.0	3158.35
5.0	3183.68
6.0	3392.57
7.0	3543.30
8.0	3474.39
9.0	3437.00
10.0	3556.57
11.0	3547.98
12.0	3559.08

Table 8 Maximal values of the fluorescence intensity at $\lambda = 480$ nm for Hoechst 33258 in Tris-HCl 50 mM buffer upon addition of SB3-12 in the absence of DNA. [Hoechst] = 2×10^{-6} M, pH = 7.5.

10^4 [SB3-12] (M)	I_{\max} ($\lambda_{\max} = 480$)
0	56.47
7.5	62.07
15.0	82.04
22.5	281.98
30.0	985.01
37.5	1714.66
45.0	2174.61
52.5	2419.59
60.0	2562.46
67.5	2686.83
75.0	2715.48
82.5	2781.18
90.0	2839.66

Table 9: Maximal values of the fluorescence intensity at $\lambda = 480$ nm for Hoechst 33258 in Tris-HCl 50 mM buffer upon addition of DDAO in the absence of DNA. $[Hoechst] = 2.0 \times 10^{-6}$ M, pH = 7.5.

$10^4[DDAO]$ (M)	$I_{\max} (\lambda_{\max} = 480)$
0	68.85
0.2	59.50
0.4	58.30
1.0	58.61
2.0	56.81
3.0	58.93
4.0	54.23
5.0	53.95
6.0	65.99
7.0	59.40
8.0	64.94
9.0	60.39
1.0	62.71
11.0	71.84
12.0	73.58

Table 10: Maximal values of the fluorescence intensity at $\lambda = 464$ nm for Hoechst 33258 in Tris-HCl 50 mM buffer upon addition of pDOAO in the absence of DNA. $[Hoechst] = 2.0 \times 10^{-6}$ M, pH = 7.5.

$10^5[pDOAO]$ (M)	$I_{\max} (\lambda_{\max} = 464)$
0	58.50
0.5	55.34
1.0	77.39
1.5	47.49
2.0	261.48
2.5	377.42
3.0	502.96
3.5	626.23
4.0	779.43
4.5	921.89
5.0	1006.70
5.5	1171.70
6.0	1277.50

Table 1: 1 Maximal values of the fluorescence intensity at $\lambda = 510$ nm for Hoechst 33258 in Tris-HCl 50 mM buffer upon addition of TMAO in the absence of DNA. $[Hoechst] = 2.0 \times 10^{-6}$ M, $pH = 7.5$.

$10^4 [TMAO]$ (M)	$I_{\max} (\lambda_{\max} = 510)$
0	70.42
3.0	62.52
6.0	54.46
9.0	54.57
12.0	50.58

APPENDIX V

Fluorescence Polarisation

Fig.1: Individual components for the polarisation of ethidium bromide –DNA complex in the absence of DDAO at pH= 5.8. [DNA]= 2.0×10^{-5} M; [EB]= 4.2×10^{-6} M

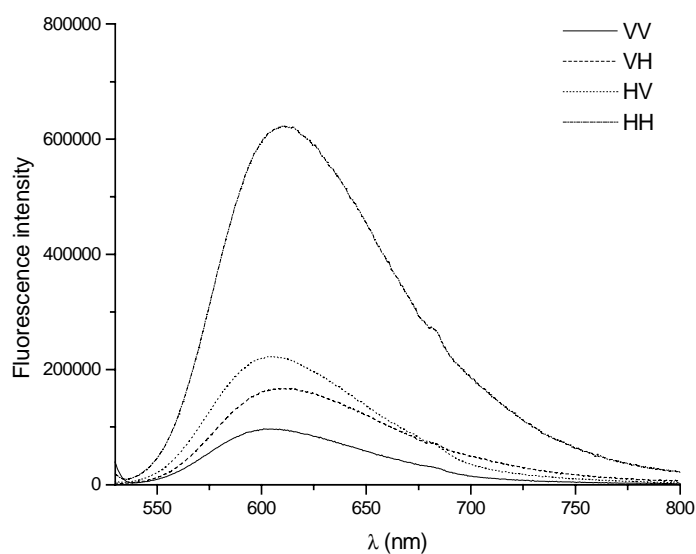


Fig.2: Individual components for the polarisation of ethidium bromide –DNA complex at [DDAO]= 2×10^{-4} M at pH= 5.8. [DNA]= 2.0×10^{-5} M; [EB]= 4.2×10^{-6} M

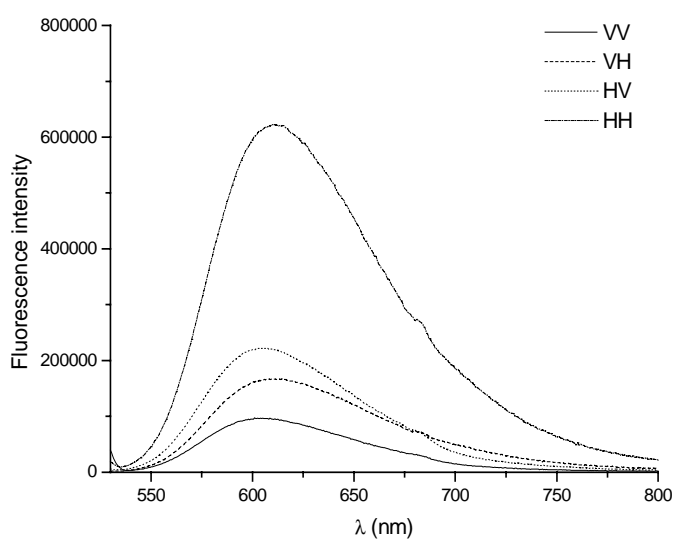


Fig.3: Individual components for the polarisation of ethidium bromide –DNA complex at $[DDAO]= 6 \times 10^{-4} \text{ M}$ at $\text{pH}= 5.8$. $[DNA]= 2.0 \times 10^{-5} \text{ M}$; $[EB]= 4.2 \times 10^{-6} \text{ M}$

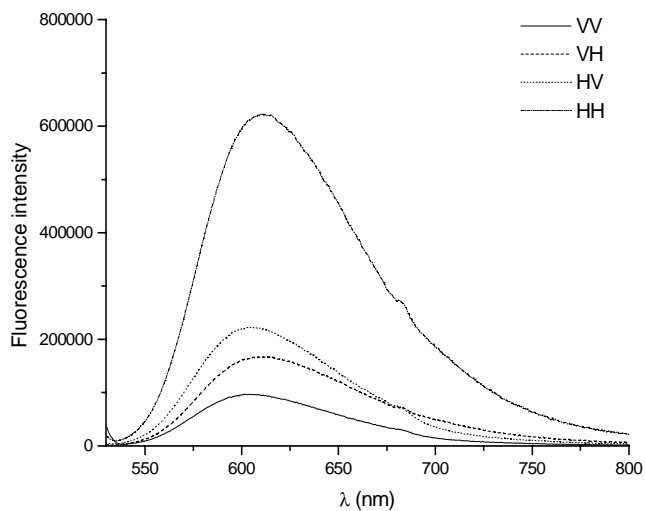


Fig.4: Individual components for the polarisation of ethidium bromide –DNA complex at $[DDAO]= 1.2 \times 10^{-3} \text{ M}$ at $\text{pH}= 5.8$. $[DNA]= 2.0 \times 10^{-5} \text{ M}$; $[EB]= 4.2 \times 10^{-6} \text{ M}$.

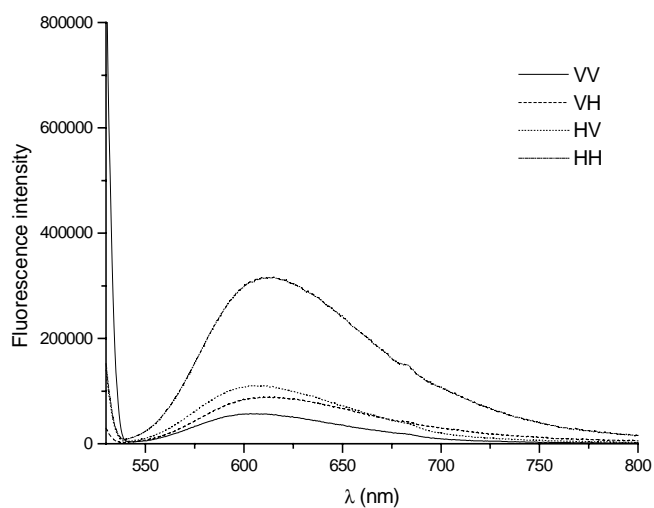


Fig.5: Individual components for the polarisation of Hoechst 33258 –DNA complex in the absence of DDAO at pH= 5.8. [DNA]= 2.0×10^{-5} M; [Hoechst]= 2.0×10^{-6} M.

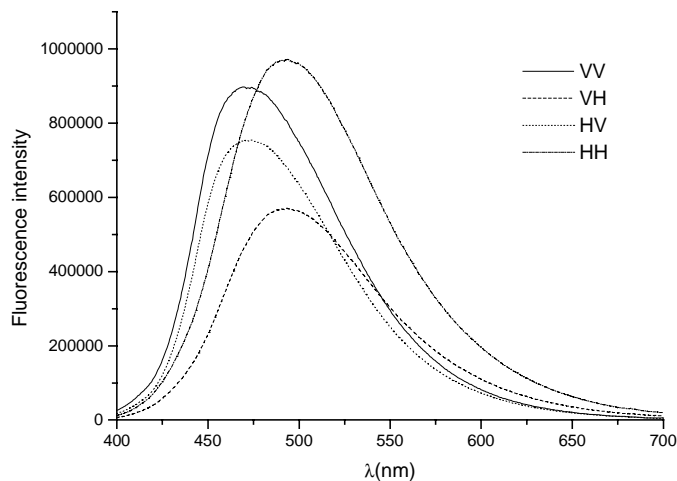


Fig.6: Individual components for the polarisation of Hoechst 33258 –DNA complex at [DDAO]= 2×10^{-4} M at pH= 5.8. [DNA]= 2.0×10^{-5} M; [Hoechst]= 2.0×10^{-6} M.

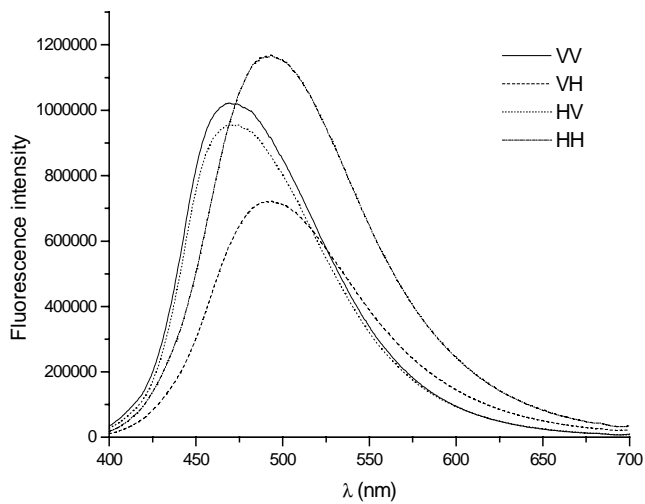


Fig.7: Individual components for the polarisation of Hoechst 33258 –DNA complex at $[DDAO]= 6 \times 10^{-4} M$ at $pH= 5.8$. $[DNA]= 2.0 \times 10^{-5} M$; $[Hoechst]= 2.0 \times 10^{-6} M$.

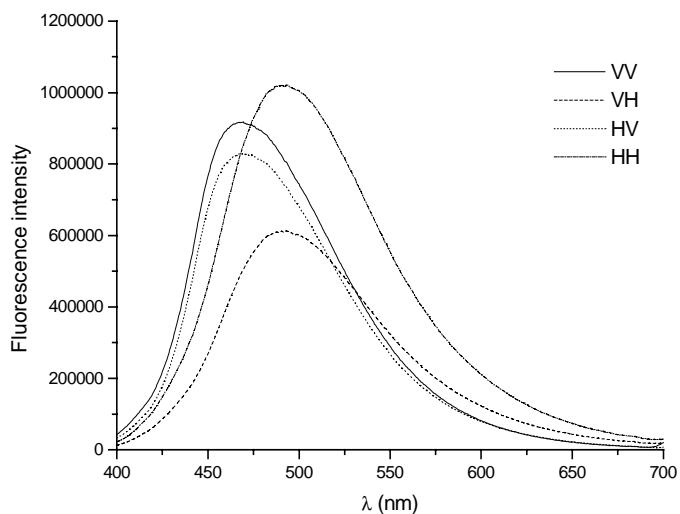


Fig.8: Individual components for the polarisation of Hoechst 33258 –DNA complex at $[DDAO]= 1.2 \times 10^{-3} M$ at $pH= 5.8$. $[DNA]= 2.0 \times 10^{-5} M$; $[Hoechst]= 2.0 \times 10^{-6} M$.

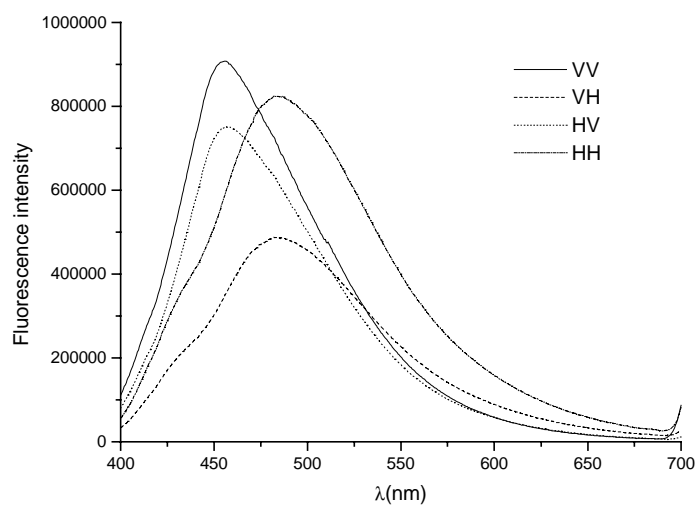


Fig.9: Individual components for the polarisation of ethidium bromide –DNA complex in the absence of pDOAO at pH= 5.8. [DNA]= 2.0×10^{-5} M; [EB]= 4.2×10^{-6} M.

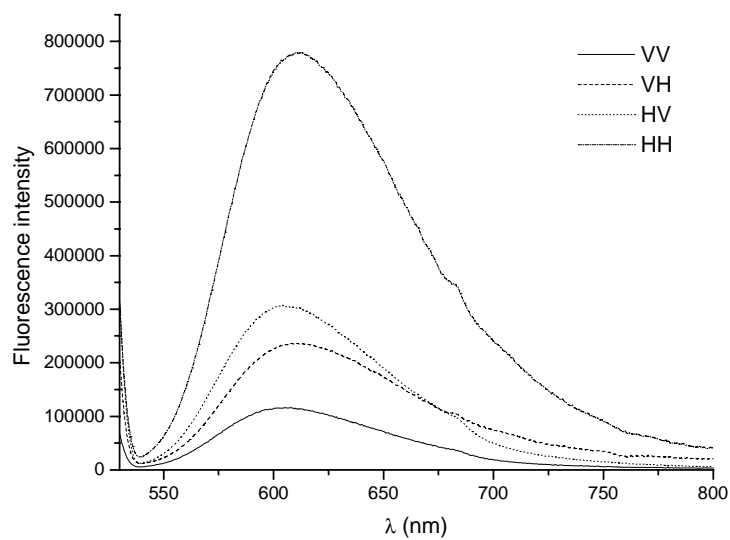


Fig.10: Individual components for the polarisation of ethidium bromide –DNA complex at [pDOAO]= 1.3×10^{-5} M at pH= 5.8. [DNA]= 2.0×10^{-5} M; [EB]= 4.2×10^{-6} M.

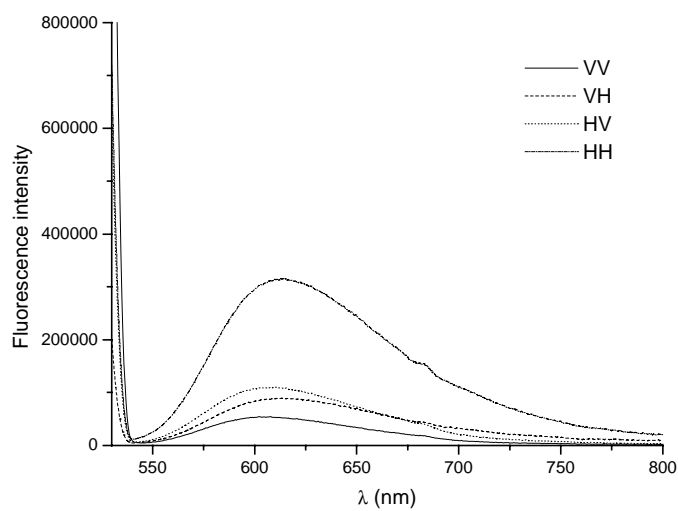


Fig.11: Individual components for the polarisation of ethidium bromide –DNA complex at $[pDOAO] = 7.3 \times 10^{-5} \text{ M}$ at $\text{pH} = 5.8$. $[\text{DNA}] = 2.0 \times 10^{-5} \text{ M}$; $[\text{EB}] = 4.2 \times 10^{-6} \text{ M}$.

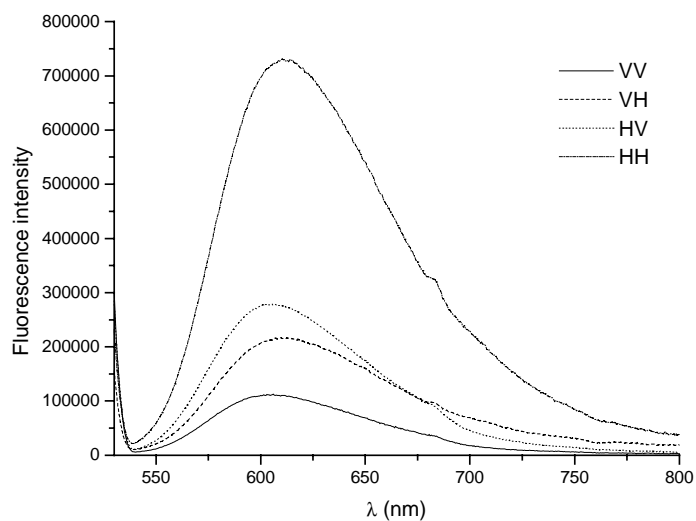


Fig.12: Individual components for the polarisation of ethidium bromide –DNA complex at $[pDOAO] = 6.8 \times 10^{-4} \text{ M}$ at $\text{pH} = 5.8$. $[\text{DNA}] = 2.0 \times 10^{-5} \text{ M}$; $[\text{EB}] = 4.2 \times 10^{-6} \text{ M}$.

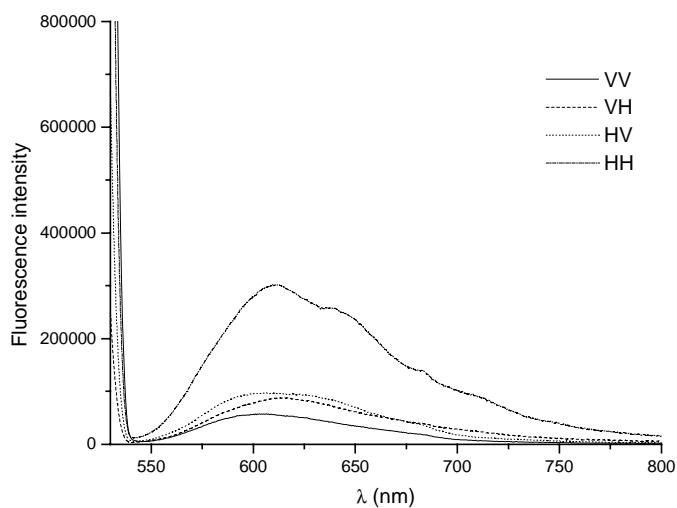


Fig.13: Individual components for the polarisation of Hoechst 33258 –DNA complex in the absence of pDOAO at pH= 5.8. $[DNA]= 2.0 \times 10^{-5} M$; $[Hoechst]= 2.0 \times 10^{-6} M$.

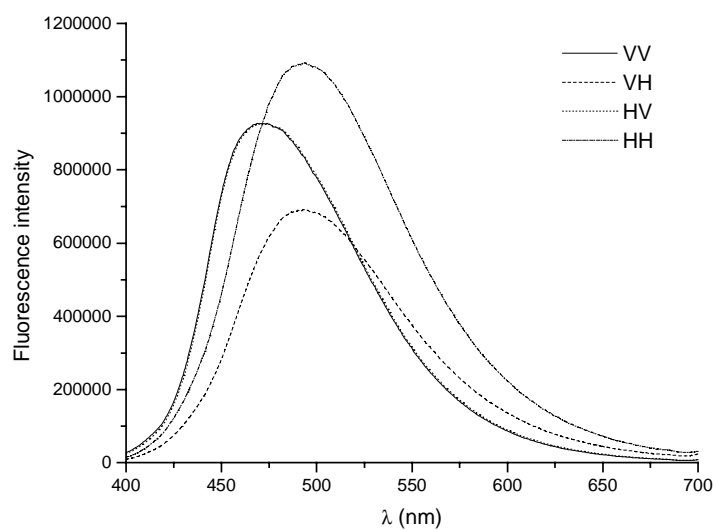


Fig.14: Individual components for the polarisation of Hoechst 33258 –DNA complex at $[pDOAO]= 1.3 \times 10^{-5} M$ at pH= 5.8. $[DNA]= 2.0 \times 10^{-5} M$; $[Hoechst]= 2.0 \times 10^{-6} M$.

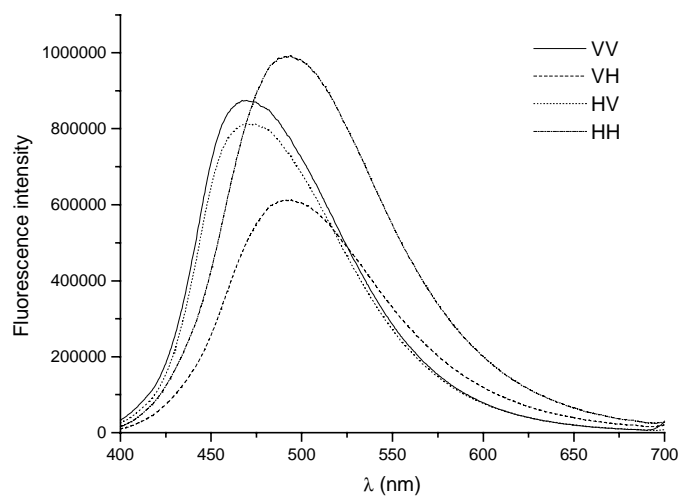


Fig.15: Individual components for the polarisation of Hoechst 33258 –DNA complex at $[pDOAO]= 7.3 \times 10^{-5} \text{ M}$ at $\text{pH}= 5.8$. $[\text{DNA}]= 2.0 \times 10^{-5} \text{ M}$; $[\text{Hoechst}]= 2.0 \times 10^{-6} \text{ M}$.

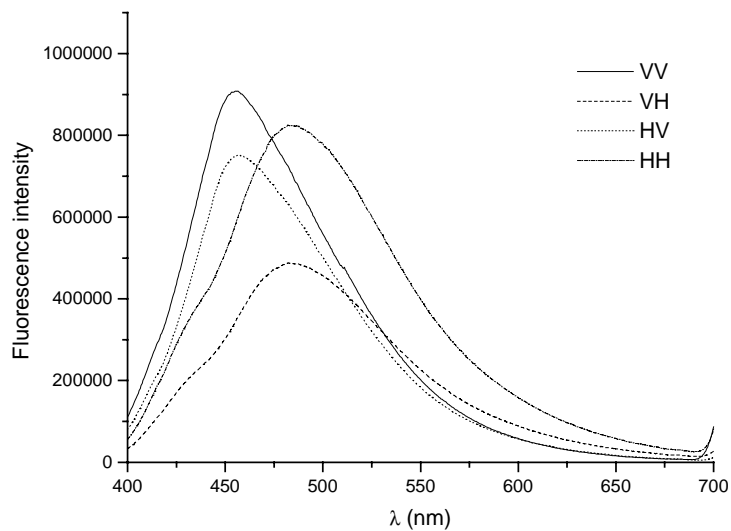


Fig.16: Individual components for the polarisation of Hoechst 33258 –DNA complex at $[pDOAO]= 6.8 \times 10^{-4} \text{ M}$ at $\text{pH}= 5.8$. $[\text{DNA}]= 2.0 \times 10^{-5} \text{ M}$; $[\text{Hoechst}]= 2.0 \times 10^{-6} \text{ M}$.

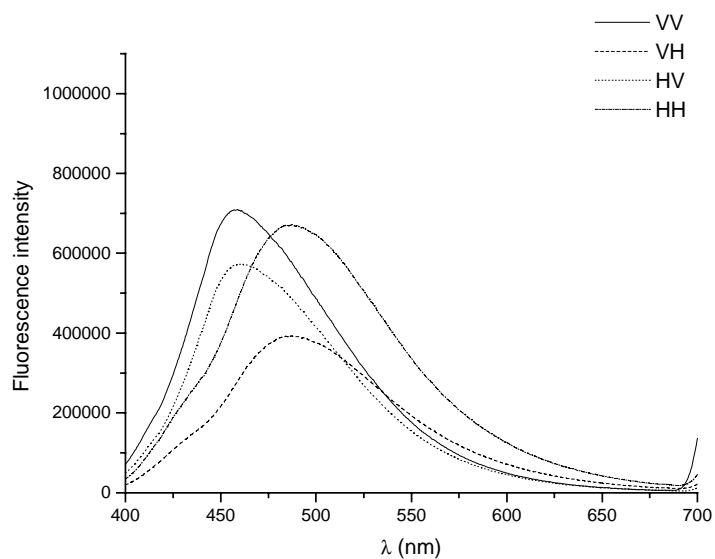


Fig.17: Polarisation curves for the DNA-ethidium bromide-pDOAO system at $pH=5.8$. $[DNA]=2.0 \times 10^{-5} M$; $[EB]=4.2 \times 10^{-6} M$.

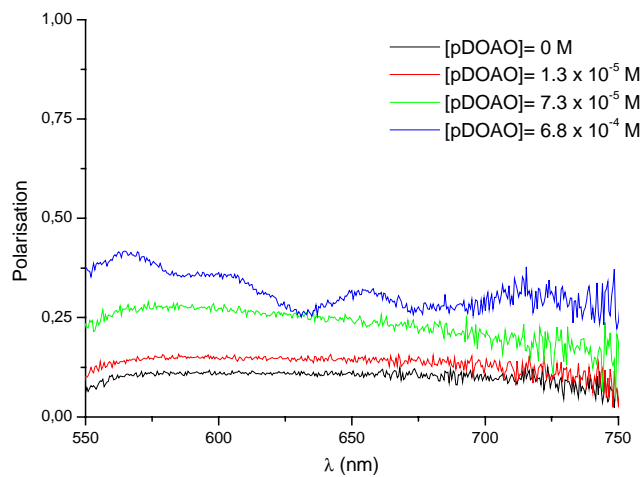
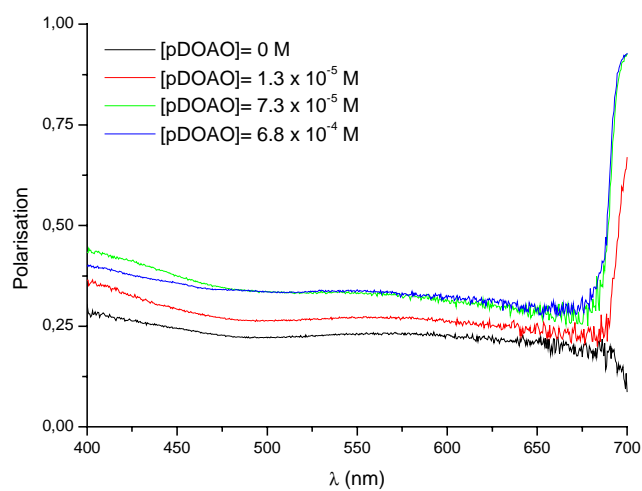


Fig.18: Polarisation curves for the DNA-Hoechst 33258-pDOAO system at $pH=5.8$. $[DNA]=2.0 \times 10^{-5} M$; $[Hoechst]=2.0 \times 10^{-6} M$.



SYMBOLS USED IN THE TEXT

c.m.c.	Critical micelle concentration
ϵ	Molar extinction coefficient
A	Absorbance
I	Fluorescence intensity
$[\theta]$	Molar ellipticity
CD	Circular Dichroism
CT	Calf-Thymus
P	Polarisation
K_{SV}	Stern-Volmer quenching constant
τ	Fluorescent lifetime of the excited state
k_q	Bimolecular quenching constant
k_s	Static quenching constant
EB	Ethidium bromide

Curriculum Vitae et Studiorum

Personal Data

Birth place: Columbus-OHIO (USA)

Day of birth: June 19th, 1976

Education

- ♦ Graduation at “Liceo Classico A. Mariotti” with mark of 60/60 (Perugia, July **1995**).

- ♦ *Laurea* in Chemistry *summa cum laude*, with a dissertation on “*Sintesi, Caratterizzazione e proprietà catalitiche di nuovi tensioattivi gemini*”, supervisors Prof. G. Savelli and Dr. R. Germani, University of Perugia (November 16th, **2000**).

- ♦ Qualification for the profession of chemist (Perugia, January **2001**).

- ♦ “Postgraduate Winter School on Organic Reactivity – WISOR XI”, Bressanone (BZ - Italy), January 6-13, **2002**.

- ♦ Fellowship from the University of Perugia for a research on “*Sintesi e caratterizzazione di molecole anfifiliche per riconoscimento molecolare e ionico*” coordinated by Prof. G. Savelli, Department of Chemistry.

- ♦ PhD student at the Laboratoire de Chimie Organique et Organometallique, at the University of Bordeaux 1 (France) for 6 months (supervisors Prof. F. Fages and Dott. D. M. Bassani).

Scientific Contributions

Communications to Conferences

1. L. Goracci, L. Brinchi, P. Di Profio, R. Germani, G. Savelli, “*Sintesi, Caratterizzazione e Proprietà Catalitiche di Nuovi Tensioattivi Gemini*”, TUMA 2001, XX Convegno Interregionale, Pisa (Italy), May 24-25, **2001**.

2. L. Goracci, L. Brinchi, P. Di Profio, R. Germani, G. Savelli, “*Synthesis and Characterization of New Gemini Surfactants*”, 5° Congresso Nazionale di Chimica Supramolecolare, Frascati (Italy), September 30-October 3, **2001**.
3. P. Di Profio, R. Germani, L. Goracci, G. Savelli, G. Onori, A. Santucci, “*Interactions of DNA with Synthetic Amphiphilic Systems as Models for Transfection Processes*”, Postgraduate Winter School on Organic Reactivity – WISOR X, Bressanone (Italy), January 6-13, **2002**.
4. P. Di Profio, R. Germani, L. Goracci, G. Savelli, “*Interactions of DNA with Synthetic Amphiphilic Systems as Models for Transfection Processes*”, TUMA 2002, XXI Convegno Interregionale, Urbino (Italy), July 15-17, **2002**.
5. P. Di Profio, L. Goracci, G. Savelli, N. Spreti, “*Amphiphilic Interactions Effect on Biomolecules in Aqueous Solution. The Case of DNA and Chloroperoxidase*”, ISSOC-4 (Italo-Spanish Symposium on Organic Chemistry), Perugia (Italy), August 31 – September 3, **2002**.
6. L. Brinchi, R. Germani, L. Goracci, G. Savelli, “*Attivazione di Nucleofili da Parte dello ione Fluoruro in Presenza di Liquidi Ionici*”, XXI Congresso Nazionale della Società Chimica italiana, Torino (Italy), June 22-27, **2003**.
7. L. Goracci, G. Savelli, D.M. Bassani, “*Using Fluorescent Probes to Study DNA-Surfactant Interactions*”, 6° Congresso Nazionale di Chimica Supramolecolare, Urbino (Italy), September 7-10, **2003**.

PAPERS

1. L. Brinchi, R. Germani, L. Goracci, G. Savelli, C.A. Bunton, “*Decarboxylation and Dephosphorylation in New Gemini Surfactants. Change in Aggregate Structures*”, **Langmuir**, 18 (21) 7821-7825 (**2002**).

Résumé

Les interactions entre l'ADN et une série de molécules amphiphiles ont été étudiées en combinant des techniques spectroscopiques anisotropes (absorption, fluorescence) et polarisées (dichroïsme circulaire, dépolarisation de fluorescence). Les résultats obtenus ont été ensuite analysés en utilisant un modèle de docking moléculaire et indiquent que l'utilisation de la sonde fluorescente bromure d'ethidium pour étudier les interactions entre ADN et amphiphiles est bien plus complexe que ce postulé actuellement dans la littérature. L'utilisation d'une nouvelle sonde, le composé Hoechst 33258, est proposée

Mots-Clés

Amphiphiles, surfactants, ADN, interactions, modélisation, Hoechst 33258, ethidium, fluorescence, dichroïsme circulaire, transfection.